PL-TR-92-2008

Lg and Other Regional Phases in South America

Ramon Cabre, S.J.
Estela R. Minaya
R. Rodolfo Ayala
Marcos Capriles

Observatorio San Calixto
P. O. Box 12656
La Paz, Bolivia

23 October 1991

Scientific Report No. 2

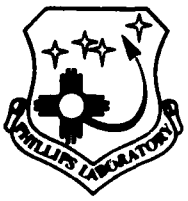

PHILLIPS LABORATORY
AIR FORCE SYSTEMS COMMAND
HANSCOM AIR FORCE BASE, MASSACHUSETTS 01731-5000

SPONSORED BY
Defense Advanced Research Projects Agency
Nuclear Monitoring Research Office
ARPA ORDER NO. 5307

MONITORED BY
Phillips Laboratory
Contract AFOSR-89-0532

This technical report has been reviewed and is approved for publication.

JAMES F. LEWKOWICZ
Contract Manager
Solid Earth Geophysics Branch
Earth Sciences Division

JAMES F. LEWKOWICZ
Branch Chief
Solid Earth Geophysics Branch
Earth Sciences Division

DONALD H. ECKHARDT, Director
Earth Sciences Division

This report has been reviewed by the ESD Public Affairs Office (PA) and is releasable to the National Technical Information Service (NTIS).

Qualified requestors may obtain additional copies from the Defense Technical Information Center. All others should apply to the National Technical Information Service.

If your address has changed, or if you wish to be removed from the mailing list, or if the addressee is no longer employed by your organization, please notify PL/IMA, Hanscom AFB, MA 01731-5000. This will assist us in maintaining a current mailing list.

Do not return copies of this report unless contractual obligations or notices on a specific document requires that it be returned.

REPORT DOCUMENTATION PAGE

Form Approved
OMB No. 0704-0188

1. AGENCY USE ONLY (Leave blank)	2. REPORT DATE	3. REPORT TYPE AND DATES COVERED
	23 October 1991	Scientific #2

4. TITLE AND SUBTITLE
Lg and Other Regional Phases in South America

5. FUNDING NUMBERS
PE 61102F
PR 9A10 TA DA WU AX

Contract AFOSR-89-0532

6. AUTHOR(S)
Ramon Cabre, S.J.
Estela R. Minaya
R. Rodolfo Ayala
Marcos Capriles

7. PERFORMING ORGANIZATION NAME(S) AND ADDRESS(ES)
Observatorio San Calixto
P. O. Box 12656
La Paz, Bolivia

8. PERFORMING ORGANIZATION REPORT NUMBER

9. SPONSORING/MONITORING AGENCY NAME(S) AND ADDRESS(ES)
Phillips Laboratory
Hanscom AFB, MA 01731-5000

Contract Manager: James Lewkowicz/GPEH

10. SPONSORING/MONITORING AGENCY REPORT NUMBER
PL-TR-92-2008

11. SUPPLEMENTARY NOTES

12a. DISTRIBUTION/AVAILABILITY STATEMENT
APPROVED FOR PUBLIC RELEASE; DISTRIBUTION UNLIMITED

12b. DISTRIBUTION CODE

13. ABSTRACT *(Maximum 200 words)*

Part I. Seismic phases, especially those following P after a short time, in records of La Paz station (LPB) for South America and neighboring coast earthquakes were revised, trying to identify their nature; a large range of diversity proves the complexity of South American tectonic structures, also in cases apparently identical. Often pP was identified; other arrivals of unclear origin were called provisorily P_1 and P_2, probably related to Nazca plate subduction; their amplitude, if observable, is much variable. Smallness of P and S phases of earthquakes occurred in zones apparently homogeneous suggests lateral variations in the mantle. Short period waves Li, Lg, Rg are recorded at LPB with a quite variable amplitude for the different South American provinces. Intermediate depth earthquakes produce in LPB those phases as large as surface quakes do. The phase Li was studied especially for Peruvian earthquakes. In spite of structural complexity, a division of South America in zones (related to Flinn and Engdahl division) was attempted. Part II. Attenuation of short period waves P, Li, Lg, Rg has been calculated for Peruvian earthquakes recorded at LPB. Provisory conclusions are in press in Revista Geofisica. Part III. At the end of the reported period improvement of the knowledge of attenuation and P wave residuals is under study.

14. SUBJECT TERMS			15. NUMBER OF PAGES
Earthquake	P derived phases	Lg	92
P	Short period surface waves	Rg	
pP	Li	Apparent velocity	16. PRICE CODE
	Q	Attenuation	

17. SECURITY CLASSIFICATION OF REPORT	18. SECURITY CLASSIFICATION OF THIS PAGE	19. SECURITY CLASSIFICATION OF ABSTRACT	20. LIMITATION OF ABSTRACT
Unclassified	Unclassified	Unclassified	SAR

TABLE OF CONTENTS

PART I

INTRODUCTION

The study of regional wave propagation allows to know the general lineaments of the internal earth structure: remarkable discontinuities, mantle and crust dynamics (Dziewonski, 1984; Jordan, 1981; Jordan et al., 1975, 1989; Johnson, 1967, 1969; Burdich et al., 1978; Lay et al., 1984).

On the othter hand the coda of P-waves for teleseisms (distance larger than 10°) helps to establish low velocity zones (LVZ) beneath different structures: those LVZ are not apparent, or do not exist at all, in shield structures and on the contrary they are ticker in tectonically active regions (Helmberger, 1973). This data informs us about thermal variations related to lateral variations in the upper mantle.

Regional waves (distance of 10° or less) help: to detect variations in the crust; more precise locations of seismic events. Local phases allow to know with more detail characteristics close to the station or to the station network.

Other important phases independent of the distance (that is, for earthquakes, either local, or regional, or teleseism) are identified with those short period waves Li, Lg, Rg, what are characteristics of continental regions; they allow a better knowledge of low velocity layers in the crust. (Nuttli, 1986; Payo Subiza, 1974; Pomeroy et al., 1980; Alcócer, 1989; Ayala, 1989; among others).

Nevertheless, those phases have different characteristics for different complex zones, meanwhile they are similar for more homogeneous zones.

South America, especially the Pacific Coast, is really complex when considering tectonic structures, crustal thickness and Nazca plate subduction. Let us distinguish two types of geological structures: stable zones (Guyana, Brazil and Patagonia Shields and the Altiplano); strong activity zones (Western and Eastern Cordilleras).

Crustal thickness: 40 km at the north, increases to 65 km in central part and then decreases to 35 km in the south (Meissner et al., 1976; Couch et al., 1981; James, 1971; Wigger et al., 1990; Fernández , 1965; Valez, 1982).

Nazca subducted plate: Subduction dipping almost null north of latitude 13°- 15°S, changes to 35° at latitude 20°S; dipping is maximum for maximum depth between 500 to 700 km (Deza, 1972; James, 1990; Minaya, 1978).

Those aspect of South America and Pacific Coast complexity have a strong influence on the waves recorded in LPB station. So the identification of those different phases is one of the highest importance.

DATA

1000 Seismic events which occurred in South America and Pacific Coast, recorded in the LPB station (La Paz - Bolivia, WWSSN type) were analysed, after excluding other about 1000 events. Epicentral data were read from the International Seismological Centre (ISC) Bulletins from 1974 through 1988.

Different phase analysis was achieved on the 3 components of analogical records.

Distance of teleseisms reach 36.5°; regional seisms are at distances between 1° and 10°. Magnitude mb is larger than 4. Depth may go down to 650 km. For local erthquakes a small error in depth influences records too much; so, to avoid that difficulty, events of the seismic-geographical region of Flinn and Engdahl 3-120 (Bolivia) were excluded from our study.

Seismic records were digitized, using a time window of 25 to 35 sec, being sample interval 0.05 sec.

Flinn and Engdahl seismic regions studied are: 7, 8, 9, 35.

METHODOLOGY

1. Seismic phases, amplitude (mm) and period were read on analogical short period records; precision depends on the abruptness of the initial phase. Particle motion helped to correct time readings for the phase after the first arrival. Epicentral distance (km) divided by travel time (second) was called apparent velocity.

2. Phase identification: Trying to identify the regional phases, frequently P was quite clear; for distance larger than 10° often pP and sP were detected; other regional phases derived from P could not be identified; but certainly other phases are present, what were called P1 and P2.

A phase type S may be Sn, but was not labeled so, considering that Moho depth is not known reliably.

We have to remark that Lg phase is clearly recorded for earthquakes north of LPB station, independently of depth; south of LPB Rg amplitude may equal that of Lg, or be lesser or also completely absent.

Particle motion helped to identify phases close to first arrival (Figs. 1, 2, 3).

3. Analysis of crustal tickness, geology and tectonics in the region and Nazca plate subduction:

Looking for the changes in crustal tickness, let us see a profile from north to south (Fig. 4):

Along the parallel 8.5°N Meissner et al. (1976) found that oceanic crust is 20 km thick close to the coast, and maximum tickness of 40 km in the continent.

At 14°S he found from west to east 20 km, then a maximum of 60 km, decreasing to 30 km in the Subandean.

Porth et al. (1990) in a profile along the parallel 21°S find a thickness of 65 km between 66° and 68.25°W; at the coast 39 km; at the west of 66°W 30 km.

Couch et al. (1981) calculate a thickness of 45 km in the continent at latitude 26°S and only 8 km in the oceanic crust.

At the latitude 38°S the same author calculates a maximum thickness of 35 km in the continent.

Geological and tectonic changes are more relevant from east to west than from north to south: Shield zones, Subandean, Cordilleras (Western, Central and Eastern), Coast Cordillera, coast and transition zone from continental to oceanic crust.

According to Deza (1972), Nazca plate has three transition zones: between 0° and 1°S; between 13° and 14°S; between 26° and 27°S. James (1990) considers the transition to begin at 15°S. Those transition zones coincide with the change of subduction angle of Nazca plate.

That analysis recommended to divide seismic regions (Fig. 2):

SEISMIC REGION	ZONE	GEOGRAPHIC REGIONS
7	7a	98, partial both 97 and 101
	7b	96, 99, 100, partial both 97 and 101
8	8a	102, 104, 105, 108, 109
	8b	103, 106, 107, 110, 111, partial both 112 and 116
	8c	113, 119, 120
	8d	partial 112, 114, 115, partial 116, 117, 118
	8e	122, 123, 124, 125, partial 127, 128, 129
	8f	partial 127, 130, 131, 132, partial 136 through 141
9	9	143 through 146
35	35	528 through 531

Earthquakes located in seismic zones 8a and 35 have no phase derived from P. Seismic record is of small amplitude. S phase is not visible. Lg is of small amplitude. We have to remark that earthquakes located in 8a have a path to LPB different of those in 35. Those in 8a are originated beneath the ocean in the coast, or in the subducted plate; those in zone 35 are shield surface quakes.

Other phases close to P were observed for the earthquakes originated in all the other provinces: 7a, 7b, 8b, 8c, 8d, 8e, 8f, 8g and 9. But there are so many differences in P derived phases that they claim for a separate description.

Seismic Region 7a. After P a larger phase arrives with an interval corresponding to depth; that means that if is a pP (Fig. 6.1).

See the gradation of amplitudes P<pP<Lg + Rg (both later phases indepent from depth). S<<P . For the corner northeast of this region P is fairly large; no other P derived phase is observed; Lg<P. 80% Of path for those earthquakes to LPB is across shield zones.

Seismic region 7b. The main difference with to appears in short period surface waves: Surface earthquakes located between 72° and 69°W and 7° to 9°N have them larger than pP (Fig. 6.2).

Intermediate earthquakes have smaller short period surface waves.

Seismic region 8a. Generally no P derived phase; in a few cases a second phase, 3 to 8 seconds after P of unknown process of generation.

Lg and Rg << P_1 ; S very small.

Seismic region 8b. In most of the records pP is observed; in some cases another phase P_1 between P and pP, 5 to 9 seconds after P.

Short period surface waves, especially Rg, are clear and large; they appear for intermediate depth as well as for surface quakes.

Three phases after P are observed, but in several cases only the phase P is observed. The whole record has a small amplitude (Fig. 6.3).

Seismic region 8c. Most of the earthquakes of this region are deep. The surface or intermediate quakes have three P phases (Fig. 6.6), being the second one pP larger than the other two (1st and 3rd this one not identified). S phase is clear for deep earthquakes (more than 500 km), but emergent for surface and intermediate quakes. Short period surface waves are larger for surface and intermediate quakes, not existent for deep quakes.

Seismic region 8d. It is considered especially complex, since record amplitude may be larger or small for the same magnitude; P derived phases may be clear or completelly absent; in some cases a regular pP was identified. We have to remark that Nazca plate dip changes gradually within this region from horizontal to 35° (Fig. 6.5,8,17).

Seismic region 8e. Records show two phases after P, one 2 to 5 seconds, the other 14 to 20 seconds after P. Looking to the envelope curve, two are clearly different:

1 The third arrival is the largest one (Fig. 6.12 through 16).

2 The first P arrival is the largest one (Fig. 6.18).

Short period surface waves are smaller than S; records are not clear, especially for surface waves, without doubt because, being regional events, wave trains recorded analogically may not be decompressed.

Seismic region 8f. A second arrival 2 to 8 seconds after P is independent from the focal depth. Deep earthquakes (h>500 km) do not show any duplication of P, that is to say, no pP.

Generally, but no always, the first phase is smaller than the second one. Short period surface waves Lg, Rg are larger than previous phases for surface quakes, are smaller for intermediate, are absent for deep ones. No Li recorded for this region. (Fig. 6.9 through 11).

Seismic region 8g. Ocean and coast. Generally the whole record is of small amplitude. A second phase, larger than P, corresponds to pP (Fig. 6.8).

Seismic region 9. 3 To 9 seconds after P, another phase is observed, and a third one after 18 seconds. Generally the coda is short, signal amplitude small. Short period surface waves are not observed at all.

Seismic region 35. This geological zone is quiet, well known, consisting mostly in Guyana and Brazil shields. One P phase of small amplitude is observed (Fig. 6.4).

Phases Li, Lg and Rg are clear. S phase has small amplitude and a rather long period, so it is read on long period records.

CONCLUSIONS AND INTERPRETATION

Analysis of the phases following the first P arrival for earthquakes occurring beneath South America and Pacific coast recorded at LPB station has shown that these phases are related to the South American and Nazca plate complex structure.

The complexity of Andean Cordillera explains the strong attenuation of waves transmitted along a path parallel to its axis across transition zones. Variation of crustal thickness appears to influence more seismic waves than source or station conditions.

Problably P_1 has its origin in a canalization of waves in the subducted Nazca plate; also a low velocity layer in the upper mantle was suggested for teleseisms of intermediate depth. For regional earthquakes of surface focus rather reflexion in the multiply layered continental crust would be the responsible of those phases; that would also explain the delay in many earthquakes recorded with small amplitude.

P_2 possibly is originated in the S to P conversion; but this possibility does not explain P_2 presence for deep earthquakes.

In a few earthquakes P is faster than expected according the tables. These cases have an irregular geographical distribution not coincident with the division of South America related to other seismic aspects. Possibly a high velocity layer in the mantle may explain that (20° discontinuity 400 km deep. Lehmann, 1970; Julian et al., 1968; Fahmi, 1964).

Nazca plate geometry is important related to conversion of wave type or its reflexion, mainly if focus is at an intermediate depth.

On the other hand the wedge of the mantle between the Moho and the Benioff zone may disturb seismic ray propagation for deeper events, those originated in plate contact.

The small amplitude and the absence of other P derived phases in the region a possibly are explained by a strong absorption of energy in the transition zone oceanic to continental crust.

The region 35 produces very small P, without any acceptable explanation for the moment.

See in a tabular form the behavior of South American regions concerning P derived phases at LPB; those of unknown origin will be called P_1 and P_2.

	ZONE	P-PHASES			
One P arrival	8a	P			
	35	P			
Two P phases	7a	P		pP	
	7b	P		pP	
Three P phases	8b	P	P_1		
	8c	P		pP	
	8d	P	P_1		P_2
	8e	P	P_1	pP	P_2
	8f	P	P_1	pP	P_2
	8g	P		pP	P_2
	9	P	P_1	pP	

A paper was presented in the General Assembly XX of the IUGG in a poster session of August 22, whose abstract is as follows:

REGIONAL PHASES SHOW ANDEAN ZONE COMPLEXITY

E. Minaya, R. Cabré S. J. and R. Ayala

Observatorio San Calixto. Cas. 12656. La Paz, Bolivia

Regional phases Li, Lg, Rg and S, P residuals, for South American earthquakes recorded at LPB station, show a regional complexity claiming for a new division in subregions of different seismic and structural characteristics.

Eastern South America, excepting the quite stable Guyana Shield, has a few anomalies, probably originated in deep fractures. In northern part of South America attenuation is higher than normal, uneven, with a tendency to increase from W to E. The Andes in Peru-Ecuador are the most complex part of the whole South America, especially Lg and Rg are different for earthquakes supposed similar in location and size. Continuing to the S, we find double phase P, but only when quakes originate in subducted plate; attenuation of Lg still appears high. Southern Argentina-Chile is the less complex part of the Andes, though Li, Lg and Rg are not recorded at all; eventually P phase is double or also triple.

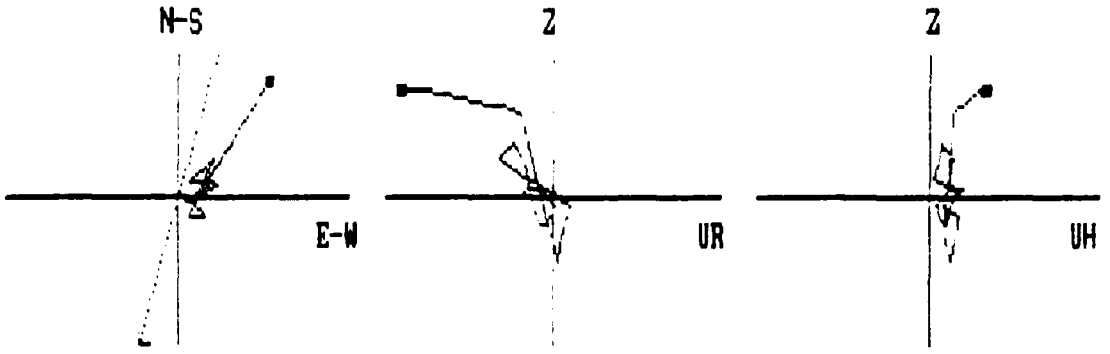

1a. Particle motion of P phase.

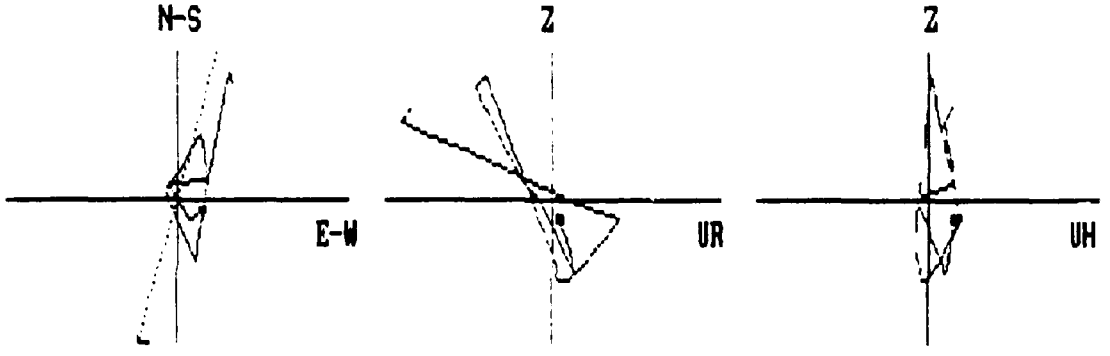

1b. Particle motion of pP phase.

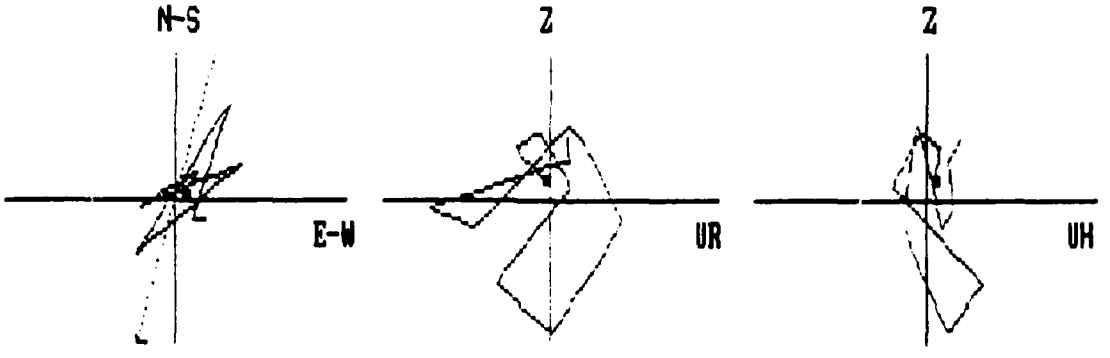

1c. Particle motion of P_2 phase.

Fig. 1. PARTICLE MOTION OF THREE P PHASES. ZONE 8f (Fig. 6.8).

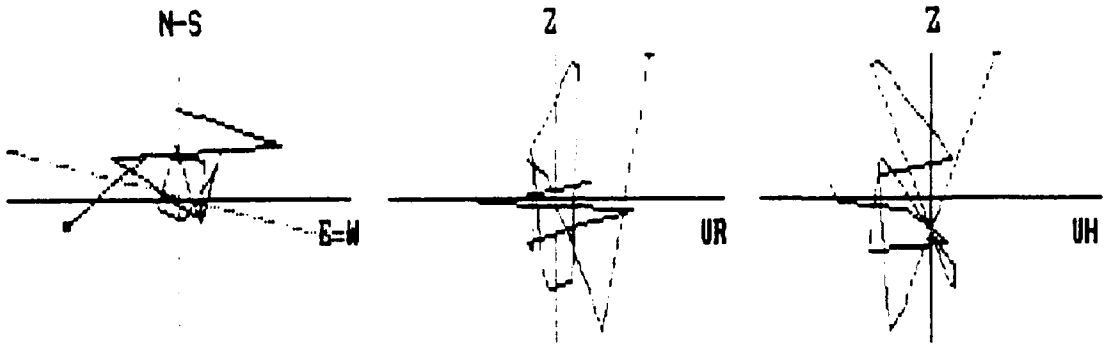

Fig. 2. PARTICLE MOTION OF COMPLEX P PHASE. ZONE 8d (Fig. 6.17).

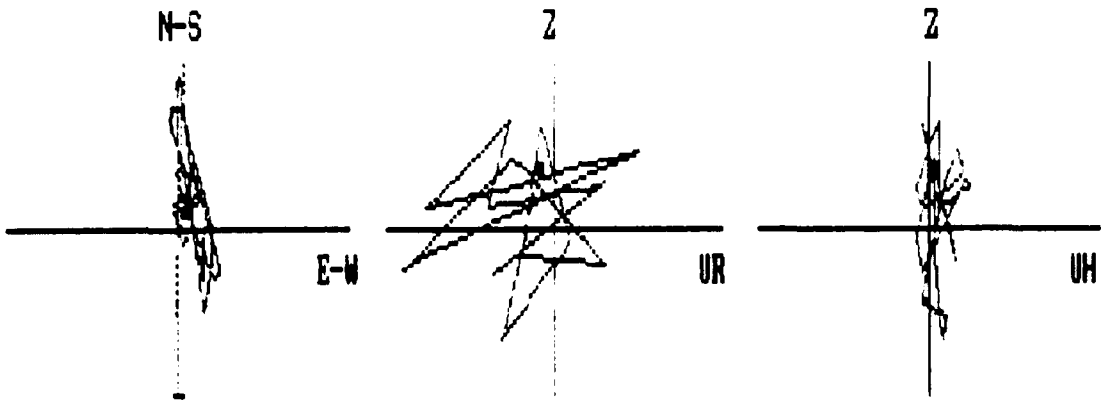

3a. Particle motion of pP phase.

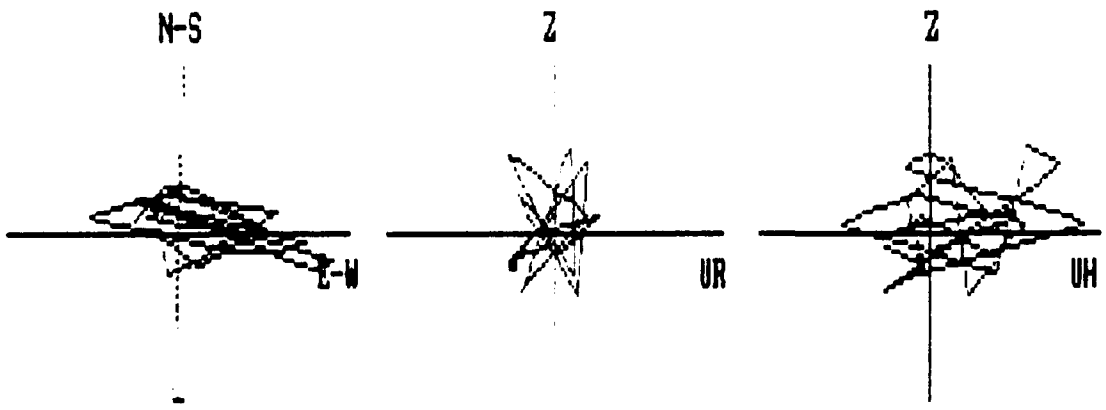

3b. Particle motion of P_2.

Fig. 3. PARTICLE MOTION OF TWO PHASES. ZONE 8f (Fig. 6.10).

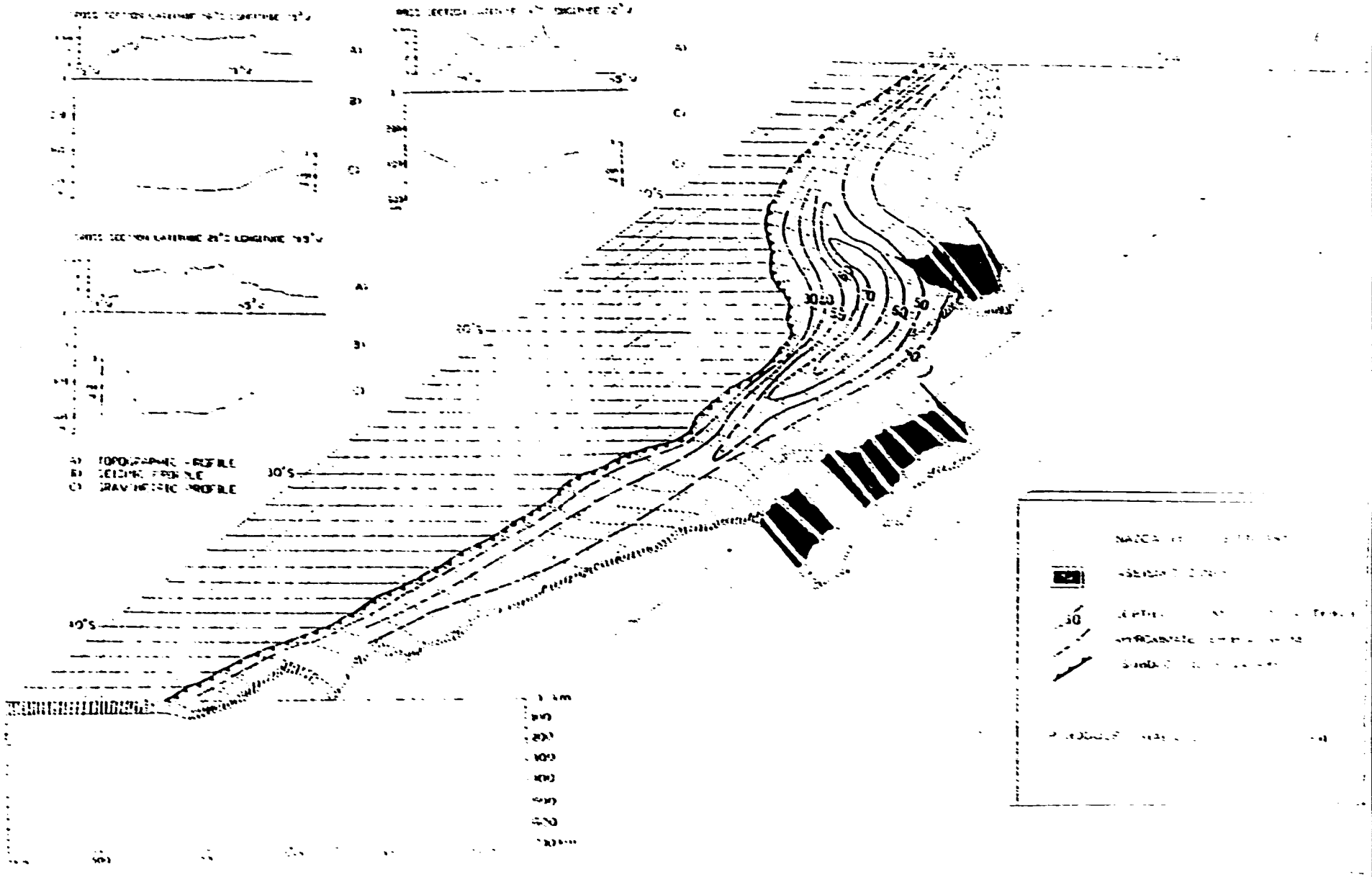

Figure 4. Nazca plate and depth of Moho

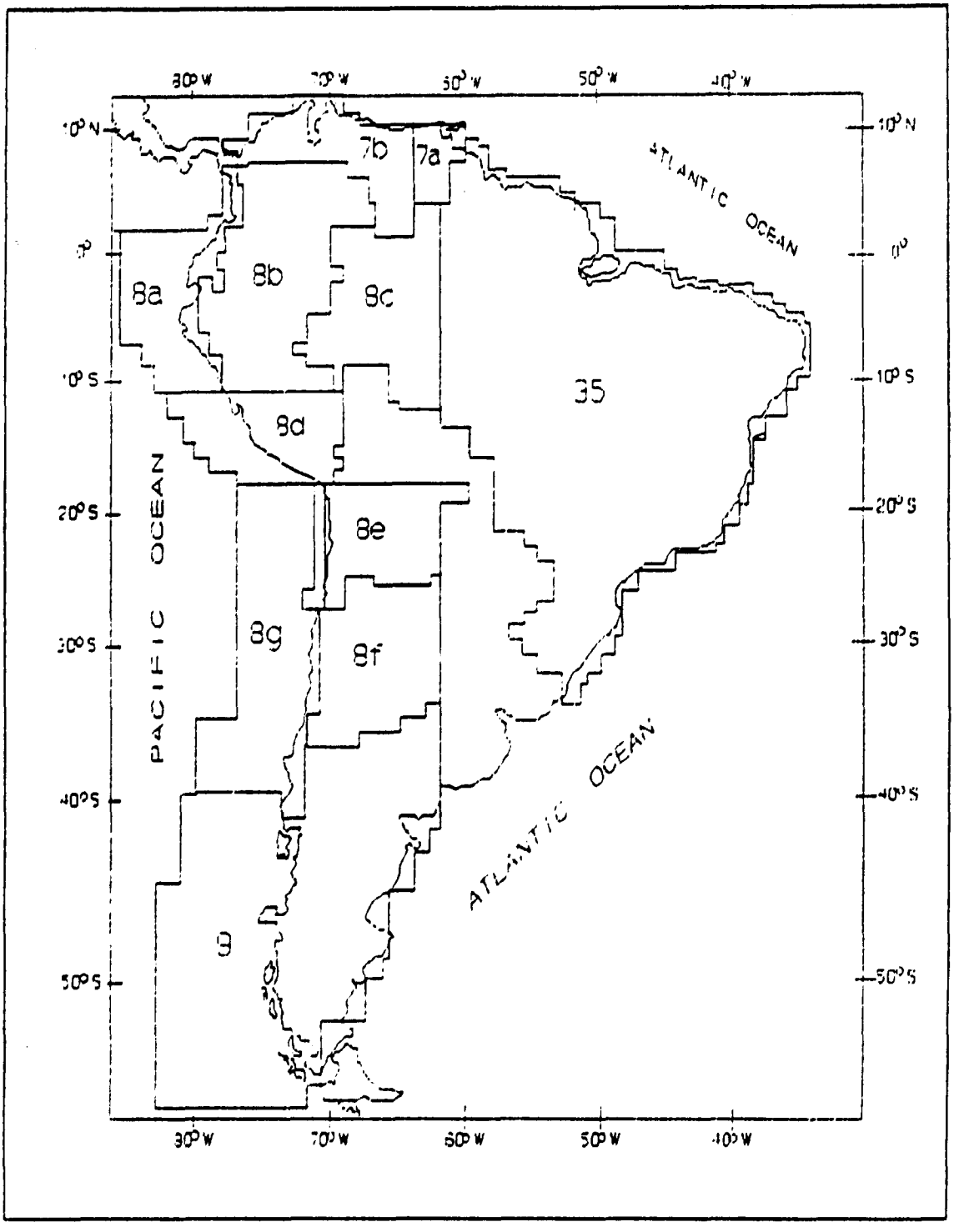

Fig. 5. MAP OF SOUTH AMERICA SHOWING THE ZONES ACCORDING TO THE SEISMIC P PHASES ANALYSED.

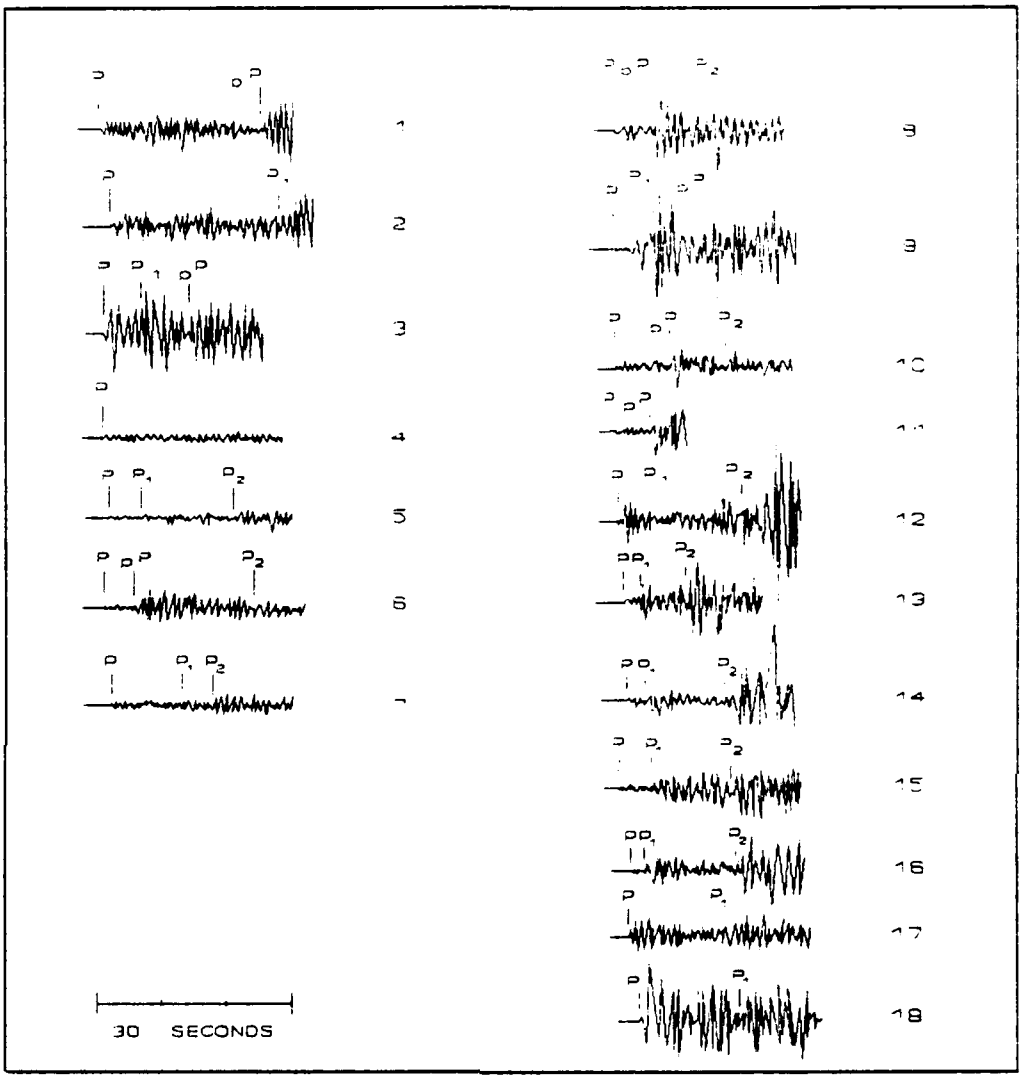

NUMBER	ZONE	D (o)	h (km)	AZIMUTH (o)	mb	NUMBER	ZONE	D (o)	h (km)	AZIMUTH (o)	mb
1	7a	27.87	112	192	4.2	8	8g	22.18	24	13	5.3
2	7b	23.73	39	170	5.0	9	8f	16.59	103	7	5.9
3	8b	22.45	91	158	5.7	10	8f	16.00	24	2	4.9
4	35	18.96	10	208	5.0	11	8f	15.03	13	358	5.6
5	8d	10.65	63	119	5.6	12	8e	8.07	66	13	5.0
6	8c	10.73	67	164	4.8	13	8e	7.31	40	17	4.8
7	8d	7.49	117	134	5.2	14	8e	7.21	47	331	4.7
						15	8e	5.53	63	24	4.9
						16	8e	4.90	115	7	4.4
						17	8d	3.90	47	108	4.7
						18	8e	3.29	33	15	4.8

Fig. 6. SEISMOGRAMS RECORDED AT LPB STATION, SHORT PERIOD VERTICAL COMPONENT, SHOWING THE DIFFERENT P PHASES.

Li OF PERU EARTHQUAKES RECORDED AT LPB

The analysis of Li waves originated in Peru, recorded at LPB (La Paz-Bolivia) station continues a previous study: La onda Lg a través de los Andes y registradas en la estación de LPB (Alcócer, 1989). Generally the beginning of Li waves is enough clear.

350 Events occurred in Perú from 1974 to 1986 could be useful for that analysis; among them 95 were selected, excluding the smaller ones, several superposed with other signals, etc. On the other hand two recent events clearly recorded in local digital stations were added for comparaison reasons (Fig. 7).

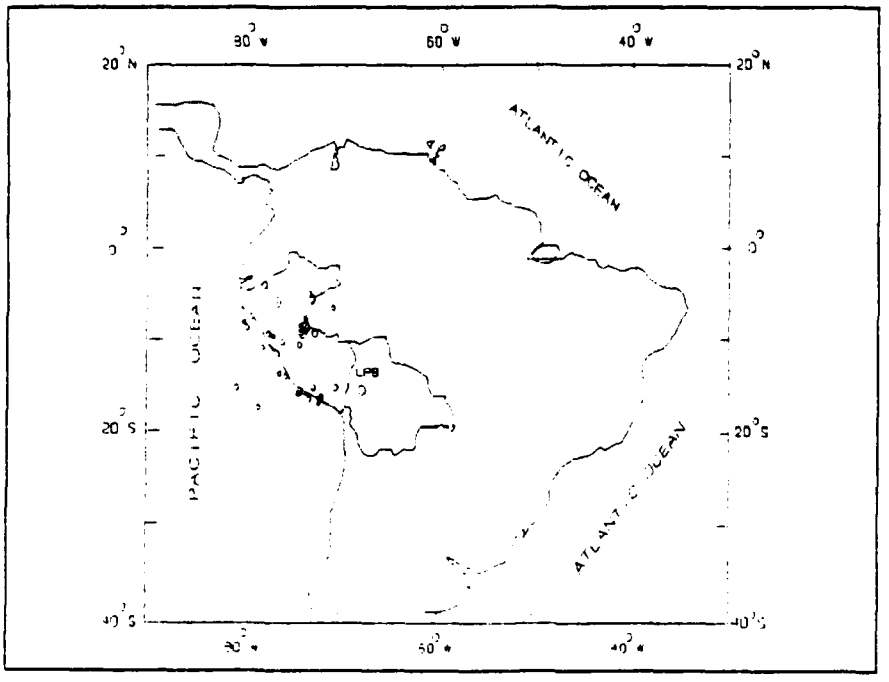

Fig. 7. Epicenters of earthquakes studied here (1974-1986).

The guided waves Li were found by M. Bath (1956), meanwhile studying in detail the following phases Lg and Rg (Press and Ewing, 1952); they propagate along a low velocity layer, supposed to extend between Conrad and Mohorovicic discontinuities; that supposition originates in the analogy of those waves with Sb waves observed for near earthquakes.If the path focus-station is ocenaic along about 100 km, Li is not recorded, but when the oceanic path is no more than 60 km, Li is recorded the same as when the path is completely continental. The non-existence of a granitic layer, together with the reduction of basaltic layer to a few km, mean that the continental crust is responsible of Li generation and transmission; so, a low velocity layer is thought to occupy the intermediate space (so it is represented by index i).

When the path of Li waves is parallel or subparallel to Andes Cordillera, Li are smaller than Lg, being the ratio Li/Lg 0.65±0.20; both trains of waves have a similar predominant period (that allows a direct comparaison of amplitudes in the record itself). If path is perpendicular to the Cordillera, Li at least equals Lg amplitude, but generally is larger, being the mean ratio 1.05±0.21.

Li are the beginning for several trains of surface, short period, low velocity waves, appearing as a continuation; so, some times the whole set of different waves is called Lg.

Particle motion of Li waves appears complex, mainly for surface earthquakes, what suggests that such waves are a composition of several arrivals.

The largest part of the energy belongs to the horizontal projection SH (transverse to the ray path); after that the largest amplitude corresponds to the component SVH (parallel to the ray path); the vertical amplitude SVV is small, practically absent for intermediate depth earthquakes.

Amplitude spectrum was obtained by fast Fourier transform; the maximum amplitude corresponds to frequencies o.75 to 1.40 Hz. WAVES.

The ground apparent velocity of Li was calculated by dividing the hypocentral distance (D) by the travel time (t):

$$V = D/t$$

Two different ranges of velocity may be distinguished corresponding to different ranges of depth (see Fig. 8).

Depth (km)	Velocity (km/s)
h≤120	3.84±0.03
h>120	3.91±0.04

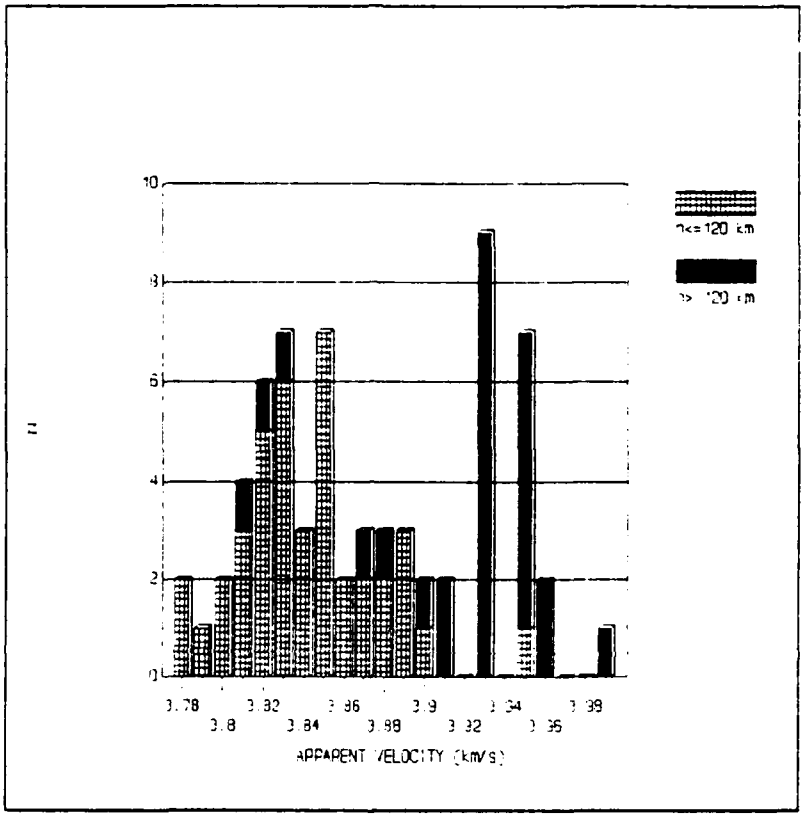

Fig. 8. Histogram showing the correspondence between frequency of apparent velocity values considering two depth ranges.

PART II

ATTENUATION OF THE SHORT PERIOD WAVES P, Li, Lg AND Rg TRHOUGH PERU - BOLIVIA, RECORDED AT LPB

R. Rodolfo S. Ayala, Ramón P. Cabré S.J. and
Estela R. Minaya
Observatorio San Calixto, La Paz, Bolivia

ABSTRACT

This preliminary study analyses the characteristics of phases P, Li, Lg and Rg of earthquakes originated in Peru, recorded at La Paz - Bolivia (LPB). See the mean apparent velocity (km/s) for those phases, according the depth:

	P	Li	Lg	Rg
h≤70 km	7.73±0.01	3.84±0.0001	3.54±0.0003	3.17±0.001
70<h≤217km	7.86±0.05	3.81±0.01	3.53±0.003	3.15±0.005

The anelastic attenuation has values quite different in two separate areas: In the Cordillera region oscillates between 0.12 and 0.17 ^{1}/degree; in Brazilian shield and Subandean oscillates between 0.12 and 0.17 ^{1}/degree. Being quality factor Q inversely related to :In the Cordillera region Q changes between 192 and 630; in Brazilian Shield and Subandean between 450 and 794. The complexity of Cordilleran structure may explain a stronger attenuation.

Remark.- The Spanish version of this paper is in press, in the Revista Geofísica (Pan American Institute of Geography and History). It is annexed to this Report. Figures in the Report are taken from the Spanish version.

INTRODUCTION

Longitudinal waves (P waves) have particle motion in the same direction as the waves propagate. Their velocity is less than 8 km/s in the crust and 8 to 10 km/s in the mantle. They are well observed in the short period vertical component.

Li waves (identified by Bath, 1956) are short period channel waves period transmitted along the intermediate layer of the crust. Their group velocity is 3.79±0.07 km/s. They are identified as S* wave at short epicentral distance, their particle motion is complex, with large horizontal component.

Lg guided waves have short period, large amplitude (discovered by Ewing and Press, 1952); they have a particle motion perpendicular to the ray path, polarized on horizontal plane; their group velocity is 3.54 km/s.

Rg were recognised (by Bath, 1954) as guided waves, short period, Rayleigh wave type, with propagation along the granitic layer, group velocity about 3.0±0.7 km/s and particle motion characteristic of Rayleigh waves.

DATA

The events studied occurred in Peru, 2° to 18° latitude south, 68° to 81° longitude west (Fig. 1), magnitude mb 4 to 5.6, depth divided in two ranges $h \leq 70$ km and $70 < h \leq 217$ km, during 1973 to 1986. The data was taken from ISC, for earthquakes recorded at LPB station.

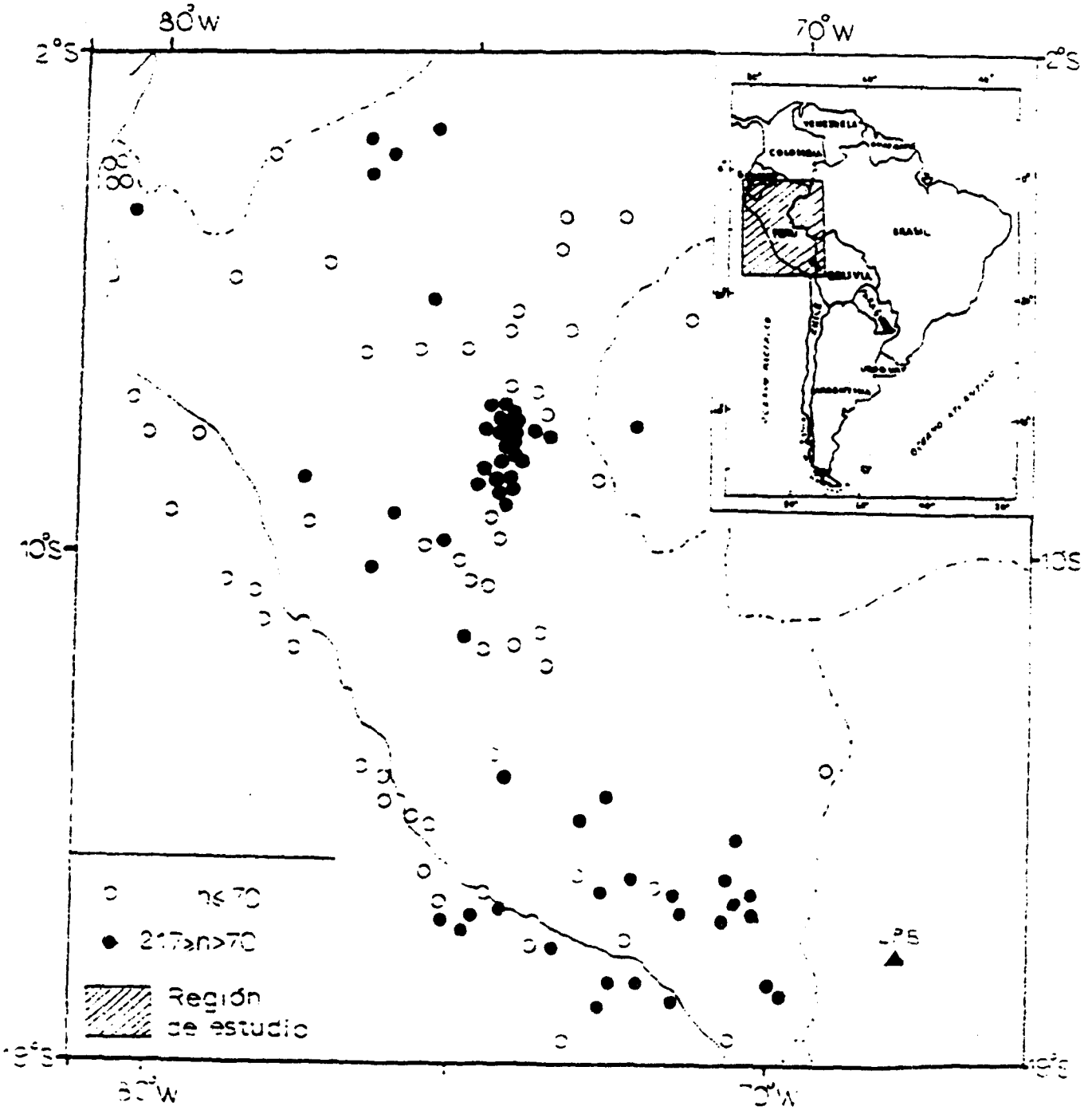

Fig. 1. Epicenter distribution Map according to depth.

METHOD

The maximum amplitude and corresponding period of P waves were measured on the short period vertical seismograms; Li, Lg and Rg maximum amplitude and period were measured on short period horizontal seismograms.

The region was divided in six diferent zones (Fig. 2) according to the back azimuth station-epicenter. In relation to the depth each zone has two levels (Table 1). The first level for shallow depth and the second one for intermediate depth.

Amplitude data were normalized at mb=5.0 in order to avoid the source effect.

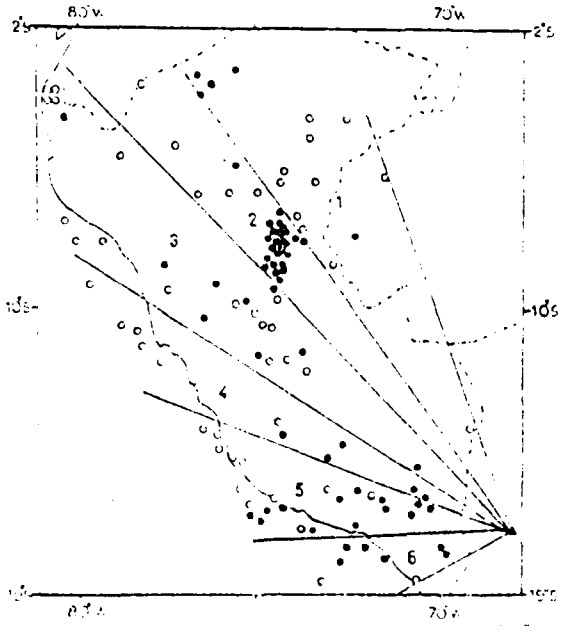

TABLE 1	
ZONE	AZIMUTH (sta-epi)
1	340° - 320°
2	320° - 310°
3	310° - 280°
4	280° - 270°
5	270° - 250°
6	250° - 160°

Fig. 2. Epicenter distribution map, showing the division by zones.

Nuttli's equation of magnitude (1973) was used to compute the C, B coefficents for each phase and zone. Coefficent of attenuation was computed from attenuation curve (Fig. 3) of Nuttli (1973), whose basic equation is:

$$A = K*(1/(D^\circ))^{1/2}*(1/(SIN(D^\circ)))^{1/2}*(e^{-\gamma*D^\circ})$$

Where A is amplitude (micrometers), K constant, D° epicentral distance and γ anelastic attenuation coefficent (^{1}/degree).

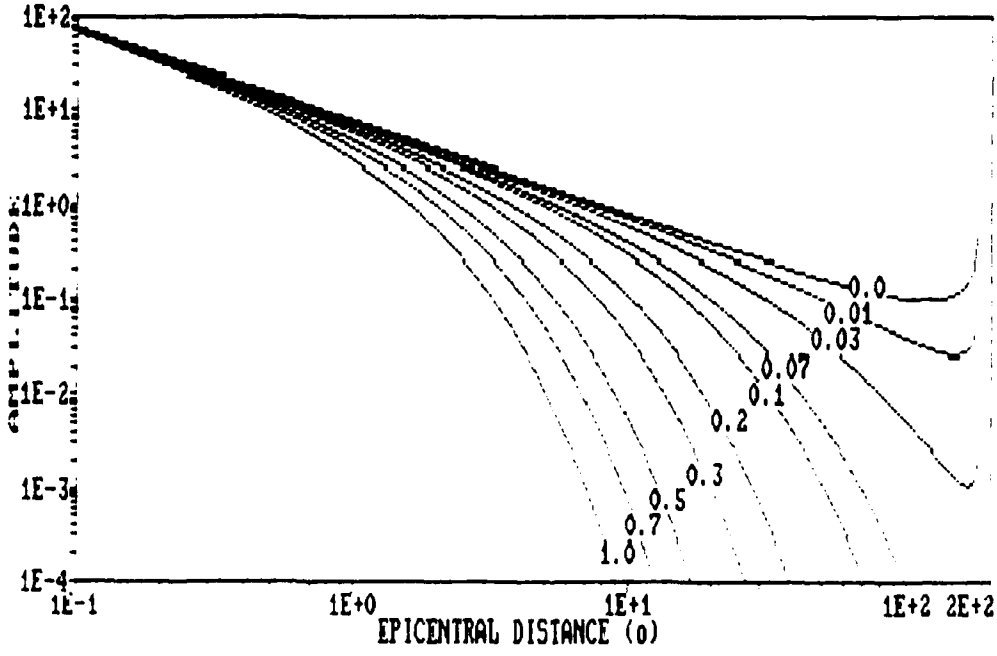

Fig. 3. Attenuation theorical curves of the amplitude in time domain, where γ is expressed in reverse of degree (Nuttli, 1973).

Units of γ were changed to ^{1}/km in order to get the quality factor Q using Nuttli equation (1973) :

$$Q = \pi / (T * \gamma * V)$$

Where T is period in seconds, γ anelastic coefficent of attenuation (^{1}/km) and V group velocity (km/s)

Herrmann (1980) method was applied to data in order to verify the Q values obtained by Nuttli's method (1973). Herrmann's method used the coda of the seismic event, considering that the main frequency fp (Hz) is inversely proportional to Q values.

The master curves were used to obtain the Q values (Fig. 4) for short period standard seismograph (WWSSN). Travel time t divided by Q is equal to t* (Fig. 4); fp (Hz) was computed taking a time band-window about 10 seconds and number of zeros that cross the mean trace of signal, after that they are divided twice by the time band-window; fp (Hz) is plotted versus t (s) and cheking with the master curve until t* becomes equal to one, then the Q value will be numerically equal to t.

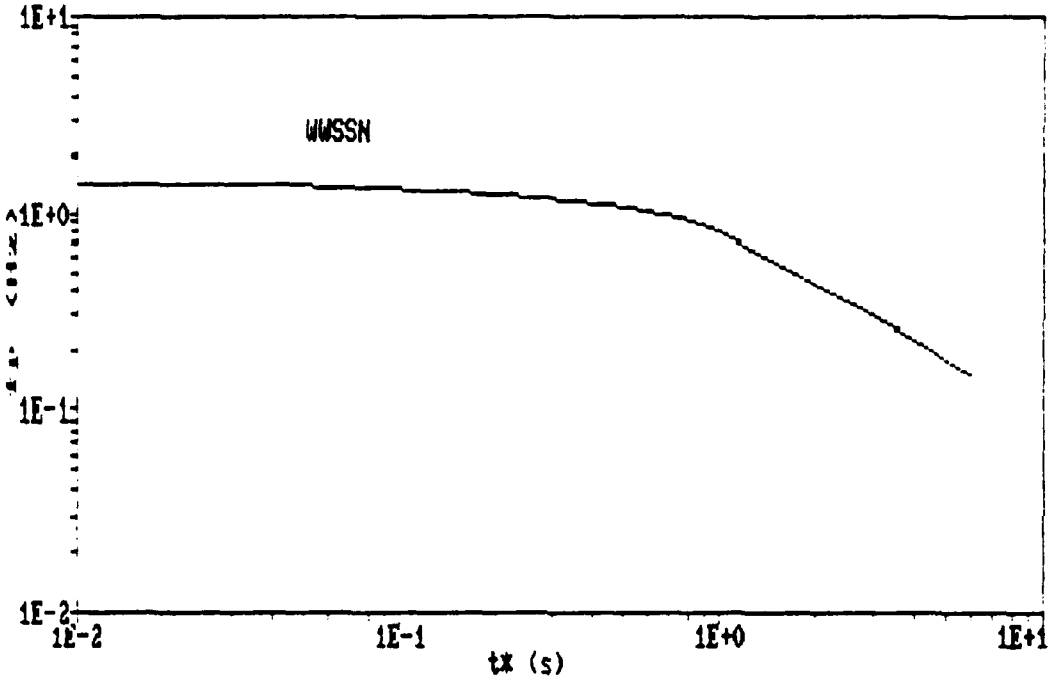

Fig. 4. Master curve of main frequency fp (Hz) versus t* for standard short period seismographs (WWSSN) (Herrmann, 1980).

Group velocity was obtained by plotting travel time versus epicentral distance fitting curve and computing it for each phase (Figs. 5a and 5b, according to depth).

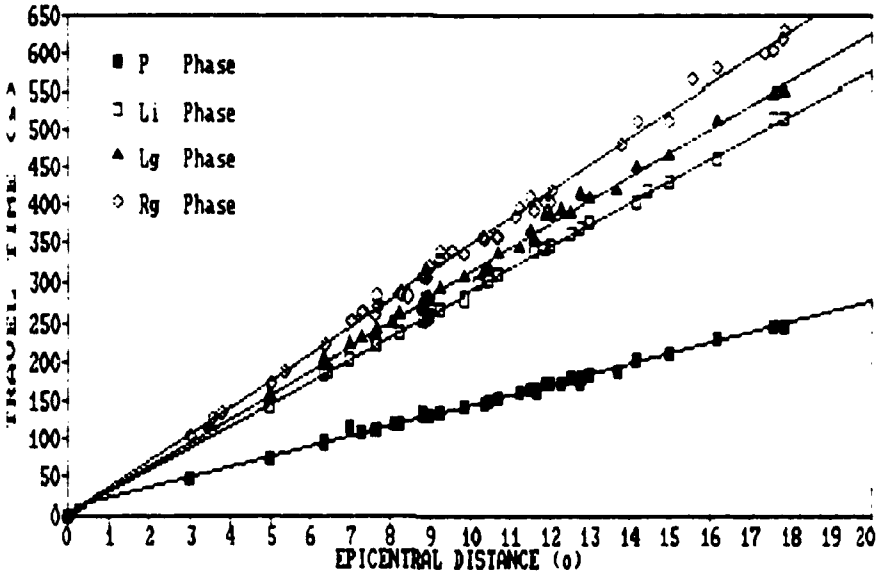

Fig. 5a. Travel time versus epicentral distance curves for shallow earthquakes.

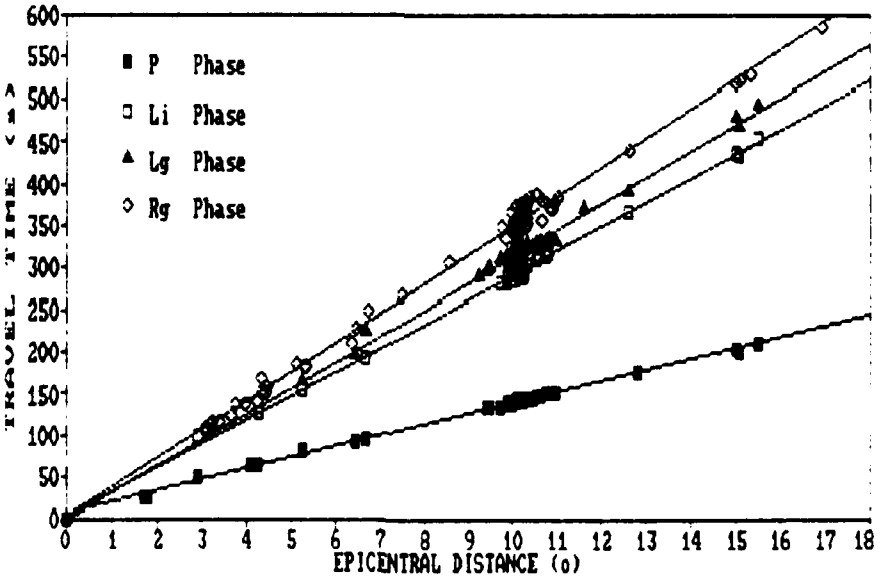

Fig. 5b. Travel time versus epicentral distance curves for intermediate earthquakes.

TECTONIC AND GEOLOGICAL ENVIRONMENT

The region studied corresponds to a convergency zone between two tectonic plates where the Nazca plate is subducted under the South America plate; the Nazca plate moves a 6 cm/year and the South America plate 3 cm/year (Minster and Jordan, 1978).

The Nazca plate is divided in five segments in this region, the first between 2° and 6° south latitude , dipping 12°E, 100 km thick, seismically active until 250 km; the second segment from 7° to 12° south latitude , dipping 20°E, 110 Km thick and seismically active until 580 km; the third segment, 12° to 15° south latitude , dipping 16°E, 100 km thick and seismically active until about 290 km; the fourth is located from 15° to 17° south latitude, dipping 21°E, 120 km thick and seismically active until about 300 km; the fifth, from 17° to 24° south latitude, dipping 29°E, 120 km thick seismically active until about 580 to 600 km (Ayala, 1991).

Both in the Northern and Southern parts there are active volcanoes, being weakness zones.

Continental plate is divided (at surface) in five geological provinces: Andean Cordillera, Altiplano, Coastal Cordillera, Coastal Plateau, Upper Basin of Amazonas, Chaco-Benian plains, Brazil and Guayana Shields.

Andean Cordillera consists of Western and Eastern Cordillera, the last one composed of Paleozoic rocks and granitic bodies, the spurs, called Subandean, are composed mainly by sedimentary Paleozoic rocks , strongly folded and fractured. Western Cordillera consists mainly of volcanic rocks.

Coastal Cordillera is made of a series of batholithic rocks parallel to the coast line. It is a local range.

Coastal Plateau separates the Coastal Cordillera from the Western Cordillera.

High Plateau corresponds to a tectonic trench lifted, of mesozoic age. It is located between Western and Eastern Cordilleras, filled with sedimentary rocks, paleozoic, cretaceous, tertiary and quaternary cover, around 12000 meters thick (Schlater and Nederlof, 1966).

Brazilian Shield consists of precambrian rocks. They are the basement of South American plate. The part outcroping in Bolivia is labeled Guapore Shield; the northern prolongation is labeled Guayana Shield. These are separated by sedimentary paleozoic rocks, of marine origin and meso-cenozoic rocks of Amazonas basin 700 meters thick (Jeffreys and Aires, 1988).

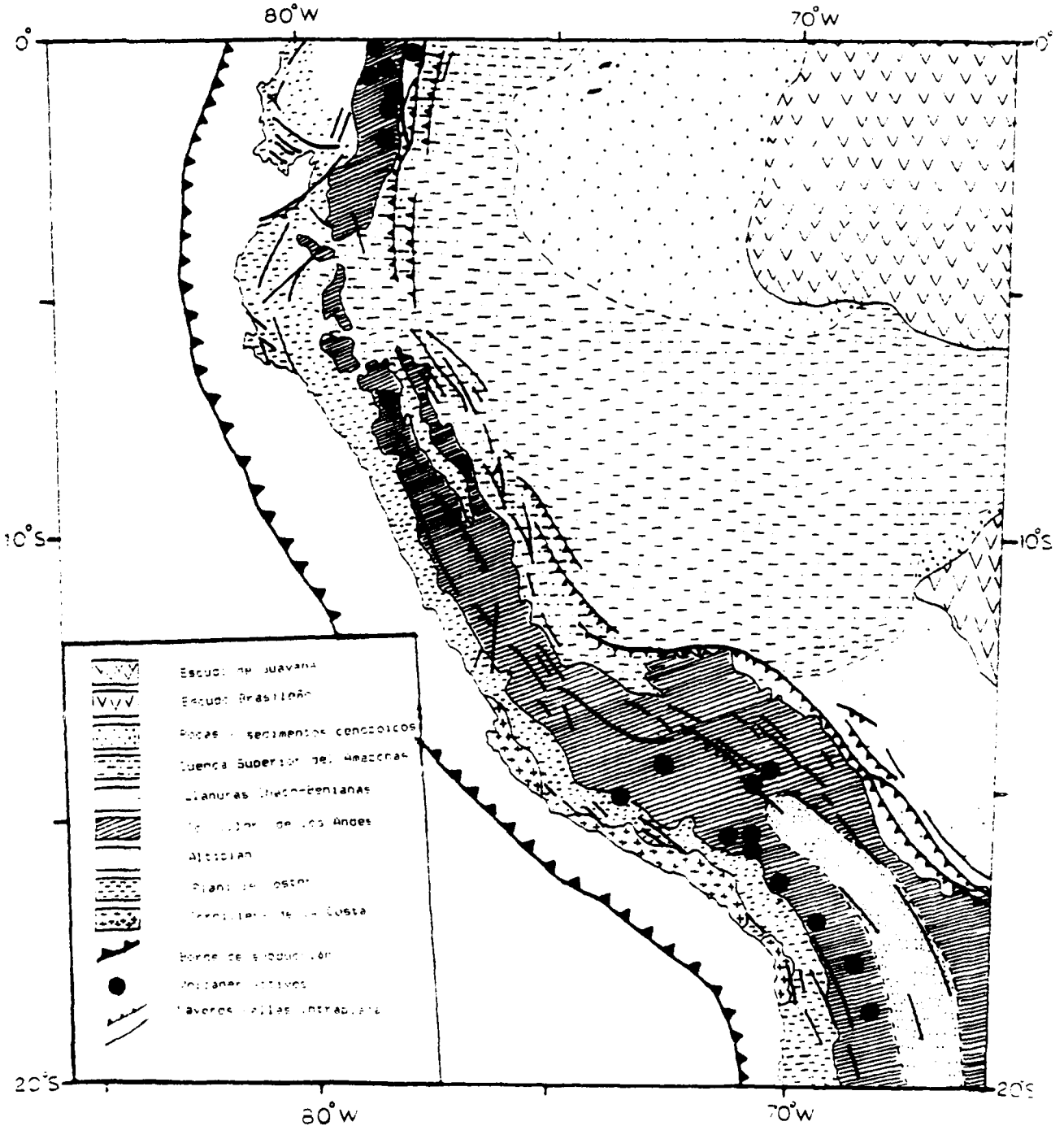

Fig. 6. Tectonic geological map (adopted from the Mapa Noetectoncio Preliminar para Sudamérica, 1985).

The Eastern part is called Upper Amazonas Basin, with Paleocene rocks. It covers the contact between Shield and Cordillera. It is about 4000 meters thick (Morrison, 1962).

Chaco-Benian plains are wide, with cambrian and paleozoic rocks, 2300 meters thick (Morrison, 1962), while along the Beni river the precambrian basement is covered with terciary rocks.

SEISMIC WAVES ORIGINATED IN THE PERU

The Fig. 7 shows the short period vertical records of Peruvian earthquakes, recorded at LPB.

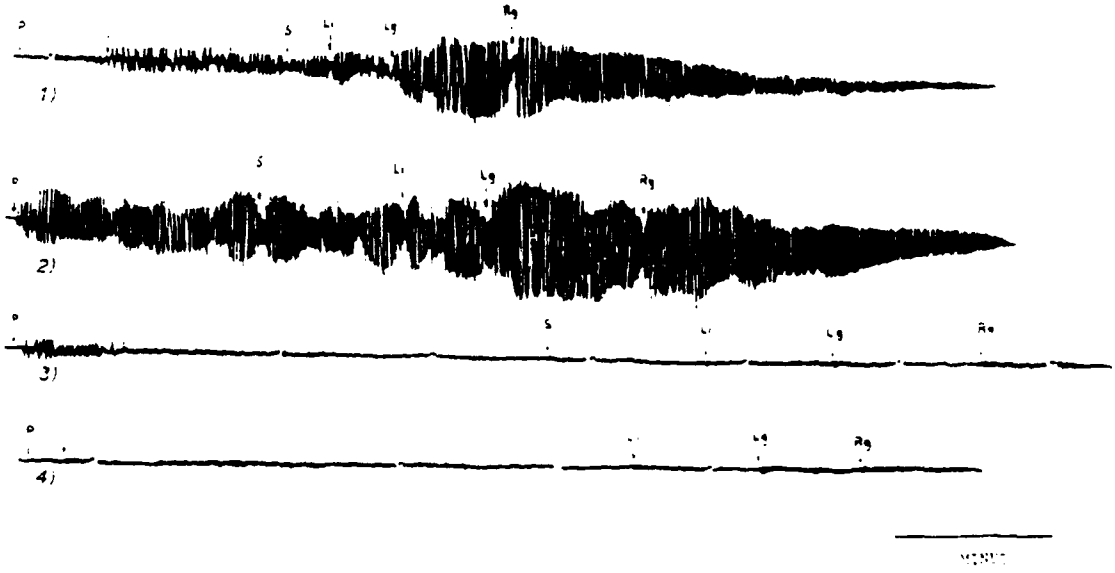

Fig. 7. Vertical short period seismograms recorded at LPB.

(1) 15-VII-1982 ; h=117 km ; mb=5.5 ; D°=10.34°

(2) 20-III-1983 ; h= 18 km ; mb=5.4 ; D°= 8.90°

(3) 21- V -1986 ; h=126 km ; mb=4.9 ; D°=15.51°

(4) 23- IV-1986 ; h= 96 km ; mb=5.4 ; D°=17.85°

P Phase

In general the Peruvian P waves have emergent beginnings; periods between 0.6 and 1.2 s; the average apparent velocity is 7.73±0.01 km/s, normalized amplitudes from 0.01 to 0.3 micrometers for shallow focus; for intermediate focus the velocity is 7.86±0.05 km/s and their normalized amplitudes from 0.02 to 1.1 micrometers. The particle motion parallels the ray propagation (in the three planes: horizontal plane formed by N-S and E-W components; vertical plane parallel to the azimuth, formed by vertical component Z with the radial proyection UR, and the vertical plane perpendicular to the azimuth, formed by the Z component and the horizontal proyection UH (Fig. 8a y 8b). These waves travel across the upper mantle, for the considered distances.

Li Phase

They are guided waves of short period, generally with emergent beginnings, transmitted by the lowest part of the continental crust; periods between 0.7 to 1.2 s; average velocity is 3.84±0.0001 km/s, their maximun amplitudes from 0.04 to 0.8 micrometers for shallow focus; apparent velocity for intermediate depth is 3.81±0.01 km/s and their maximum amplitudes from 0.1 to 3.4 micrometers. Particle motion shows predominant movement almost perpendicular to the ray path with some horizontal polarization (Fig. 9a),record is clearer for intermediate focus (Fig. 9b); this phase may be a superposition of higher modes of Love waves.

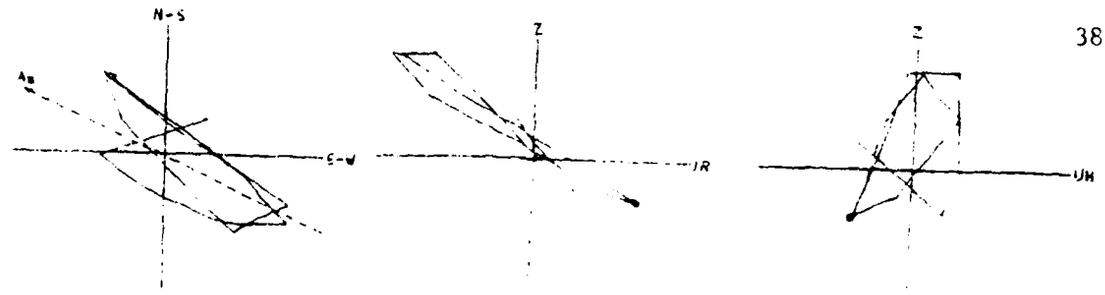

Fig. 8a . Movimiento de partícula Fase P, sismo superficial.

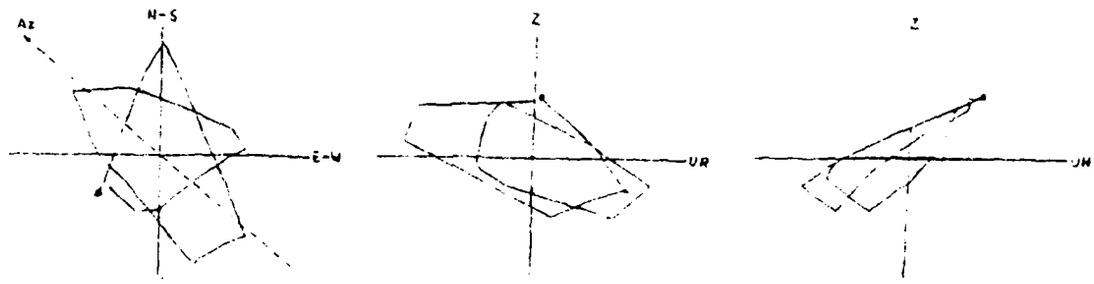

Fig. 8b . Movimiento de partícula Fase P, sismo intermedio.

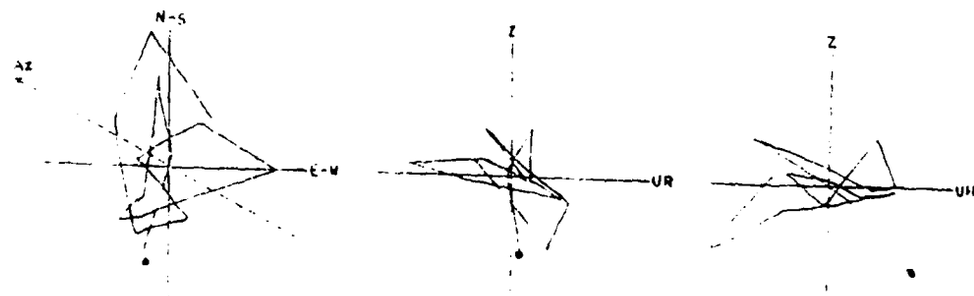

Fig. 9a . Movimiento de partícula Fase S, sismo superficial.

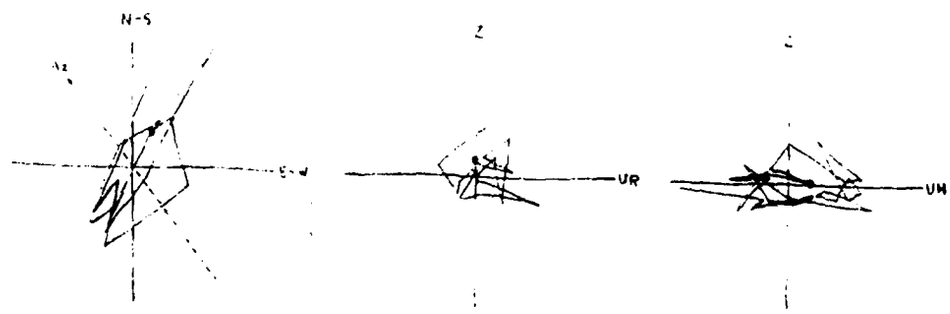

Fig. 9b . Movimiento de partícula Fase S, sismo intermedio.

Lg Phase

They are guided waves of short period, generally with emergent beginnings ; transmitted by the higher part of the continental crust, with periods between 0.6 to 1.5 s; average velocity is 3.54±0.0003 km/s, their maximum amplitudes from 0.02 to 0.9 micrometers; for intermediate focus is 3.53±0.003 km/s and their amplitudes from 0.09 to 2 micrometers. Their particle motions are perpendiculars to the ray path, with a strong horizontal polarization (Fig. 10a), major in the intermediates (Fig. 10b).

Rg Phase

They are guided waves of short period, generally with emergent beinnings; interfered by the previous phases coda; it is transmitted by the higher part of the continental crust; predominant periods between 0.6 to 1.4 s; average velocity is 3.17±0.001 km/s, their maximum amplitudes from 0.03 to 0.2 micrometers for shallow focus; for intermediate focus velocity is 3.15±0.005 km/s and their maximum amplitudes between 0.04 to 1.1 micrometers. Particle motion is parallel to the ray path (Figs. 11a and 11b), being a composition of much higher modes of Rayleigh phase.

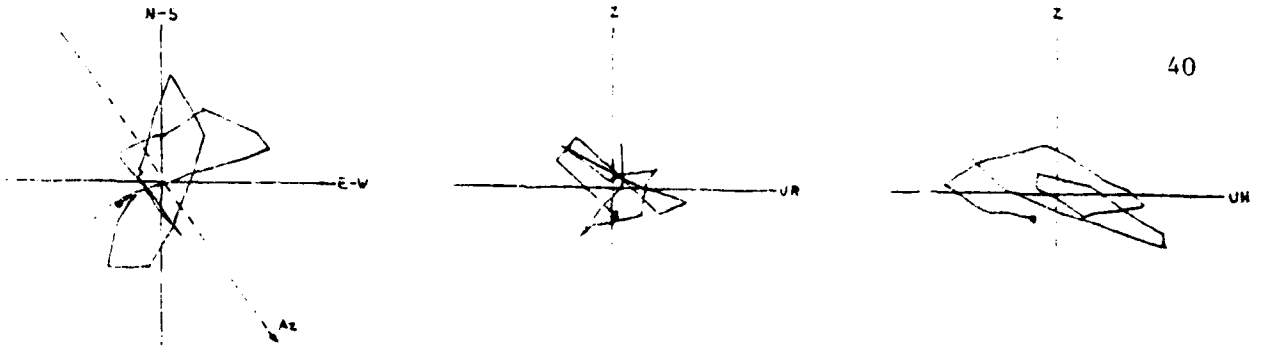

Fig. 10a . Movimiento de partícula Fase Lg, sismo superficial.

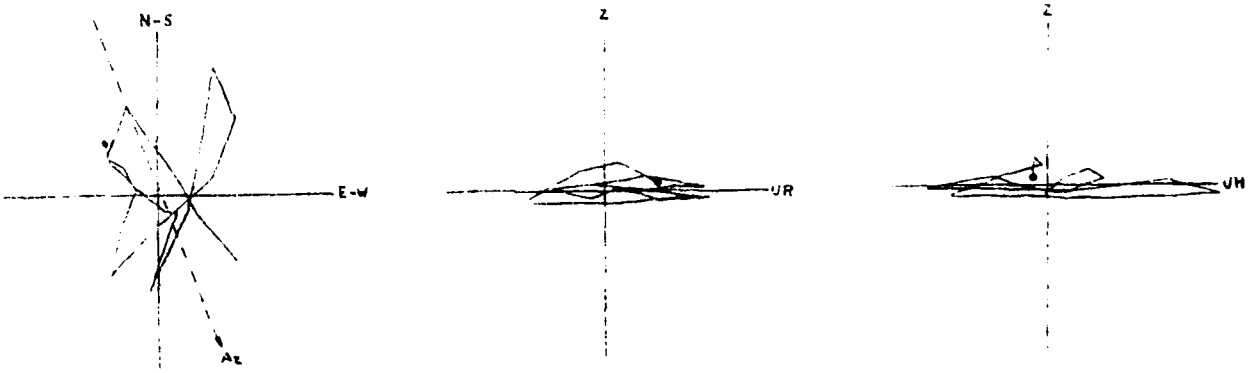

Fig. 10b . Movimiento de partícula Fase Lg, sismo intermedio.

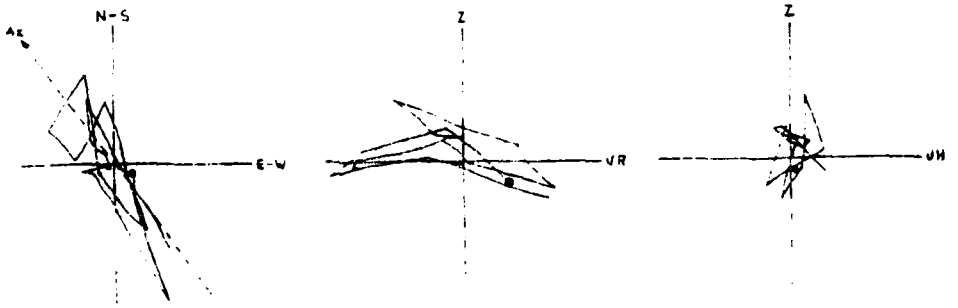

Fig. 11a . Movimiento de partícula Fase Rg, sismo superficial.

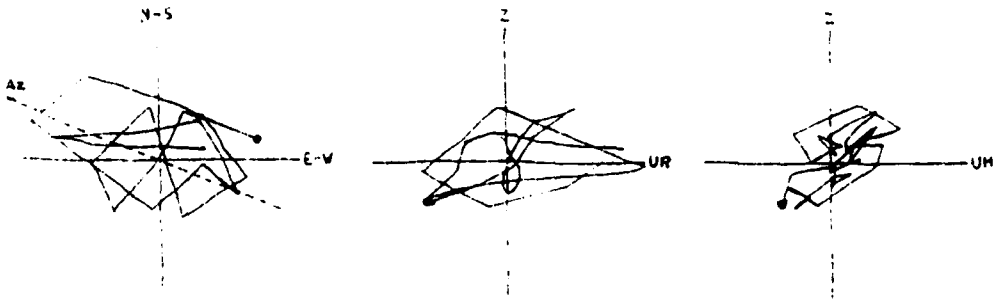

Fig. 11b . Movimiento de partícula Fase Rg, sismo intermedio.

ANELASTIC ATTENUATION COEFFICIENT

In order to estimate the anelastic attenuation coeficients (γ), first the amplitudes read for each zone and for different depth levels were normalizated, to mb=5.0. Real values were superposed to the theorical curves (Fig. 3) obtaining γ the values (in 1/degrees) for each considered phase.

The Figs. 12a to 18a show the γ values for each phase, zone and depth level analysed. The values of period (T) and average γ and their respectives standard deviations are detailed in the Table 2.

QUALITY FACTOR

With the obtained values the formuled (II) was applyed to calculate the apparent Q values for each zone, considering different focal depths.

Plotting fp versus t, was appropopiated through the metod of seismic wave coda form (Herrmann, 1980), that may confirm the Q values calculated by the Nuttli's method (Figs. 19a to 26b).

The computed Q values were plotted on a map to obtain the regions of similar Q value (Figs. 27a to 30b).

Group velocity values (V) and average Q for each zone and by depth levels and their standard desviations are expressed in the Table 2.

TABLE 2

PHASE	ZONE	T (s)	γ (1/degree)	V (km/s)	Q_N	Q_H
P *	1	0.85±0.01		7.71±0.03		
	2	0.80±0.01	0.12±0.004	7.88±0.02	458±1	450
	3	0.90±0.06		7.80±0.05		
	4	0.80±0.04	0.16±0.00007	7.77±0.05	357±10	350
	5	0.90±0.06	0.30 0.005	7.59±0.02	181 12	200
P **	1	0.85±0.02		8.01±0.03		
	2	0.85±0.04	0.12±0.0005	7.96±0.002	447±26	450
	3	0.80±0.02		7.90±0.04		
	5	0.80±0.007	0.30±0.0008	7.65±0.006	192±11	200
	6	0.95±0.02		6.98±0.25		
Li *	1	1.0±0.007		3.84±0.003		
	2	1.0	0.12±0.00005	3.84±0.003	753±1	750
	3	1.0		3.84±0.005		
	4	0.95 0.01		3.84 0.007		
	5	0.90±0.02	0.16±0.01	3.84±0.006	601±9	600
Li **	1	0.90±0.01		3.83±0.004		
	2	1.0	0.12±0.00008	3.81±0.004	794±5	780
	3	1.0		3.81±0.001		
	4	1.0		3.84		
	5	0.9±0.06	0.16±0.0002	3.77±0.005	630±23	600
	6	1.0		3.73		
Lg *	1	1.0±0.03		3.54±0.002		
	2	1.2±0.24	0.15±0.00004	3.54±0.004	614±8	600
	3	1.0±0.06		3.54±0.003		
	4	1.0±0.06		3.54±0.001		
	5	1.0±0.03	0.20±0.006	3.54±0.003	480±5	480
Lg **	1	1.0		3.54±0.001		
	2	1.0±0.03	0.15±0.00003	3.54±0.004	630±5	650
	3	0.90±0.04		3.54±0.002		
	5	1.0	0.20±0.0004	3.52±0.003	512±6	500
	6	1.0±0.07	0.23±0.06	3.48±0.07	420±10	400
Rg *	1	1.0±0.03		3.18±0.004		
	2	1.0±0.01	0.16±0.003	3.18±0.004	664±4	650
	3	1.1±0.03		3.18±0.006		
	4	1.0		3.18±0.003		
	5	1.05±0.01	0.20±0.002	3.17±0.004	529±19	500
	6	1.10±0.07		3.17±0.002		
Rg **	1	1.0±0.06		3.17±0.002		
	2	1.0±0.006	0.17±0.002	3.17±0.001	652±23	650
	3	1.0±0.10		3.16±0.003		
	4	1.0±0.06		3.10±0.01		
	5	1.1±0.04	0.20±0.0008	3.11±0.004	534±6	500
	6	1.0±0.03		3.11±0.009		

* shallow focus ** intermediate focus

N Nuttli's method (1973) H Herrmann's method (1980)

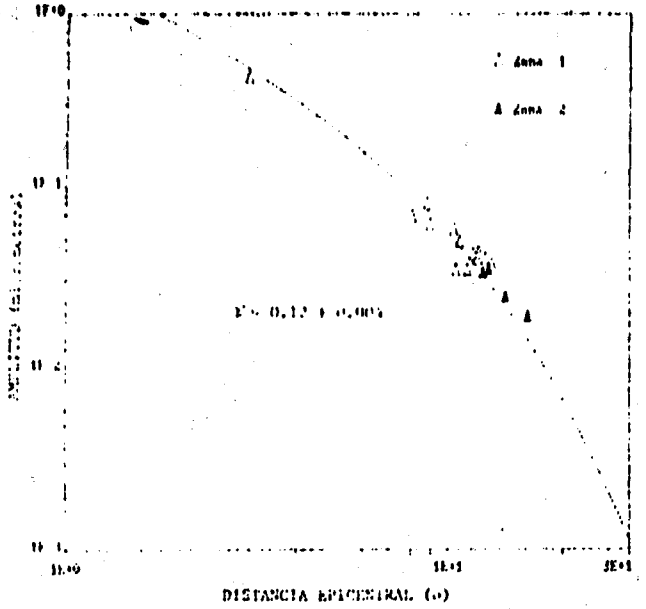

Fig. 12a. Valor de λ Fase P, sismos superficiales.

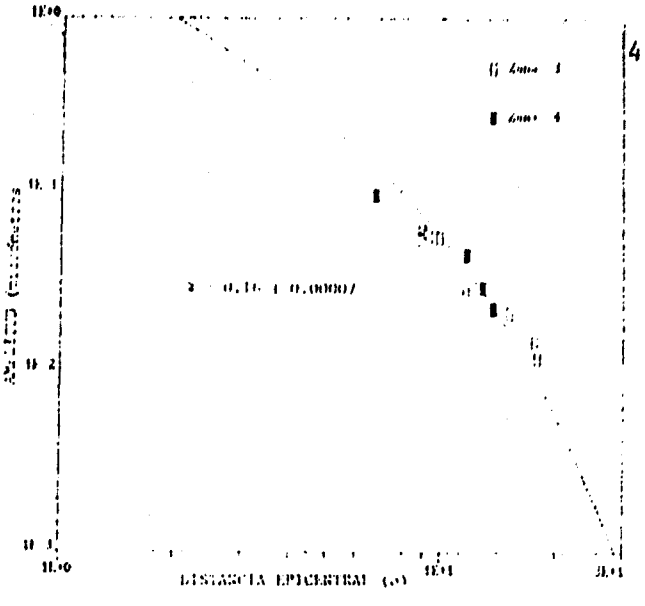

Fig. 12b. Valor de λ Fase P, sismos superficiales.

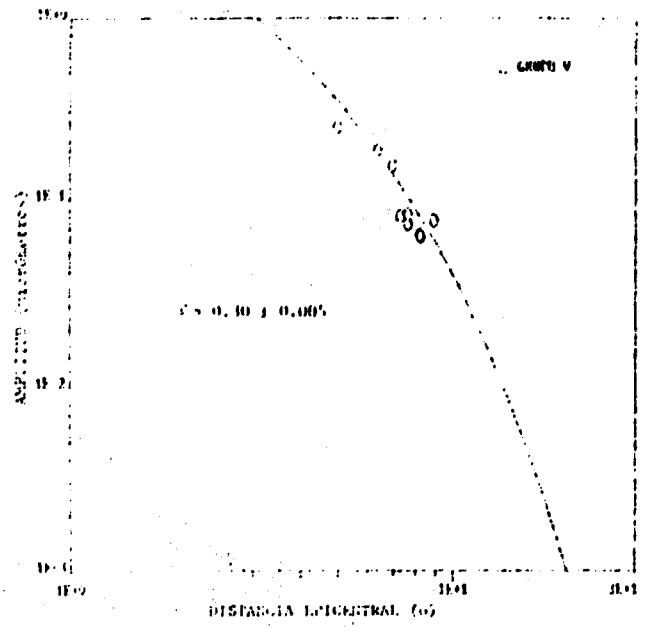

Fig. 12c. Valor de λ Fase P, sismos superficiales

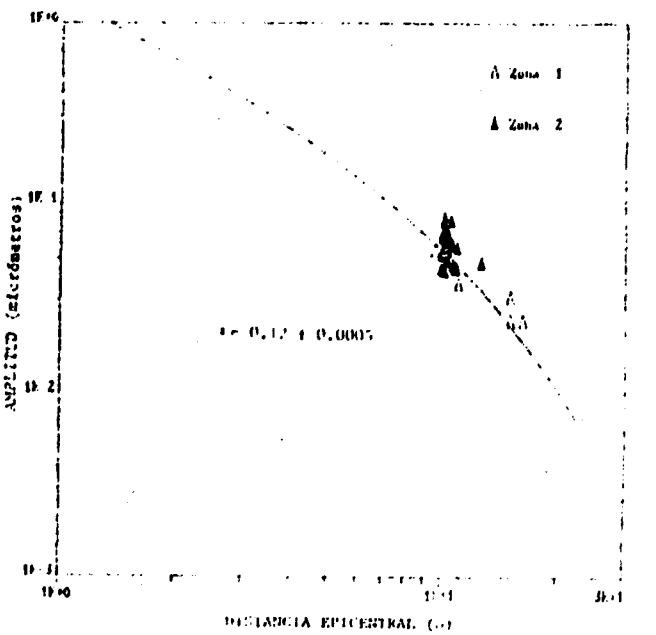

Fig. 13a. Valor de λ Fase P, sismos intermedios

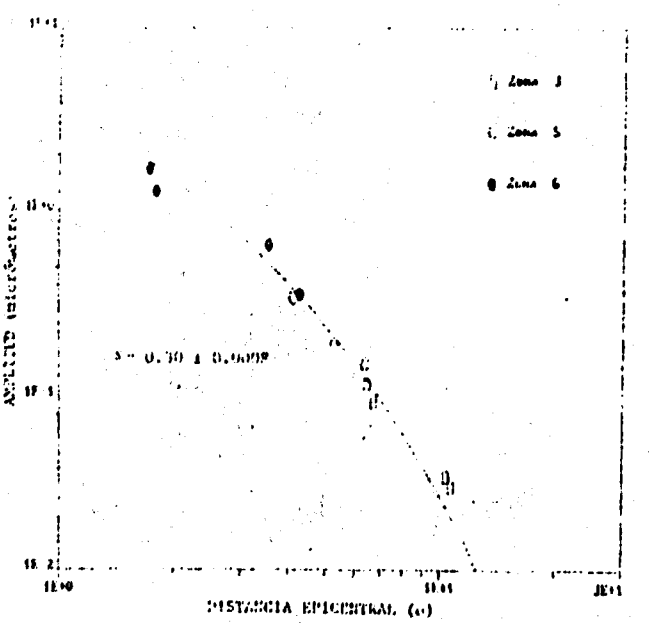

Fig. 13b. Valor de λ Fase P, sismos intermedios.

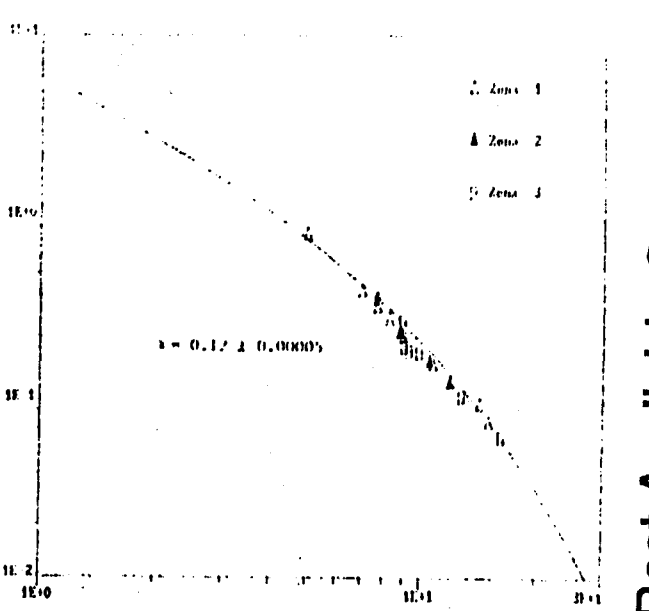

Fig. 14a. Valor de λ Fase Lf, sismos superficiales

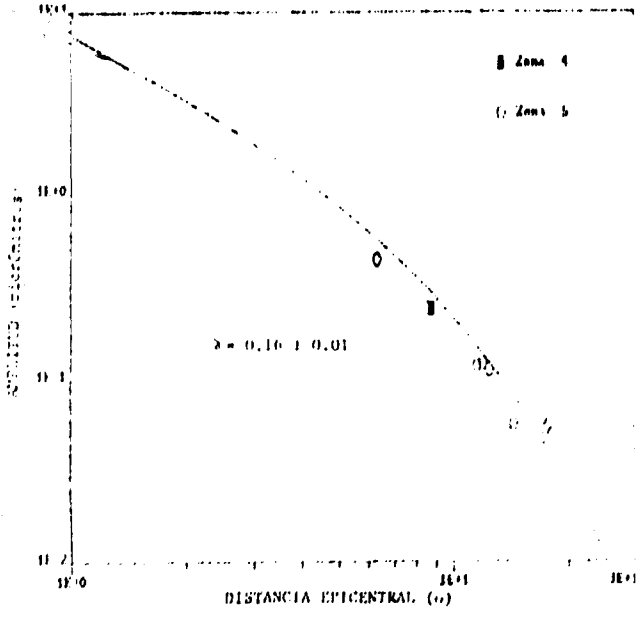

Fig. 14b. Valor de γ Fase Lf, sismos superficiales.

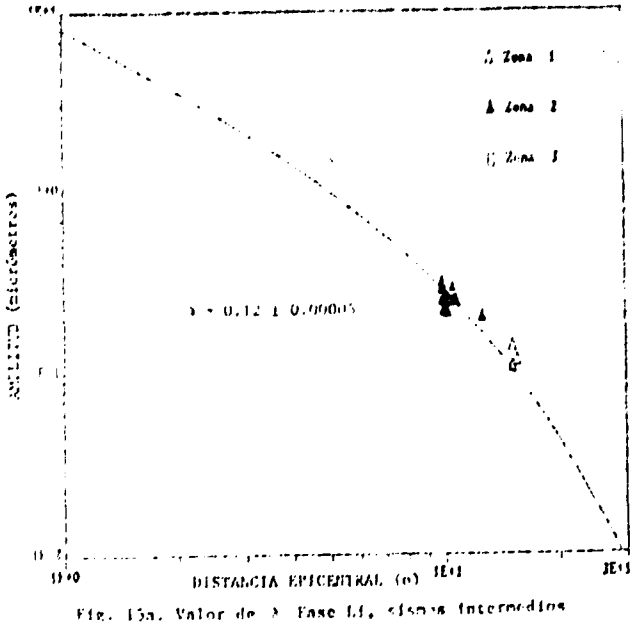

Fig. 15a. Valor de γ Fase Lf, sismos intermedios

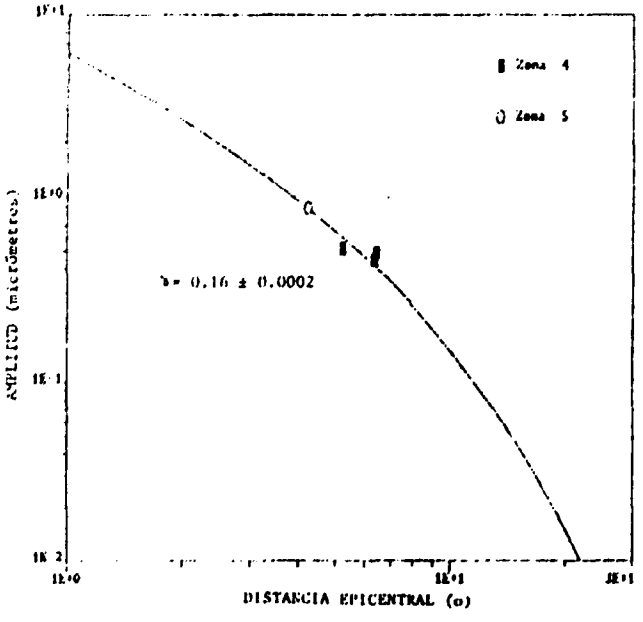

Fig. 15b. Valor de γ Fase Lf, sismos intermedios

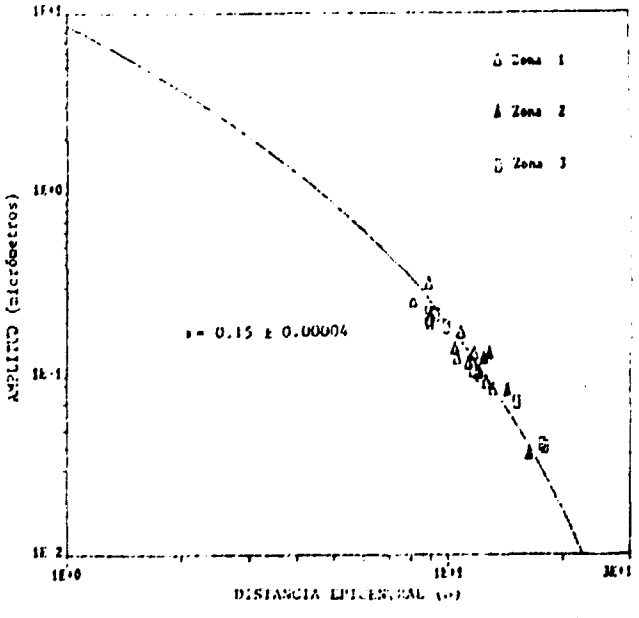

Fig. 16a. Valor de γ Fase Lg, sismos superficiales

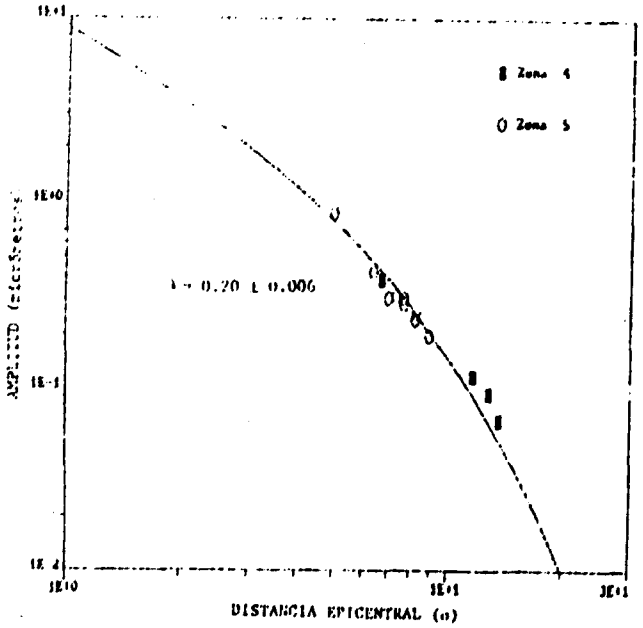

Fig. 16b. Valor de γ Fase Lg, sismos superficiales.

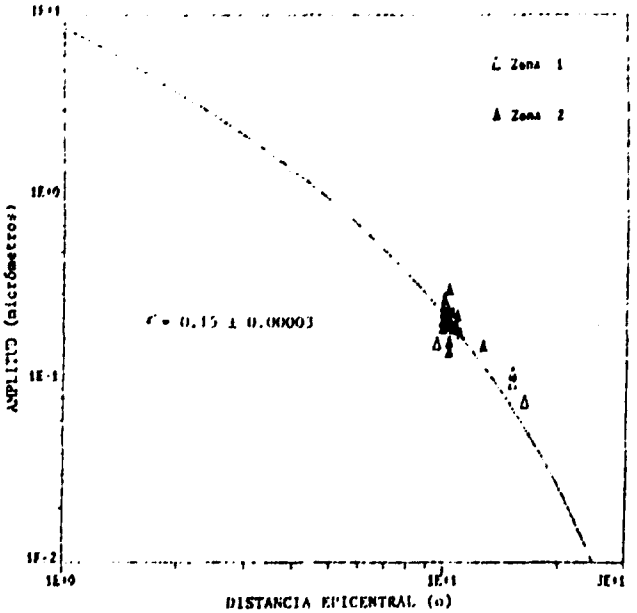

Fig. 17a. Valor de γ Fase Lg, sismos intermedios.

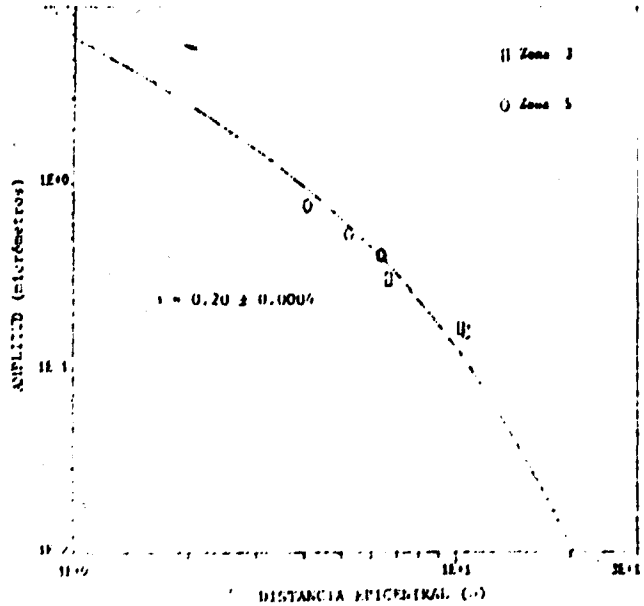

Fig. 17b. Valor de γ Fase Lg, sismos intermedios.

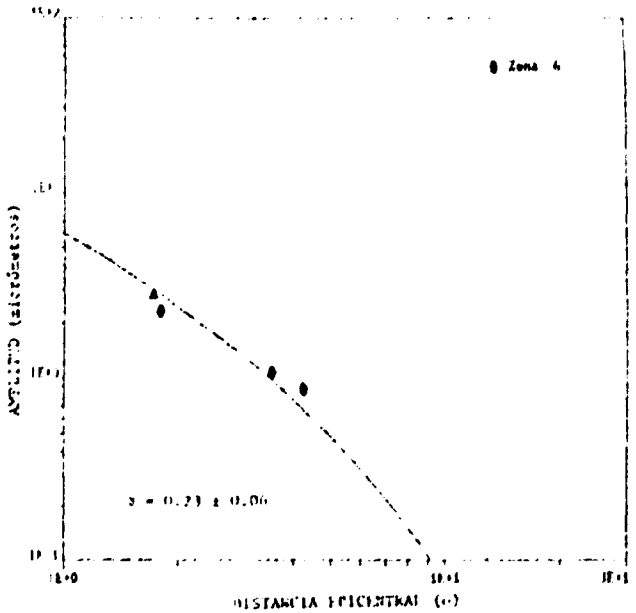

Fig. 17c. Valor de γ Fase Lg, sismos intermedios.

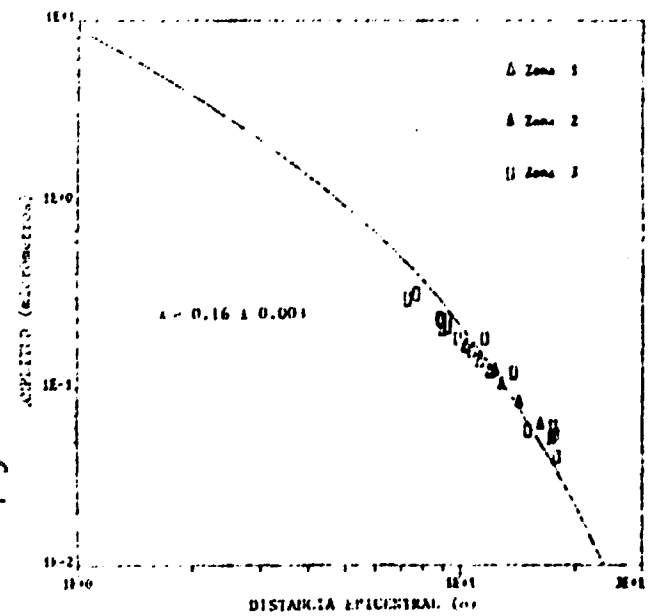

Fig. 18a. Valor de γ Fase Rg, sismos superficiales.

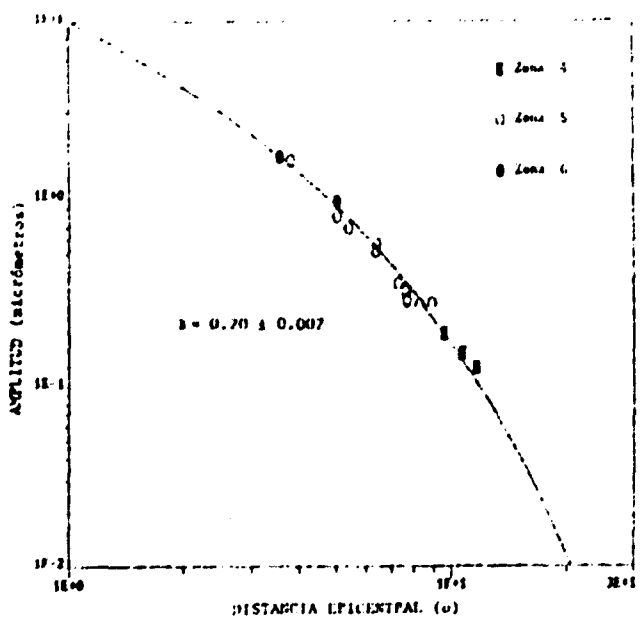

Fig. 18b. Valor de γ Fase Rg, sismos superficiales.

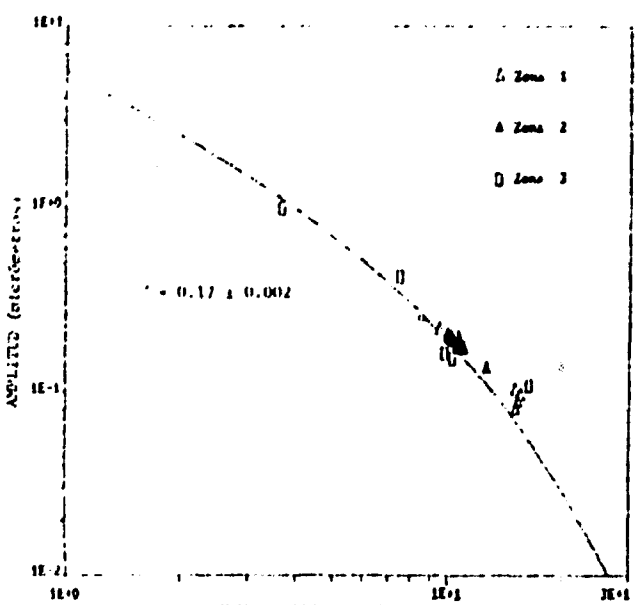

Fig. 19a. Valor de γ Fase Rg, sismos intermedios.

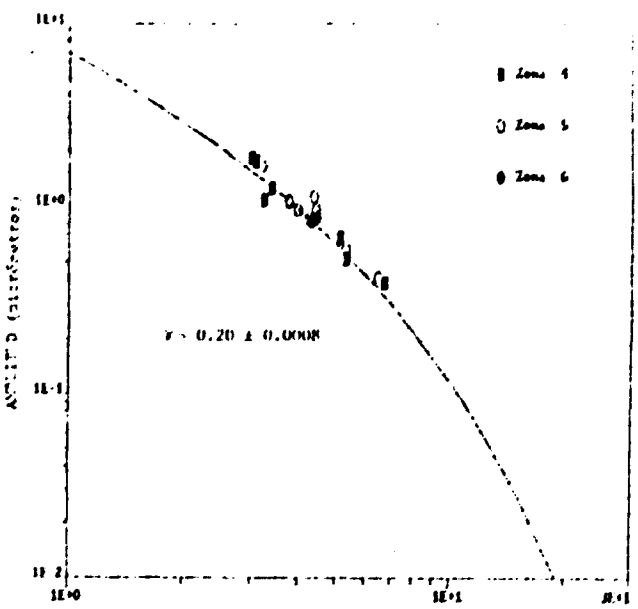

Fig. 19b. Valor de γ Fase Rg, sismos intermedios.

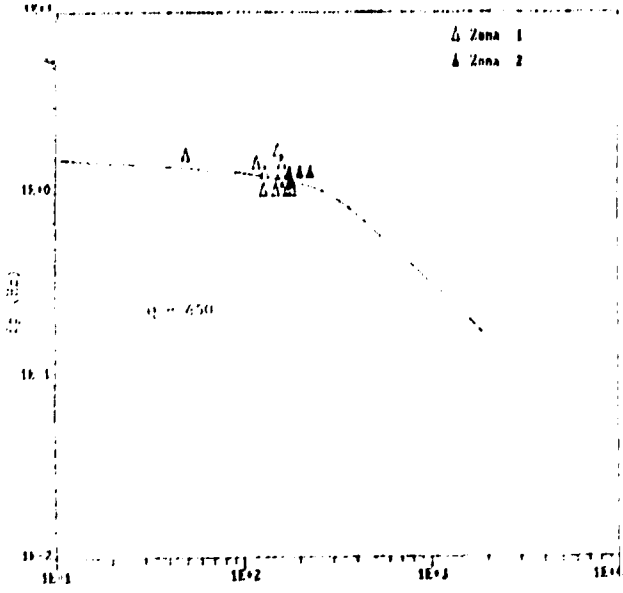

Fig. 20a. Valor de Q Fase P, sismos superficiales

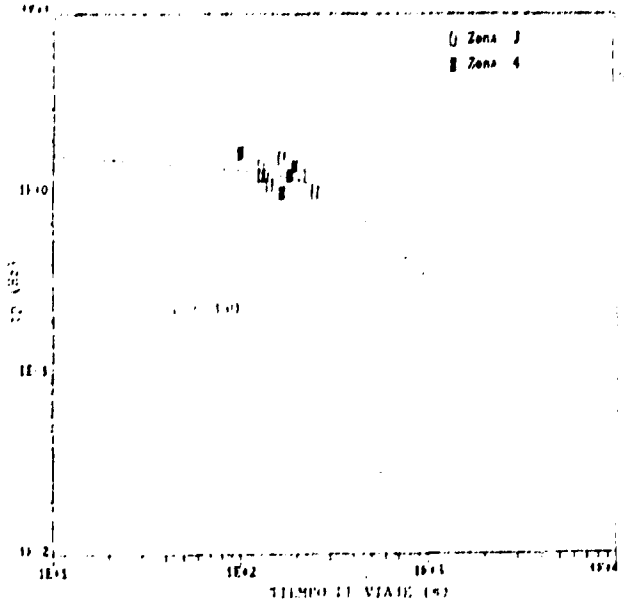

Fig. 20b. Valor de Q Fase P, sismos superficiales

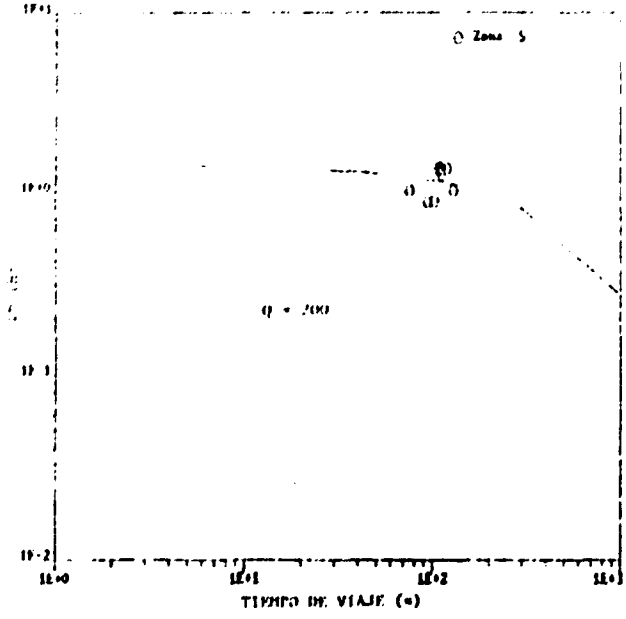

Fig. 20c. Valor de Q Fase P, sismos superficiales

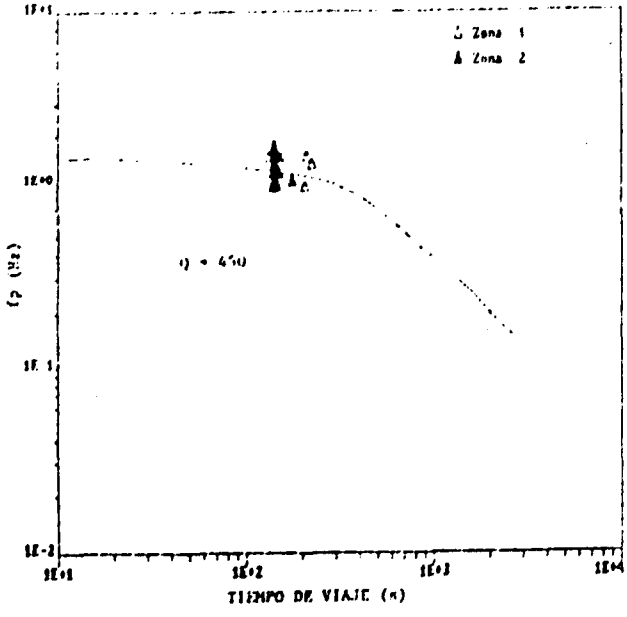

Fig. 21a. Valor de Q Fase P, sismos intermedios

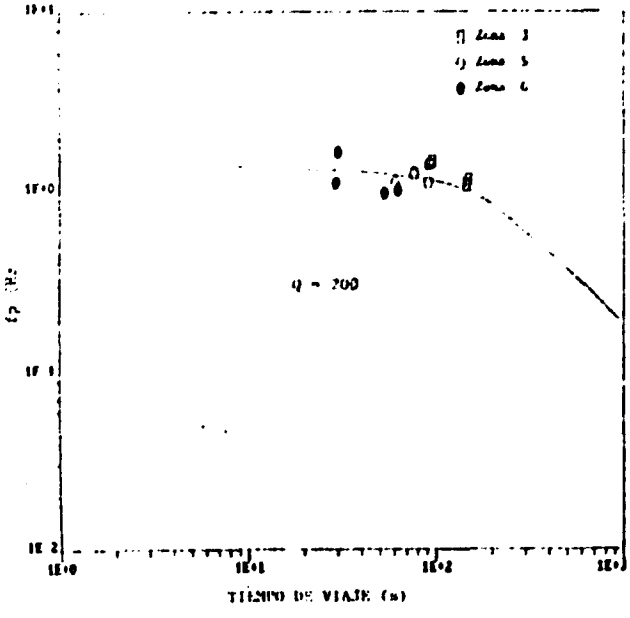

Fig. 21b. Valor de Q Fase P, sismos intermedios

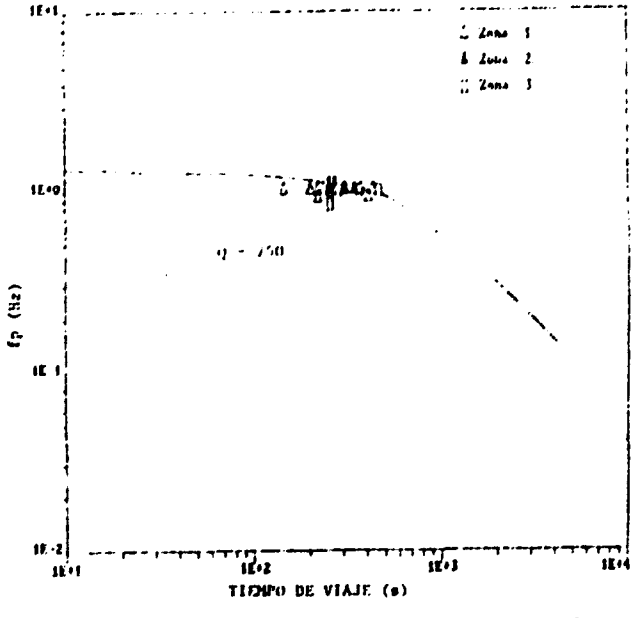

Fig. 22a. Valor de Q Fase L.I. sismos superficiales.

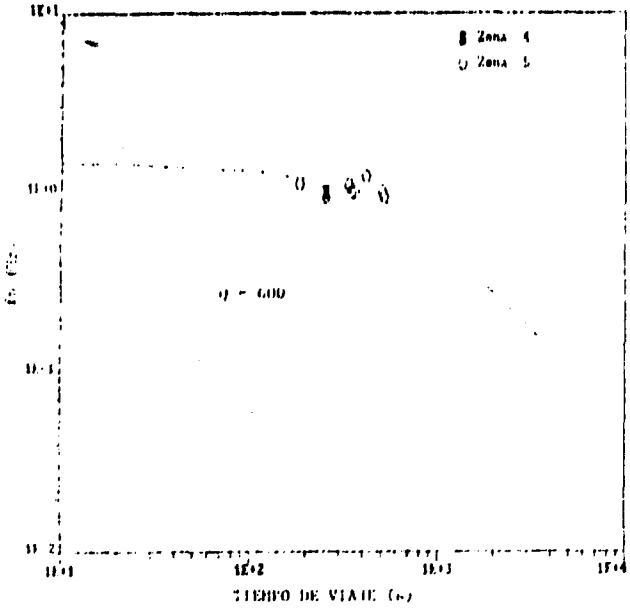

Fig. 22b. Valor de Q Fase Lt, sismos superficiales.

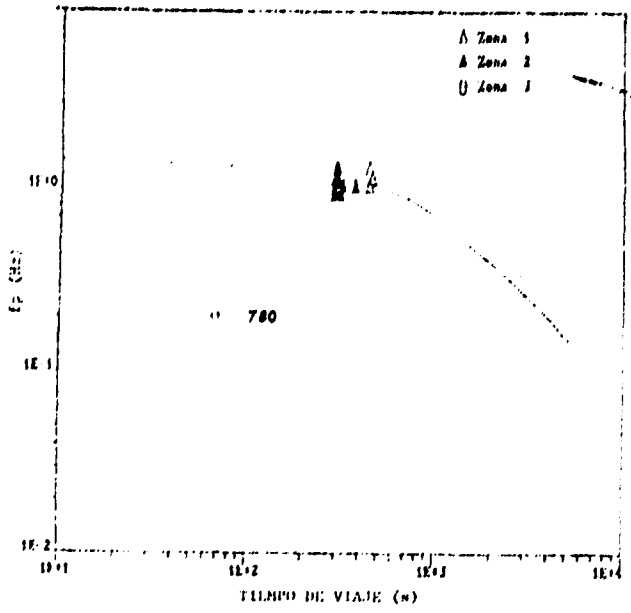

Fig. 23a. Valor de Q Fase Lt, sismos intermedios

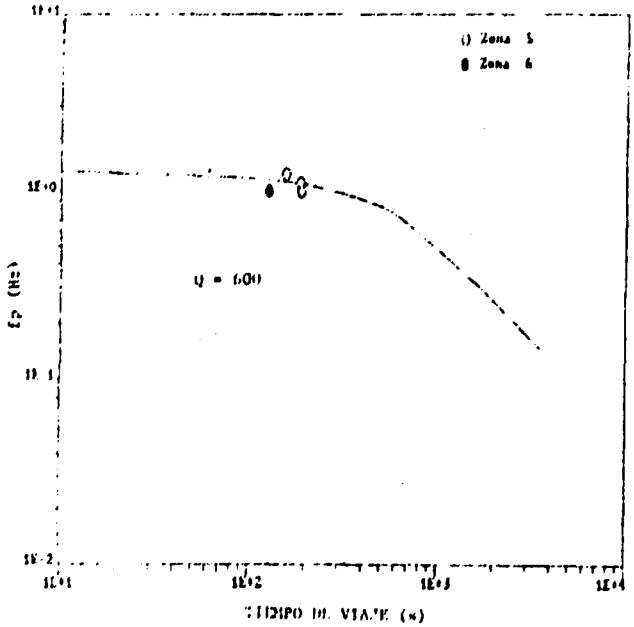

Fig. 23b. Valor de Q Fase Lt, sismos intermedios

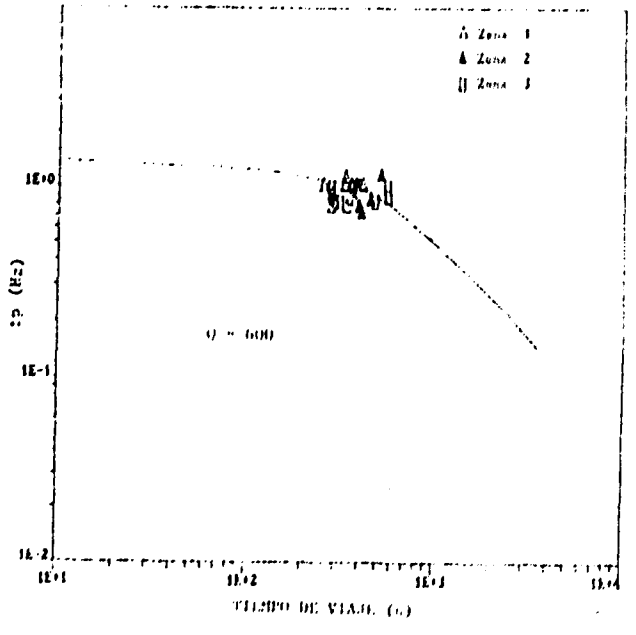

Fig. 24a. Valor de Q Fase Lg, sismos superficiales

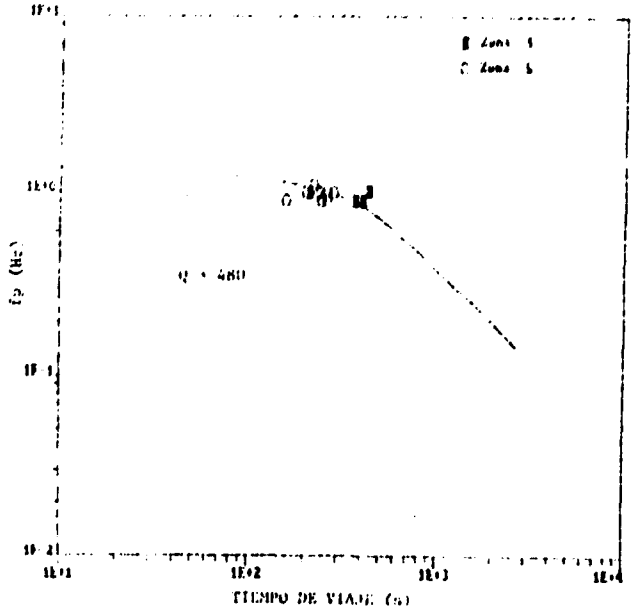

Fig. 24b. Valor de Q Fase Lg, sismos superficiales.

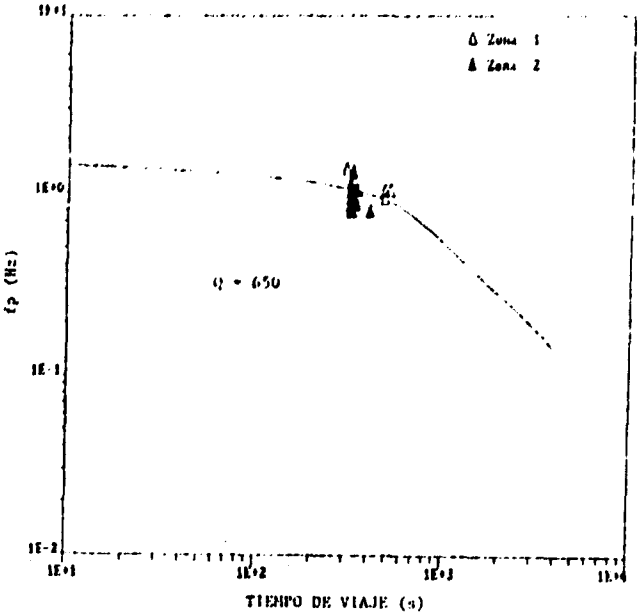

Fig. 25a. Valor de Q Fase Lg, sismos intermedios.

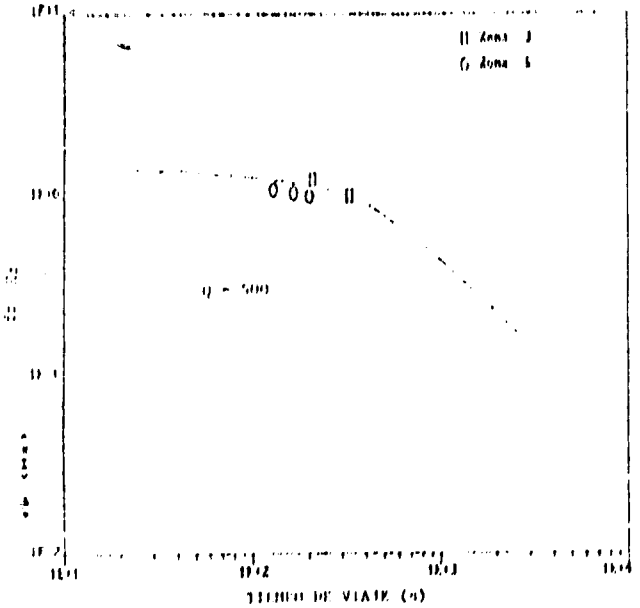

Fig. 25b. Valor de Q Fase Lg, algunos intermedios

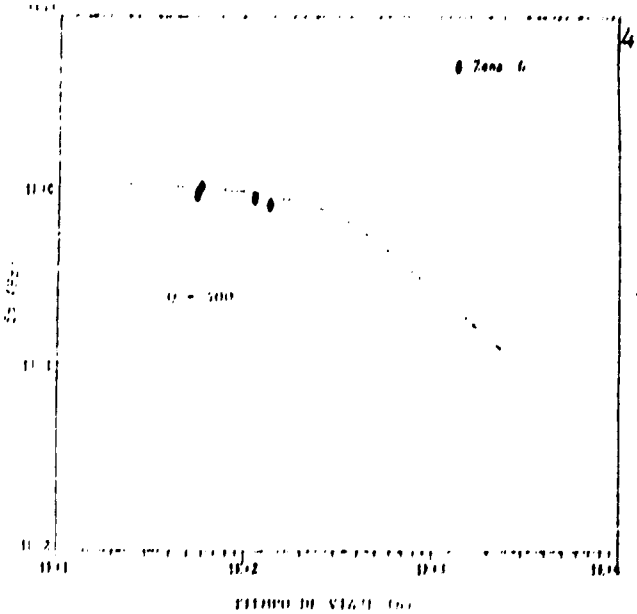

Fig. 25c. Valor de Q Fase Lg, algunos intermedios

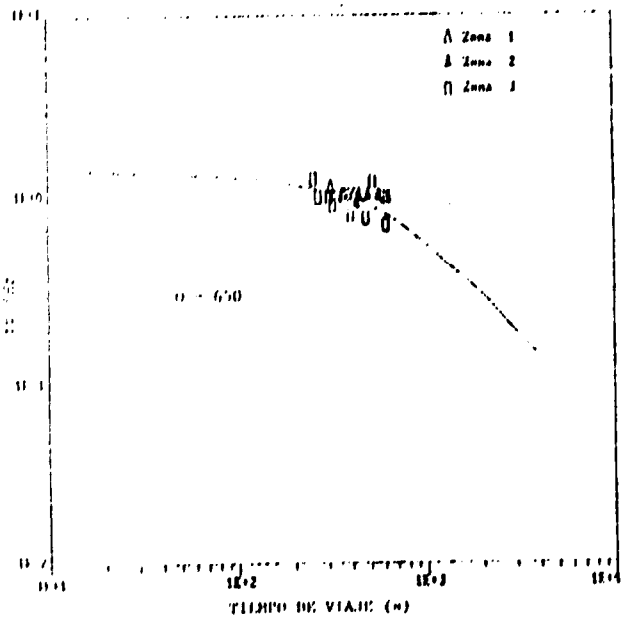

Fig. 26a. Valor de Q Fase Rg, algunos superficiales.

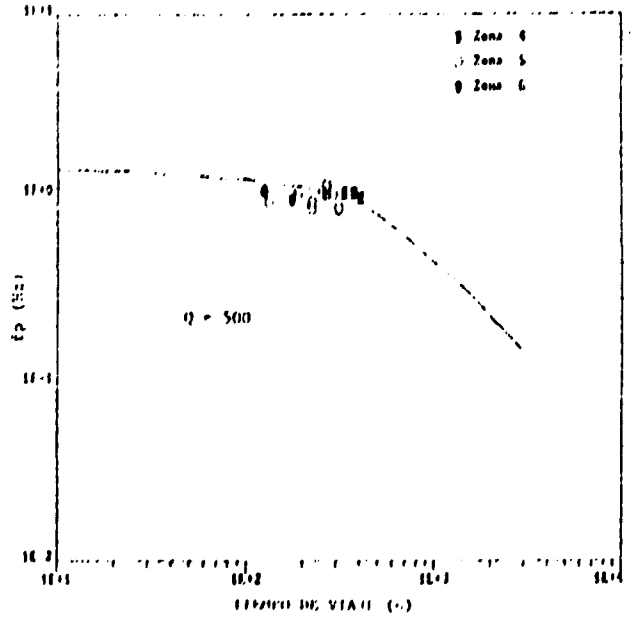

Fig. 26b. Valor de Q Fase Rg, algunos superficiales.

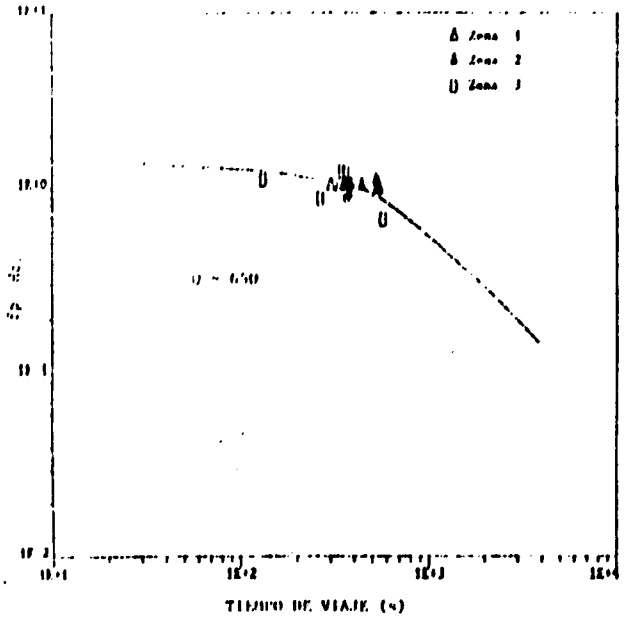

Fig. 27a. Valor de Q Fase Rg, algunos intermedios.

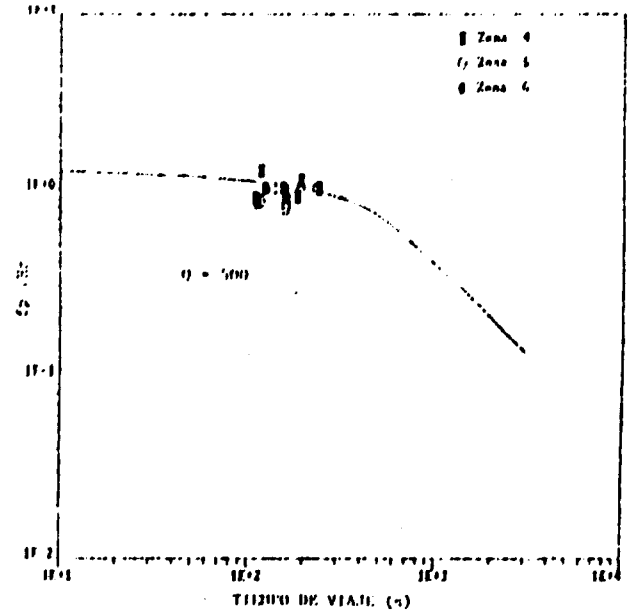

Fig. 27b. Valor de Q Fase Rg, algunos intermedios.

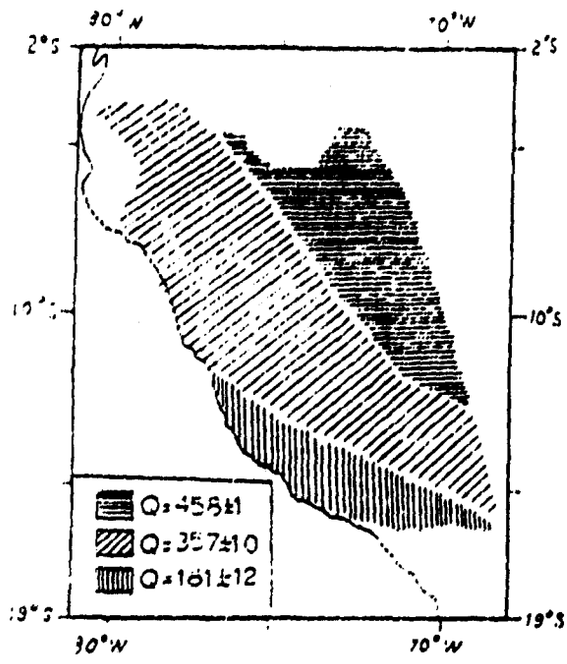

Fig. 28a. Regiones de Q Fase P, focos superficiales.

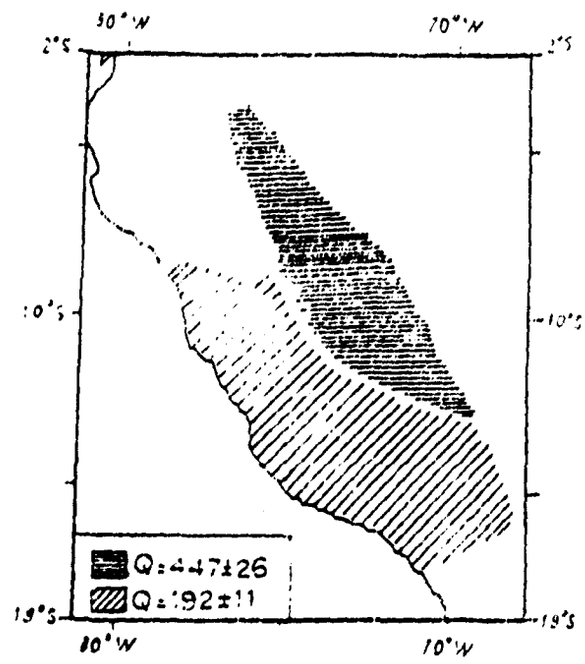

Fig. 28b. Regiones de Q Fase P, focos intermedios.

Fig. 29a. Regiones de Q Fase Ll, focos superficiales.

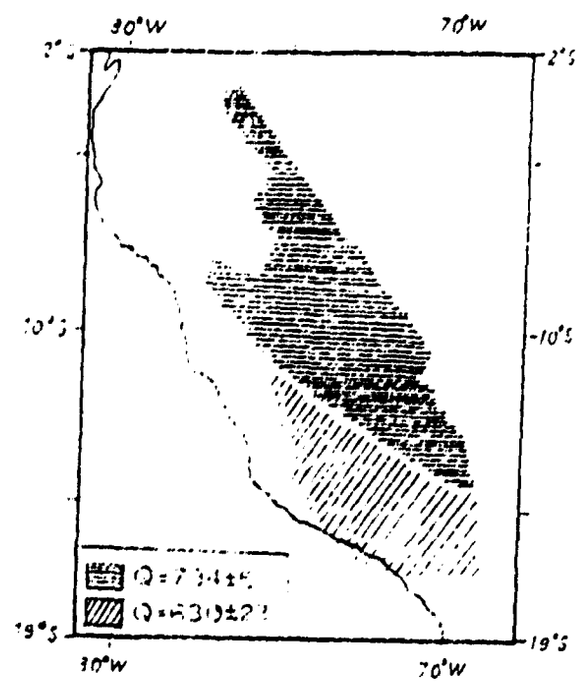

Fig. 29b. Regiones de Q Fase Ll, focos intermedios.

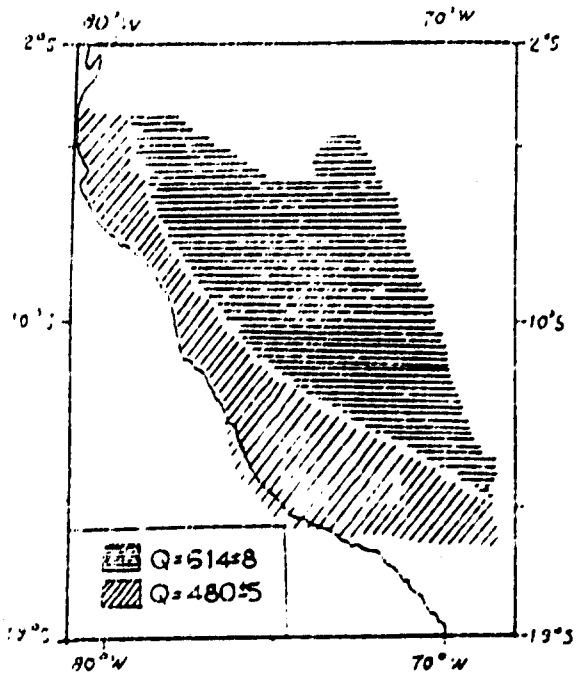

Fig. 30a. Regiones de Q Fase Lg, focos superficiales.

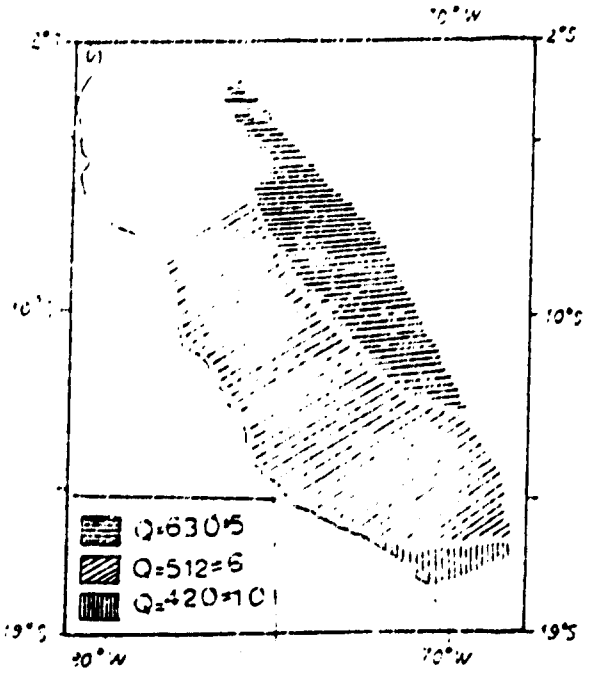

Fig. 30b. Regiones de Q Fase Lg, focos intermedios.

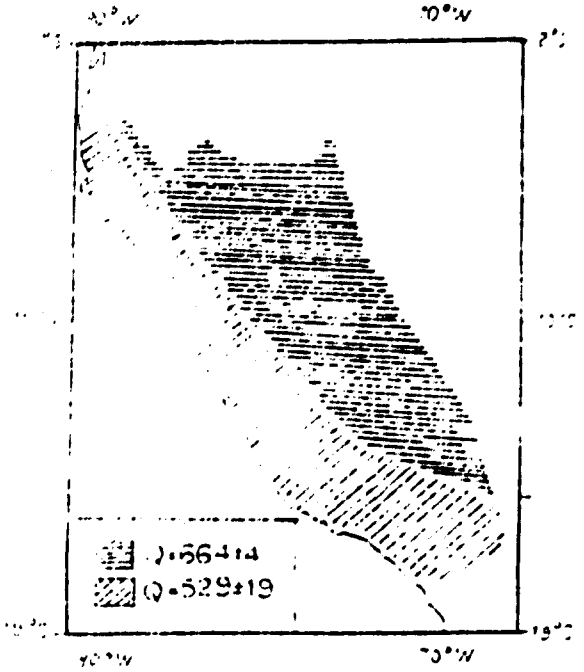

Fig. 31a. Regiones de Q Fase Rg, focos superficiales.

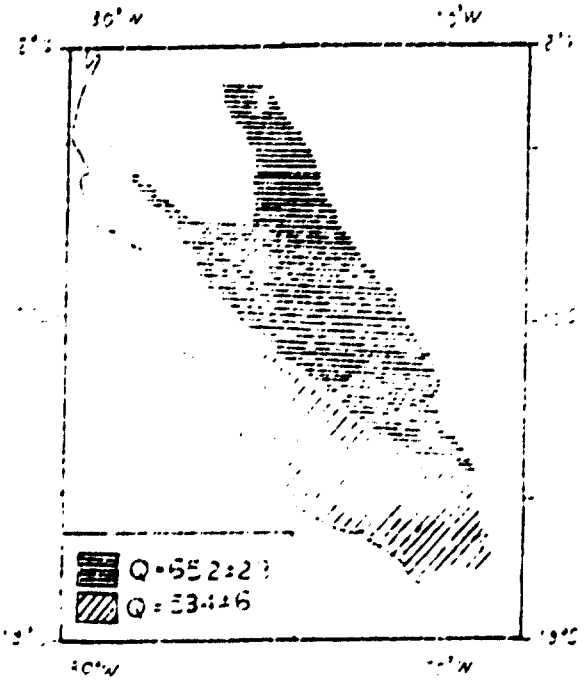

Fig. 31b. Regiones de Q Fase Rg, focos intermedios.

INTERPRETATION

Comparing the group velocity calculated for the P waves with the regional velocity model (Fig. 32) (Ayala, 1991), we notice that these waves are transmitted through the higher mantle, including its low velocity layer. For shallow focus three regions are distinguished in relation to Q, the first one with lowest attenuation corresponds to Brazilian Shield and Subandean zone with the highest values of Q; the second zone corresponds to the Cordillera, with a larger attenuation, caused without doubt by the structure complexity, and the third sone for the Altiplano and active part of Western Cordillera. For intermediate focus two regions are distinguised with an increased attenuation towards the West; the first for the Brazilian Shield, Subandean and Eastern Cordillera and the second for the Altiplano and Western Cordillera.

The Q calculated values of Table 2 correspond to an average of the whole trajectory; analysing these values as function of the epicentral distance, a tend to a little increase of Q with the distance appears, that will be studied later. For more distant events there is a deeper penetration of the P waves corresponding to increased density and homogeneity of mantle material.

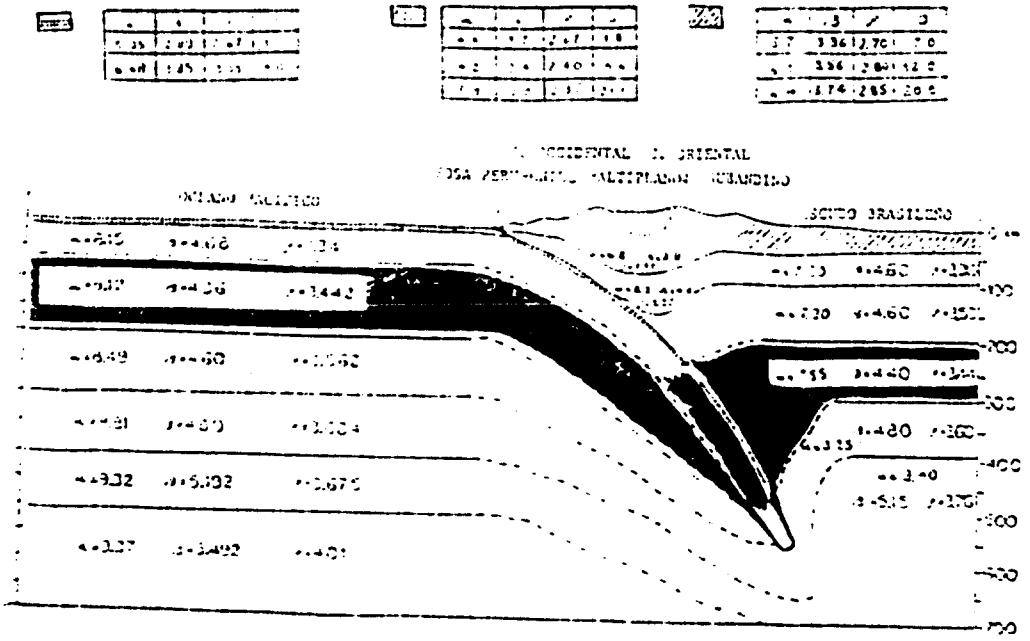

Fig. 32. Modelo generalizado de velocidad para la corteza y manto superior, entre Perú y Bolivia (Ayala, 1991).

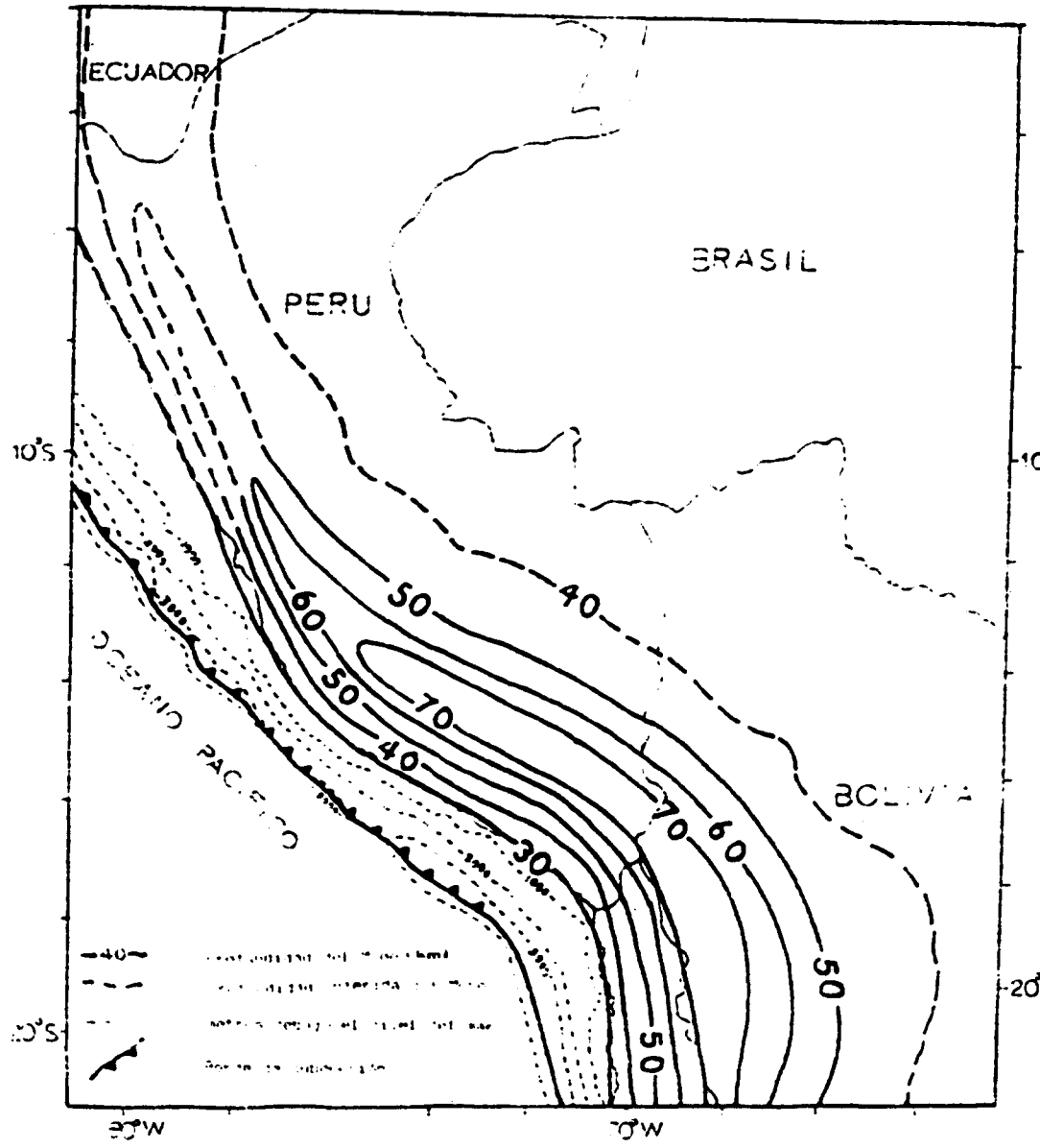

Fig. 33. Mapa mostrando la profundidad de la discontinuidad de Mohorovicic (mod. de James, 1971).

The Fig. 33 shows the depth variation of the Mohorovicic discontinuity between Peru and Bolivia (modified from James, 1971), the maximun thickness of the crust below the central Andes is 70 km (Fernández, 1968; James, 1971 and Molina, 1977), it diminishes eastwards until 40 km, to become constant with a thickness of 39 km for the Brazilian Shield region (Oblitas, 1972); westwards the thickness of oceanic crust in the Nazca plate is 5 kilometers (Guzmán, 1972).

Two cases of guided waves; shallow focus, two regions according to Q values, may be distinguished concerning attenuation is small in the shield region, it increases westwards beneath the Cordillera.

For intermediate foci there is a better resolution, possibly because the attenuating effect of the sedimentary package of the continental crust is lesser; studyng the quality factor values, we can discriminate two regions and also three for Lg; noticing a larger Q value (minor attenuation) for the Brazilian Shield and Shield-Cordillera border (Subandean); Q diminishes in the Eastern Cordillera (larger attenuation), and much more in the Altiplano and Western Cordillera; these vertical and lateral changes in the structure appear trough Q changes; sea it in a preliminary model of Q for the continental crust between Peru and Bolivia (Fig. 34) to show the complex structure below the Central Andes.

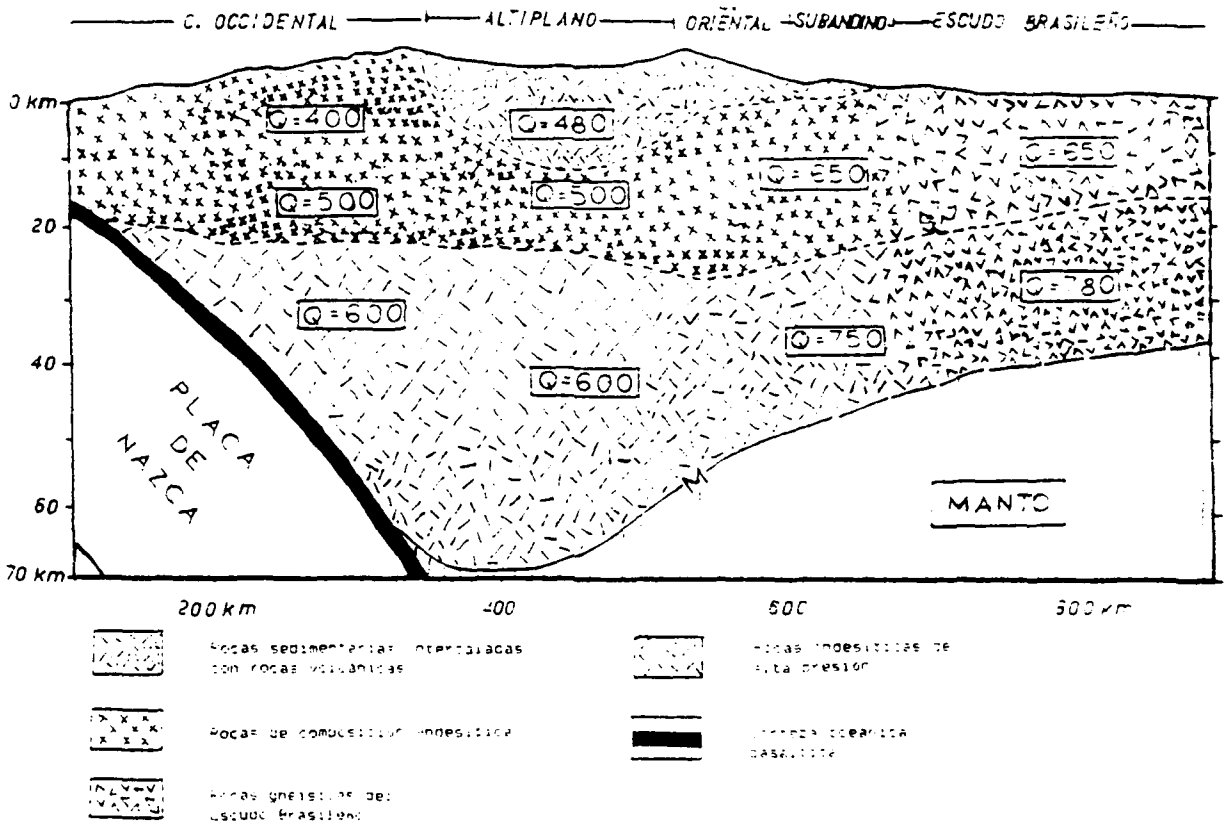

Fig. 34. Preliminar model of Q for the continental crust between Peru and Bolivia (according to James, 1976).

The attenuation study of guided waves of short period and intermediate focus allows to discriminate better different structures.

REFERENCES

Part I

Alcócer, I. J., 1989, Estudio de las ondas Lg registradas en la estación LPB a través de la Cordillera de los Andes, Tesis de Grado, UMSA, La Paz, Bolivia.

Ayala, R.R., 1989, Estudio de las ondas Lg registradas en la estación de LPB a través del Escudo, Tesis de Grado, UMSA, La Paz, Bolivia.

Bath, M., 1956, A continental chammel wave guided by the intermediate layer in the crust, Geofis. pura Appl., 38, 19-31.

Burdick,L. J., and D.V. Helmberger, 1977, The upper mantle P velocity structure of the Western United States, J. Geophys Res., 83, 1699-1712.

Couch, R. R., Whitsett, B. Huehn, L. Briceño-Guarupe, 1981, Structures of the continental margin of Peru and Chile, Geol.Soc. of Am, Memoir 154.

Deza, M. A., 1972, Zonas de transición Sismotectónica en Sudamérica, estudio preliminar de la zona de transición en el Perú, Simposio sobre los resultados de investigaciones del manto superior con enfasis en America Latina, Comité del Manto Superior, Buenos Aires, Argentina, vol. II.

Dziewonski, A. M., 1984, Mapping the lower mantle: determination of lateral heterogeneity in P wave velocity up to degree order 6, J. Geophys Res., 89, 5929-5952.

Fahmi, K. J., 1964, On the possible existence of the 20° discontinuity beneath South America, Scientific Research Council Baghdad Iraq

Fernandez, L.M., 1965, The determination of crustal thickness from the spectrum of P waves, Scientific Report Nº 13 AFCRL, 67-76.

Helmberger, D. V., 1973, On the Structure of the low velocity zone, Geophys J. R. astr. Soc.,34, 251-263.

James, E.D., 1971, Plate tectonic model for the evolution of the Central Andes, Bull. Geol. Soc. Am., vol. 82, 3325-3346.

James, E. D., 1990, Structure of the continental lithosphere and subducting Plate beneath East-Central Peru, EOS, Transactions American Union, vol 71 Nº43, 1463.

Johnson, L.R., 1967, Array measurements of P velocity in the upper mantle, J. Geophys Res.,72, 6309-6325.

Johnson, L. R., 1969, Array measurements of P velocity in the lower mantle, Bull. Seism. Soc. Am., 59,973-1008.

Jordan, T. H. and N. L. Frazer, 1975, Crustal and upper mantle from SP phases, J. Geophys Res., 80, 1504-1513.

Jordan, T. H., 1981, Global tectonic regionalization for seismological data analysis, Bull. Seism. Am., 71, 1131-1141.

Jordan, H.T., J.S. Revenaugh and S.L. Gee, 1989, Investigation of Eurasian seismic sources and upper mantle structure, Final Report: Geophysics Laboratory AFSC Massachusetts, USA. GL-TR-89-0143, ADA211806

Julian, B.R. and D.L. Anderson ,1968, Travel time, Apparent velocities and amplitudes of body waves, Bull. Seism. Soc. Am., 58, 339-366.

Lay, T., T. C. Wallace and D. V. Helmberger, 1984, The effects of tectonic release on short-period P waves from NTS explotions, Geophys J. R. astr. Am., 74, 819-842.

Lehmann, I., 1970, The 400 Km discontinuity, Geophys J. astr. Soc.,21,359-372.

Meissner, R., F. Fluch, F. Stibane and E. Berg, 1976, Dynamics of the active plate boundary in South-West Colombia according to recent geophysical meassurements, Tectonopfysics, vol.35,115-136.

Minaya,R. E., 1978, Relaciones físico-quimicas de la Placa de Nazca el emplazamiento de yacimientos minerales, Tesis de grado, UMSA, La Paz, Bolivia.

Nuttli, O., 1986, Yield estimation of Nevada test site explosions obtained from seismic Lg waves, J. Geophys Res., 91, 2137-2151.

Payo Subiza, G., 1974, Estudio sobre las ondas superficiales Lg, Rg y Li en los registros del Observatotio de Toledo, Revista de Geofísica, vol 5, Nº 75, 227-247.

Porth, R., M. Schmitz, G. Schwarz, S. Strunk and P. Wigger, Berlin: Data Compilations along two sections of the Southern Central Andes, Molility of active Continental Margins, FU, TU, Berlin, Federal Republic of Germany.

Press, F. and M. Ewing, 1952, Two slow surface wave across North America, Bull. Seism. Soc. Am., 42, 219-228.

Pomeroy, P. and W. Cheng, 1980, Regional seismic wave propagation, Final Technical Report, Rondout Associates, INC, Stone Ridge, N.Y.

Valez, B., 1982, Structure de la croute terrestre sous le Huayna Potosi (Bolivie), These, Paris, France.

Wigger, P., P. Giese, W.D. Heinsohn, P. Röwer, M. Schmitz, M. Araneda and J. Viramonte, 1990, Crustal structure of N-Chile and NW-Argentina lower crustal anomalies between coastal range and the Puna, Molility of active Continental Margins, FU, TU, Berlin, Federal Republic of Germany.

REFERENCES

Part II

Ayala, R. (1991). Deriva continental y tectónica de placas con relación a la evolución de la placa de Nazca y los Andes Centrales (en prensa).

Bath, M.(1954). The Elastic waves Lg and Rg along Euroasiatic paths, Arkiv. Geofys. 2, 295-324.

Bath, M. (1956). A continental channel wave guided by the intermediate layer in the crust, Geofis. Pura Appl. 38, 19-31.

Bollinger, G. A. (1979). Attenuation of the Lg Phase and the determination of mb in the Southeastern United States, Bullletin Seismological Society of America, Vol. 69, No. 1, 45-63.

Cabré, R. S.J., E. Minaya, I. Alcócer and R. Ayala (1989). Propagation and attenuation of Lg waves in South America, Final Report, Geophysics Laboratory, Air Force Systems Command, United States Air Force, Hanscom Air Force Base, Massachusetts 01731-5000. GL-TR-89-0273, ADA218853

Cabré, R. S.J., E. Minaya, R. Ayala and C. Mora (1990). Lg and other regional phases in South America, Final Report, Geophysics Laboratory, Air Force Systems Command, United States Air Force, Hanscom Air Force Base, Massachusetts 01731-5000. GL-TR-90-0298, ADA232087

Centro Regional de Sismología, CERESIS (1985). Mapa Neotectónico Preliminar de América del Sur, Proyecto SISRA, Instituto Geográfico Militar de Chile.

Fernández, L. and J. Careaga (1968). The Thickness of the crust in Central United States and La Paz, Bolivia, from the Spectrum of longitudinal Seismic Waves, Bulletin Seismological Society of America, Vol. 58, No. 2, 711-741.

Guzmán, R. J.(1972). Estructura de la Placa de Nazca a partir de la dispersión de ondas superficiales, Tesis de Grado, Universidad de Chile, Santiago, Chile.

Herrmann, R. B. (1980). Q estimates using the coda of local earthquakes, Bulletin Seismological Society of America, Vol. 70, No. 2, 447-468.

James, D. E. (1971). Andean Crustal and Upper Mantle Structure;J.Geophys. Res., Vol. 76, Number 14, 3246-3271.

James, D. E. (1976). Evolución de los Andes Centrales, Deriva Continental y Tectónica de Placas, Selecciones de Scientific American, H. Blume, Madrid, España.

Jeffreys, A., J. R. Aires (1988). Gravity anomalies and flexure of the Lithosphere at the Middle Amazon Basin, Brazil, J. Geophys. Res., Vol. 93, Number B-1, 415-428.

Molina, A. (1977). Estructura de los Andes Centrales a través de residuos y atenuación de ondas sísmicas, Tesis de Grado, Universidad Mayor de San Andrés.

Minster, J. B. and T. H. Jordan (1978). Present day Plate Motion, J. Geophys. Res.,Vol. 76, Number B11, 5331-5354.

Morrison R., P. (1962). A Resume of the Geology of South America, Institute of Earth Sciences, University of Toronto.

Nuttli, O. W. (1973). Seismic wave attenuation and magnitude relations for Eastern North América, J. Geophys. Res., Vol. 78, Number 5, 876-885.

Nuttli, O. W. (1980). The Excitation and Attenuation of seismic crustal phases in Iran, Bulletin Seismological Society of America, Vol. 70, No. 2, 469-485.

Oblitas, L. (1972). Estructura del Escudo Brasileño a partir de la dispersión de las ondas superficiales, Tesis de Grado, Universidad de Chile, Santiago, Chile.

Press, F. and M. Ewing (1952). Two slow surface wave across North America, Bulletin Seismological Society of America, 42, 219-228.

Raoof, M. M. and Nuttli, O. W. (1984). Attenuation of High Frecuency Earthquake Waves in South America, PAGEOPH., Vol. 22, 619-644.

Schlater,I., E., Nederlof (1966). Bosquejo de la Geología y Paleogeografía de Bolivia, Bol. Geobol No. 8.

ANNEX 1

The previous preliminary study was proposed for publication in Spanish in the Revista Geofísica (Pan American Institute of Geography and History) and is in press when this report is written. It is annexed to the report.

ATENUACION DE LAS FASES DE CORTO PERIODO P, Li, Lg y Rg A TRAVES DE PERU - BOLIVIA, REGISTRADAS EN LPB

Rene Rodolfo Ayala S.
Ramon Cabre Roige S.J.
Estela Minaya Ramos *

ABSTRACT

This preliminary study analyzes the characteristics of phases P, Li, Lg, and Rg of earthquakes originated in Peru, recorded at La Paz-Bolivia (LPB).

	P	Li	Lg	Rg
h≤70 km	7.73±0.01	3.84±0.0001	3.64±0.0003	3.17±0.001
217≥h>70km	7.86±0.05	3.81±0.01	3.53±0.003	3.15±0.005

The anelastic attenuation γ has values quite different in two separate areas: In Cordillera region γ oscillates between 0.16 and 0.30 1/degree; in Brazilian Shield and Subandean γ oscillates between 0.12 and 0.17 degree.

Being quality factor Q inversely related to γ : In the Cordillera region Q changes between 192 and 630; in Brazilian Shield and Subandean between 450 and 794. The complexity of Cordilleran structure may explain a stronger attenuation.

* Observatorio San Calixto. La Paz. Bolivia

RESUMEN

El presente estudio preliminar analiza las caracteristicas de las fases P, Li, Lg y Rg, de sismos del Perú, registradas en La Paz - Bolivia (LPB).

La velocidad promedio (km/s) para las fases consideradas es:

	P	Li	Lg	Rg
h≤70 km	7.73±0.01	3.84±0.0001	3.54±0.0003	3.17±0.001
217≥h>70km	7.86±0.05	3.81±0.01	3.33±0.003	3.15±0.005

Se tienen en general dos valores del coeficiente de atenuación anelásticaγ, para la región de la Cordillera γ=0.12 a 0.17 1/grados y para el Escudo Brasileño y Subandino γ=0.16 a 0.30 1/grados; en relación inversa con el factor de calidad Q; siendo Q=192 a 630 y Q=450 a 794 respectivamente; correspondiendo la mayor atenuación de las ondas a la region de la cordillera, debido a la complejidad en la estructura.

INTRODUCCION

Las ondas primarias P, u ondas longitudinales, tienen un movimiento de particula paralelo a la dirección de propagación del rayo. Presentan velocidades menores a 8 km/s en la corteza y de 8 a 10 km/s en el manto. Se registran mejor en los sismogramas verticales de corto periodo.

Las ondas Li (identificadas por Bath, 1956) corresponden a ondas guiadas de corto periodo, que se transmiten por la capa intermedia de la corteza (de ahi el subindice i), con velocidades de grupo de 3.79±0.07 km/s, y equivalen a la fase S* observada para sismos cercanos; presentan un movimiento de particula complejo, con una mayor componente horizontal.

Las ondas Lg son ondas guiadas de corto periodo y gran amplitud, que se supone se propagan por la denominada capa granitica de la corteza, de ahi el subindice g; las descubrieron Ewing y Press en 1952; presentan un movimiento de particula perpendicular a la direccion de propagacion del rayo, polarizadas en el plano horizontal, con velocidad de grupo de 3.54 km/s. Se registran mejor en los sismogramas horizontales de corto periodo.

Las ondas Rg (reconocidas por Bath, 1954) son ondas guiadas de corto periodo, de tipo Rayleigh, que se transmiten por la denominada capa granitica de la corteza; presentan un movimiento de particula paralelo a la dirección de propagacion del rayo, eliptico y retrogrado en el plano vertical; una velocidad de grupo de 3.0±0.7 km/s. Se registran mejor en la componente vertical de corto periodo.

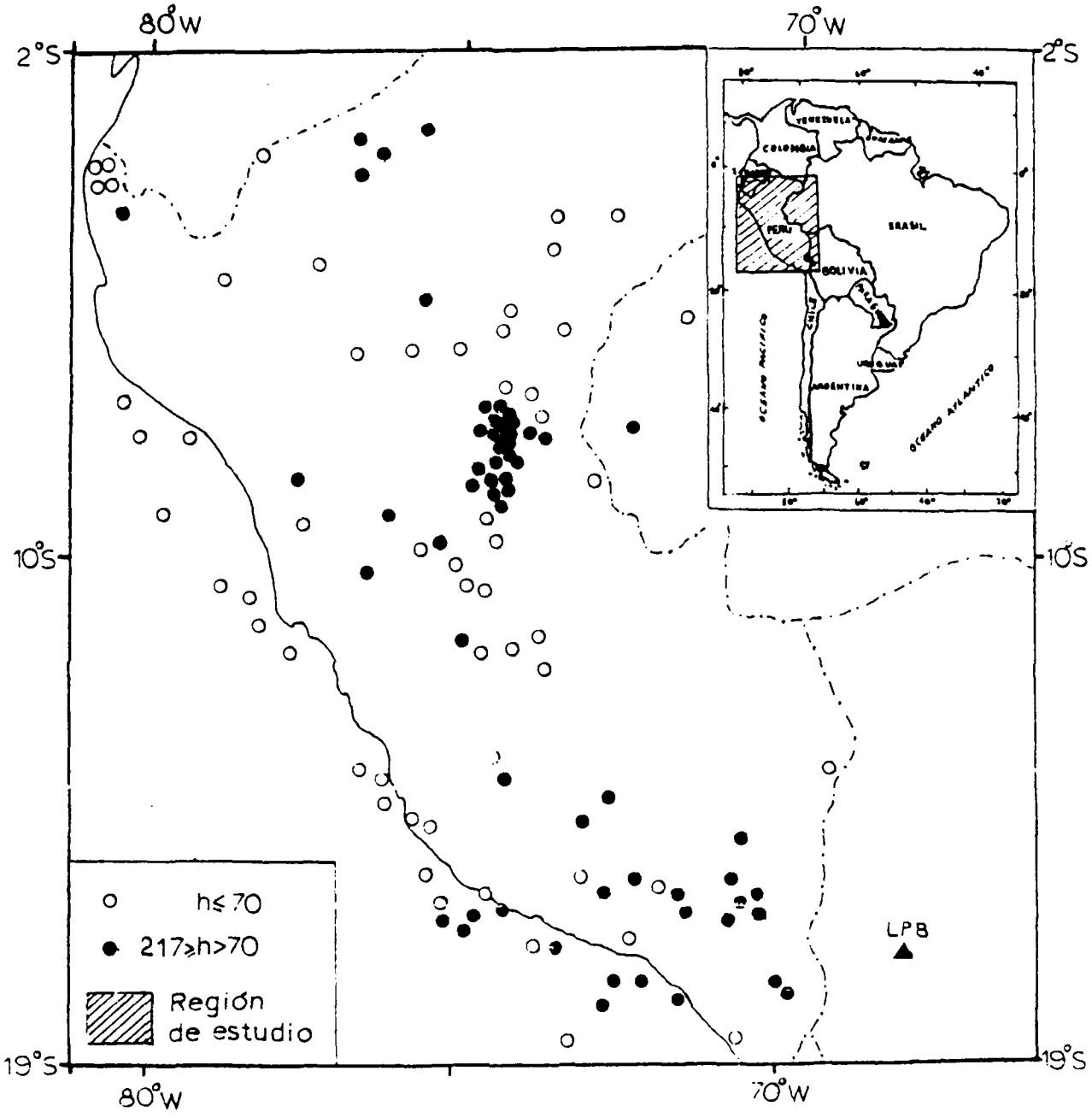

Fig. 1. Mapa de distribución de epicentros de acuerdo a la profundidad.

DATOS UTILIZADOS

La región de estudio está comprendida entre los 2° a 18° latitud sur y 68° a 81° longitud oeste; se consideraron los sismos provenientes del Perú (Fig. 1), *con magnitudes mb (magnitud de las ondas de cuerpo)* desde 4.0 a 5.6, de los años 1977 a 1986, tomados de los Catálogos de Sismos del International Seismological Center (I.S.C.), registrados en las componentes de corto período de la estación sismológica de La Paz, Bolivia (LPB) de la WWSSN (World Wide Seismographic System Network).

Los sismos utilizados varían desde profundidades superficiales ($h \leq 70$ km) hasta intermedios con profundidades ($70 < h \leq 217$ km).

PROCEDIMIENTO Y METODO

Para medir las amplitudes se consideraron los siguientes aspectos: para las ondas P se midieron las máximas amplitudes y los períodos correspondientes de los sismogramas verticales de corto período y para las ondas guiadas Lg, Li y Rg, las máximas amplitudes y períodos de los sismogramas horizontales de corto período.

La región de estudio se dividió en 6 zonas diferentes (Fig. 2), de acuerdo al azimut (estación-epicentro). Considerando la división por profundidad para cada zona, se tienen dos niveles por cada una de ellas (Tabla 1); el primero con los sismos superficiales y el segundo con los intermedios.

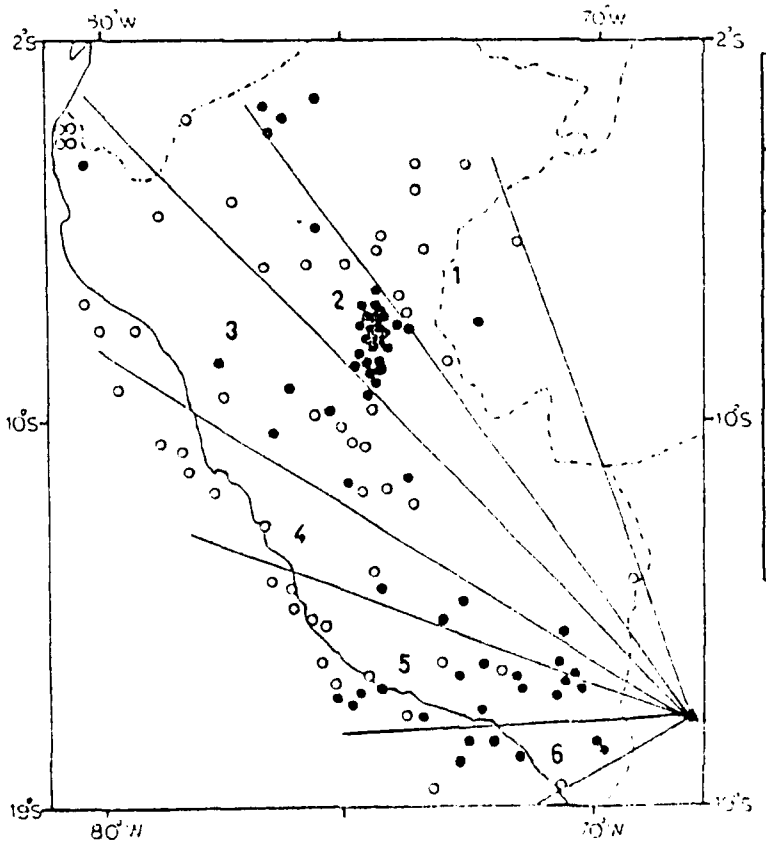

TABLA 1

ZONA	AZIMUT (est-epi)
1	340° - 320°
2	320° - 310°
3	310° - 280°
4	280° - 270°
5	270° - 250°
6	250° - 160°

Fig. 2. Mapa de distribución de epicentros, mostrando la división por zonas.

Con los datos de amplitud y períodos leídos, se procedió a normalizar la amplitud para cada zona a una magnitud mb=5.0, considerando similares niveles de profundidad, para evitar el efecto de foco; a partir de la fórmula de magnitudes (Nuttli, 1973):

$$mb = C + B(\log \Delta^\circ) + \log(A/T) \qquad (I)$$

Donde:

mb = magnitud de las ondas de cuerpo
C = umbral de detectabilidad
B = coeficiente de atenuación
Δ° = distancia epicentral en grados
A = amplitud máxima en micrómetros
T = período de las ondas de amplitud máxima en segundos

Primero se determinaron los coeficientes C y B para cada fase y zona; después se despejó de la fórmula (I) la amplitud; reemplazando todos los datos conocidos se normalizó la amplitud a una determinada magnitud (mb=5.0) y rango de profundidad.

Seguidamente se utilizaron las curvas de atenuación (Fig. 3) de Nuttli (1973) para calcular el coeficiente de atenuación γ; en base a la ecuación:

$$A = K*(1/(\Delta^\circ)^{1/2})*(1/(SIN(\Delta^\circ))^{1/2})*(e^{-\gamma*\Delta^\circ})$$

Donde:

A = amplitud de la onda en micrómetros
K = constante
Δ° = distancia epicentral en grados
γ = coeficiente de atenuación anelástica en (1/grados)

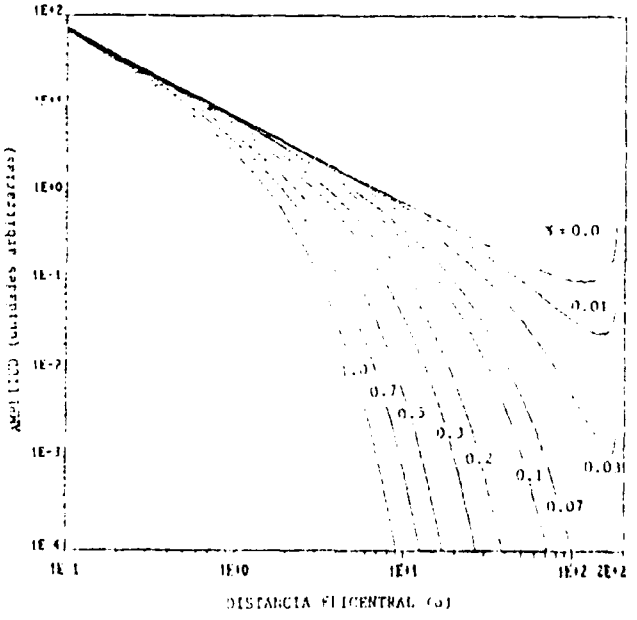

Fig. 3. Curvas teóricas de atenuación de la amplitud en el dominio del tiempo, donde γ está expresado en el inverso de grados (Nuttli, 1973).

Para calcular el factor de calidad Q se cambiaron las unidades de γ a 1/km y se empleó la fórmula (Nuttli, 1973):

$$Q = \pi/(T*\gamma*V) \qquad (II)$$

Donde :

π = 3.1416
T = periodo en segundos
γ = coeficiente de atenuación anelástica en 1/kilómetros
V = velocidad de grupo en kilómetros por segundo

Para comprobar los valores de Q obtenidos con el método de Nuttli, se utilizó también el método de la forma de la coda (Herrmann, 1980), el cual explica que la frecuencia predominante (fp) es inversamente proporcional a Q, para lo que utilizaremos la curva maestra fp versus t* (Fig. 4) para instrumentos de corto periodo de la red standard (WWSSN), donde t* es igual t/Q, siendo t el tiempo desde el origen en segundos. Para este propósito se calcula la fp de cada fase analizada en Hertz, que consiste en tomar un tiempo de medida 10 segundos o más (ventana de tiempo) y contar el número de ceros que cruzan la traza media del sismograma y dividirlos por dos veces el tiempo (ancho) de la ventana; se plotean fp (Hz) versus t (s) y son sobreimpuestos encima de la curva maestra (Fig. 4) hasta que t*=1, entonces el valor de Q será numéricamente igual a t.

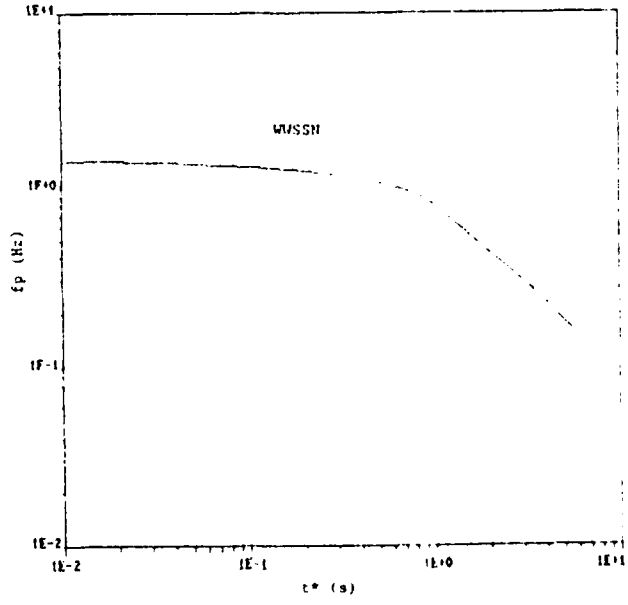

Fig. 4. Curva maestra de la frecuencia predominante de la coda fp (Hz) versus t* (s) para instrumentos de corto periodo de la WWSSN (Herrmann, 1980).

Para determinar la velocidad de grupo de cada fase, se plotearon los tiempos de viaje (tiempo origen menos tiempo de llegada de la fase; en segundos) y la distancia epicentral en grados (Δ°), de acuerdo a la profundidad (Fig. 5a y 5b), haciendo un ajuste lineal; para después calcular la velocidad de grupo para cada tipo de onda.

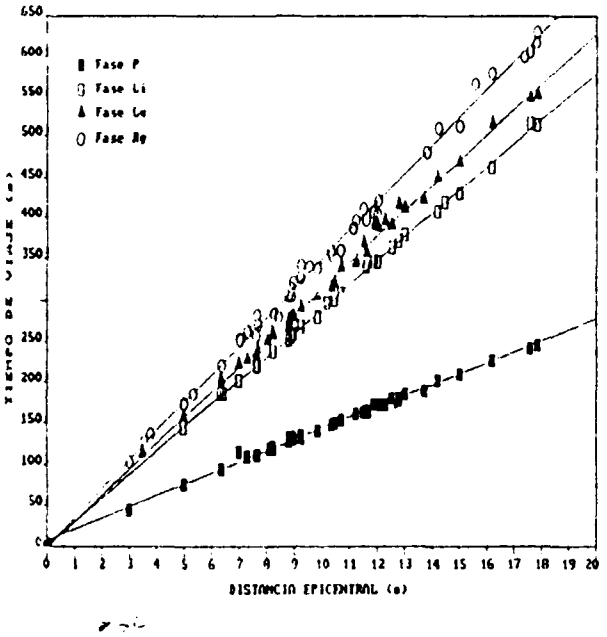

Fig. 5a. Curvas de tiempo viaje versus distancia para sismos superficiales.

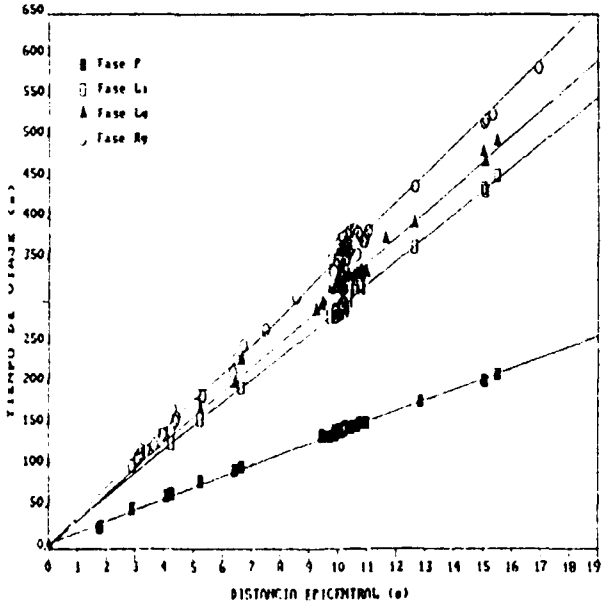

Fig. 5b. Curvas de tiempo de viaje versus distancia para sismos intermedios.

Los valores del factor de calidad Q obtenidos fueron ploteados en un mapa y con ayuda de la tectónica y geología de la región se realizó la interpretación.

MARCO TECTONICO - GEOLOGICO

La región de estudio corresponde a una zona de convergencia de dos placas tectónicas, donde la placa de Nazca se está subduciendo debajo de la placa Sudamericana; la velocidad de avance de la placa de Nazca es de 5 cm/año y para la placa Sudamericana de 3 cm/año (Minster y Jordan, 1978).

La placa de Nazca en la región de estudio presenta cinco segmentos; el primero entre los 2° a 6° latitud sur, con un buzamiento 12°E, espesor de 100 km y actividad sísmica hasta la profundidad de 250 km; el segundo desde los 7° a 12° latitud sur, con un buzamiento de 20°E, espesor de 110 km y profundidad de 580 km; el tercero desde los 12° a 15° latitud sur, con un buzamiento de 16°E, espesor aproximado 100 km y profundidad de 290 km; el cuarto desde los 15° a 17° latitud sur, buzamiento de 21°E, espesor de 120 km y profundidad de 300 km; el quinto desde 17° a 24° latitud sur, buzamiento de 29°E, espesor de 120 km y profundidad de 580 a 600 km (Ayala, 1991).

En la parte norte y sur se presentan volcanes activos, mostrando zonas de debilidad.

En la placa continental se tienen varias provincias geológicas (Fig. 6): Cordillera de los Andes, Altiplano; Cordillera de la Costa; Planicie Costera; Cuenca Superior del Amazonas; Llanuras Chaco-Benianas; Escudo Brasileño y el Escudo de Guayana.

La cordillera de los Andes se divide en cordillera Oriental y Occidental; la primera constituida por rocas paleozoicas y muchos cuerpos intrusivos graníticos; las estribaciones orientales de la misma se denominan Subandino y son rocas sedimentarias paleozoicas, fuertemente plegadas y fracturadas; la cordillera Occidental esta constituida por una serie de volcanes y mesetas volcánicas.

La cordillera de la Costa, constituye una serie de elevaciones paralelas a la costa en la parte sur del Perú, formada por cuerpos batolíticos; siendo una cordillera de tipo local.

La Planicie Costera, separa la cordillera de la Costa de la cordillera Occidental.

El Altiplano corresponde a una fosa tectónica levantada, de edad mesozoica terciaria, ubicada entre la cordillera Oriental y Occidental, rellenada por rocas sedimentarias, paleozoicas, cretácicas, terciarias y cubierta cuaternaria, con un espesor de 12000 m (Schlater y Nederlof, 1966).

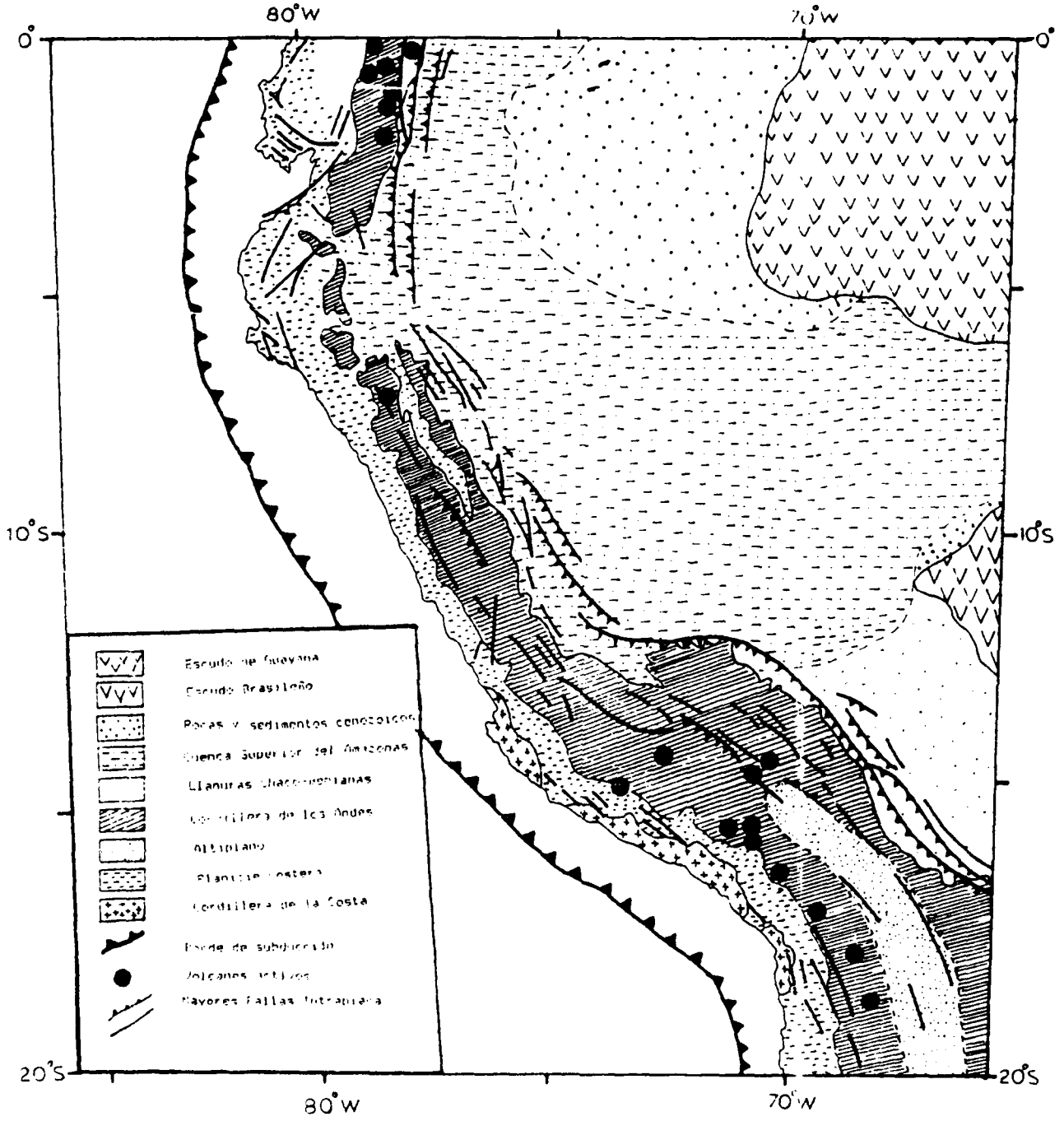

Fig. 6. Mapa tectónico-geológico, en base al Mapa Neotectónico Preliminar para Sudamérica, 1985.

El Escudo Brasileño está formado por rocas de edad precámbrica, que constituyen el basamento del continente sudamericano (la parte que aflora en Bolivia se denomina Cratón de Guaporé); la prolongación de éste en la parte norte se denomina Escudo de Guayana; separados por rocas sedimentarias de edad paleozoica de origen marino y rocas meso-cenozoicas de la cuenca del Amazonas; ésta tiene un espesor de 7000 m (Jeffreys y Aires, 1988); la parte más occidental se denomina Cuenca Superior del Amazonas, con rocas paleo-cenozoicas, que cubren el contacto entre el escudo y la cordillera, con un espesor aproximado de 4000 m (Morrison, 1962).

Las Llanuras Chaco-Beníanas son amplias llanuras constituidas por rocas paleozoicas y cámbricas, con un espesor aproximado de 2300 m (Morrison, 1962); mientras que a lo largo del río Béni el basamento precámbrico solo está cubierto por rocas terciarias.

ONDAS SISMICAS ORIGINADAS EN EL PERU

La Fig. 7 muestra los registros verticales de corto período para sismos del Perú, registrados en LPB.

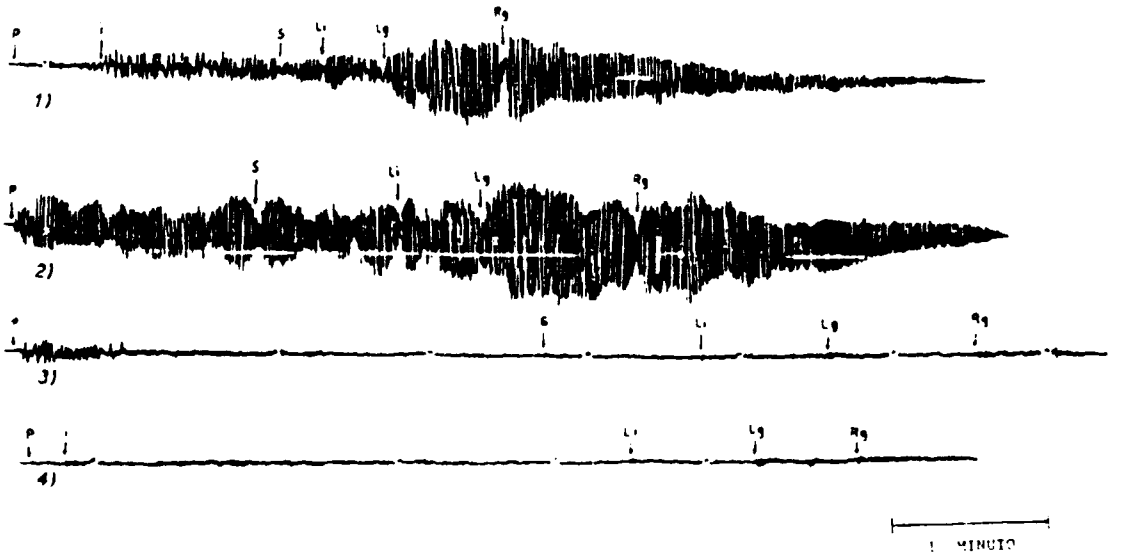

Fig. 7. Sismogramas verticales de corto periodo registrados en LPB.

(1) 15-VII-1982 ; h=117 km ; mb=5.5 ; D°=10.34°
(2) 20-III-1983 ; h= 18 km ; mb=5.4 ; °= 8.90°
(3) 21- V -1986 ; h=126 km ; mb=4.9 ; °=15.51°
(4) 23- IV-1986 ; h= 96 km ; mb=5.4 ; °=17.85°

Fase P

Las ondas P del Perú en general tienen comienzo emergente; presentan periodos entre los 0.6 a 1.2 s; su velocidad promedio es 7.73±0.01 km/s, sus amplitudes normalizadas varian entre los 0.01 a 0.3 micrómetros (1 micrómetro=0.001 mm) para focos superficiales; para los intermedios es 7.86±0.05 km/s y sus amplitudes varian entre 0.02 a 1.1 micrómetros. Exhiben un movimiento de particula paralelo a la dirección de propagación del rayo (en los tres planos: plano horizontal formado por las componentes N-S y E-W; plano vertical paralelo al azimut, formado por la componente vertical Z con la proyección radial UR y el plano vertical perpendicular al azimut, formado por la componente Z y la proyección horizontal UH (Figs. 8a y 8b). Son ondas que viajan por la parte superior del manto, para las distancias que en nuestros casos interesan.

Fase Li

Son ondas guiadas de corto periodo, con comienzo generalmente emergente, que se transmiten por la parte inferior de la corteza continental; sus periodos están entre los 0.7 a 1.2 s; su velocidad promedio es de 3.84±0.0001 km/s, sus amplitudes varian entre los 0.04 a 0.8 micrómetros para focos superficiales; para intermedios es 3.81±0.01 km/s y sus amplitudes entre 0.1 a 3.4 micrómetros. Presentan un movimiento de particula próximo a la perpendicular a la dirección de propagación del rayo con alguna polarización horizontal (Fig. 9a), más claro para los focos intermedios (Fig. 9b); pudiendo ser una sobreposición de modos superiores de la onda Love.

Fase Lg

Son ondas guiadas de corto periodo, generalmente claras, pero con comienzos no impulsivos; se transmiten por la parte superior de la corteza continental, con periodos de 0.6 a 1.5 segundos; su velocidad promedio es 3.54±0.0003 km/s, sus amplitudes varian de 0.02 a 0.9 micrómetros; para focos intermedios es 3.53±0.003 km/s y sus amplitudes entre 0.09 a 2 micrómetros. Sus movimientos de particula son perpendiculares a la dirección de propagación del rayo, con una fuerte polarización horizontal (Fig. 10a), mayor en los intermedios (Fig. 10b); corresponden a modos superiores de la fase Love.

Fase Rg

Son ondas guiadas de corto periodo, con comienzos generalmente emergentes; interferidas por la coda de las fases previas; que se propagan por la parte superior de la corteza terrestre; presenta periodos entre los 0.6 a 1.4 s; su velocidad promedio es de 3.17±0.001 km/s, sus amplitudes varian entre los 0.03 a 0.2 micrómetros para focos superficiales; para focos intermedios es 3.15±0.005 km/s y sus amplitudes entre 0.04 a 1.1 micrómetros. Muestran un movimiento de particula paralelo a la dirección de propagación del rayo (Figs. 11a y 11b); siendo un composición de varios modos superiores de la fase de Rayleigh.

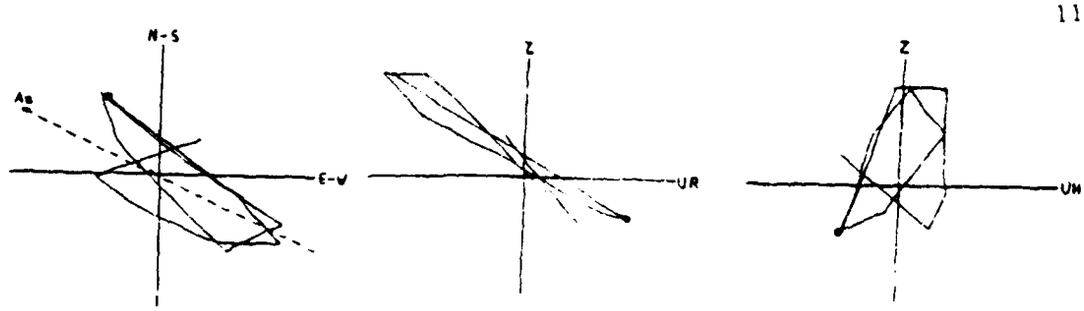

Fig. 8a . Movimiento de partícula Fase P, sismo superficial.

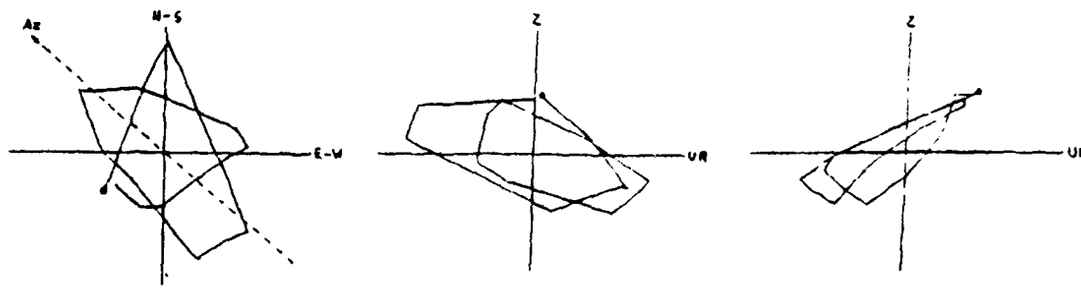

Fig. 8b . Movimiento de partícula Fase P, sismo intermedio.

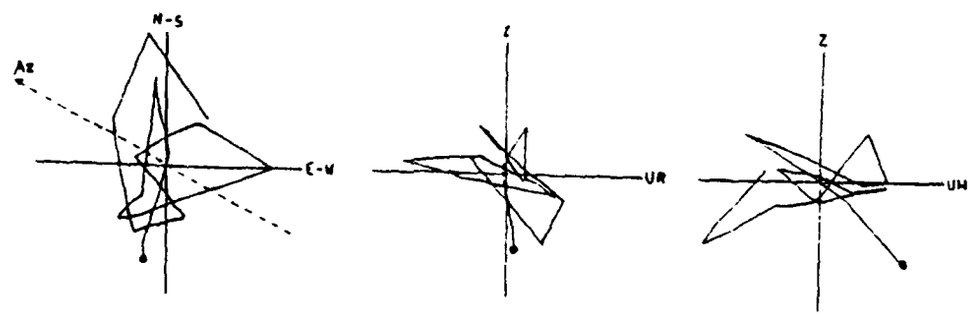

Fig. 9a . Movimiento de partícula Fase Li, sismo superficial.

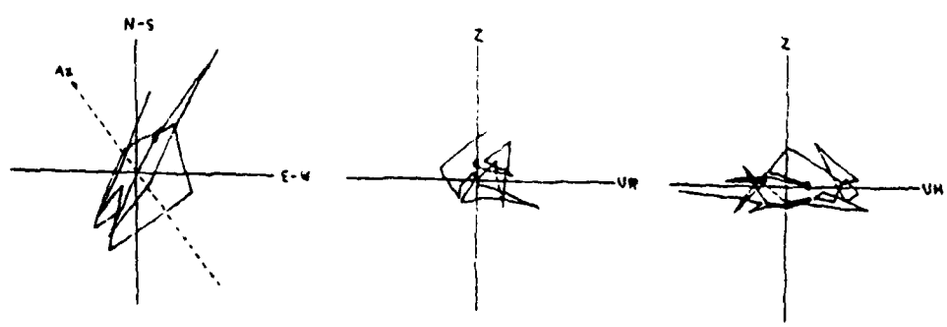

Fig. 9b . Movimiento de partícula Fase Li, sismo intermedio.

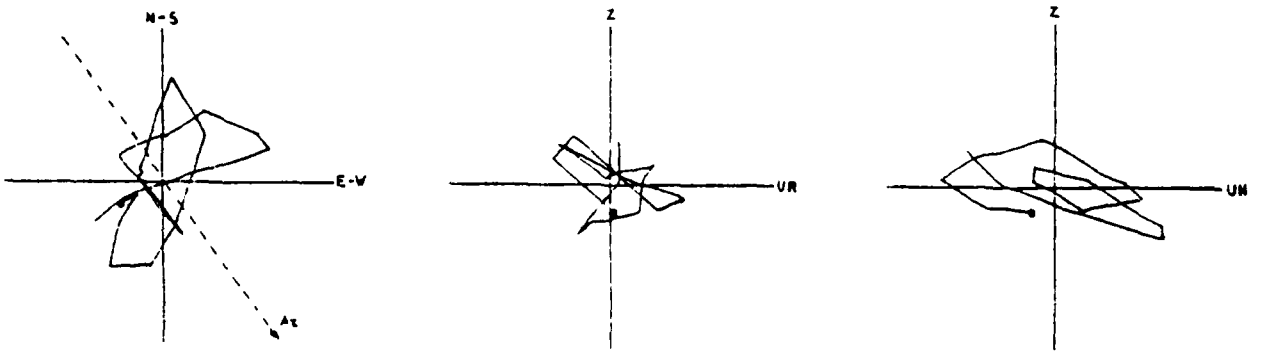

Fig. 10a . Movimiento de partícula Fase Lg, sismo superficial.

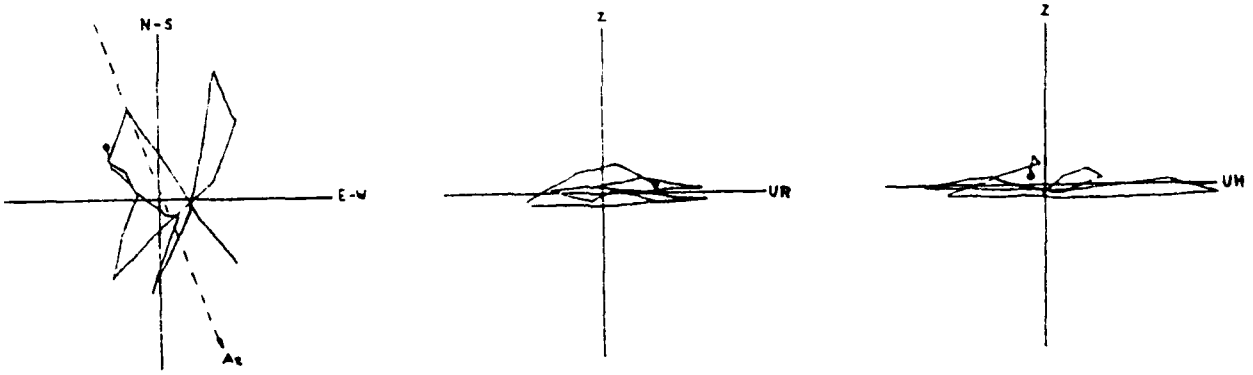

Fig. 10b . Movimiento de partícula Fase Lg, sismo intermedio.

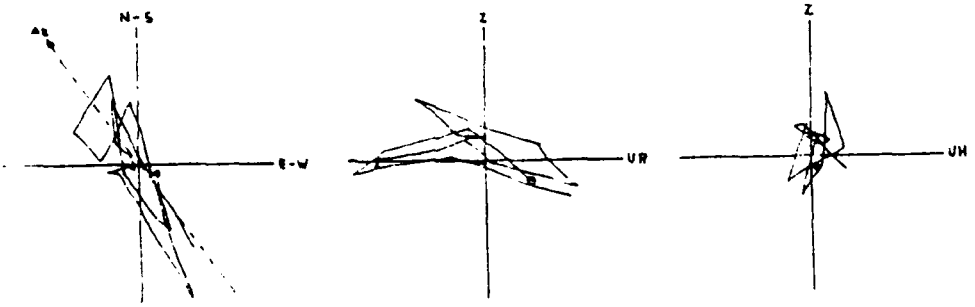

Fig. 11a . Movimiento de partícula Fase Rg, sismo superficial.

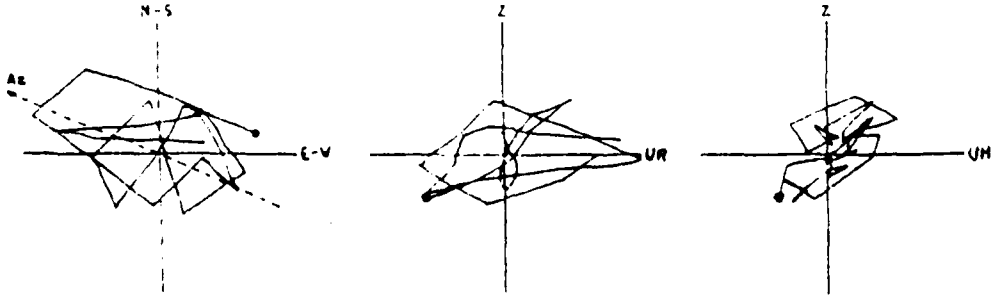

Fig. 11b . Movimiento de partícula Fase Rg, sismo intermedio.

COEFICIENTE DE ATENUACION ANELASTICA

Para determinar los coeficientes de atenuación anelástica (γ), primero se normalizaron las amplitudes leidas para cada zona y por niveles de profundidad, a mb=5.0. Ajustando los valores a las curvas teóricas (Fig. 3), obteniendo los valores de γ (en 1/grados) para cada fase considerada.

Las Figs. 12a a 19b muestran los valores de γ para cada fase, zona y niveles de profundidad analizados; los valores del periodo (T) y γ promedios y sus respectivas desviaciones standard están detallados en la Tabla 2.

FACTOR DE CALIDAD

Con los valores de γ obtenidos se aplicó la fórmula (II) para calcular los valores de Q aparente para cada zona, considerando diferentes niveles de profundidad de foco.

Ploteando fp y t, se procedió a determinar Q por el método de la forma de la coda de las ondas sísmicas (Herrmann, 1980), que servirán para corroborar los anteriores valores calculados de Q (Figs. 20a 27b).

Los valores de Q obtenidos fueron ploteados sobre un mapa para obtener regiones de similar valor de Q (Fig. 28a 31b).

Los valores de velocidad de grupo (V) y Q promedios para cada fase y por niveles de profundidad y sus desviaciones standard están expresados en la Tabla 2.

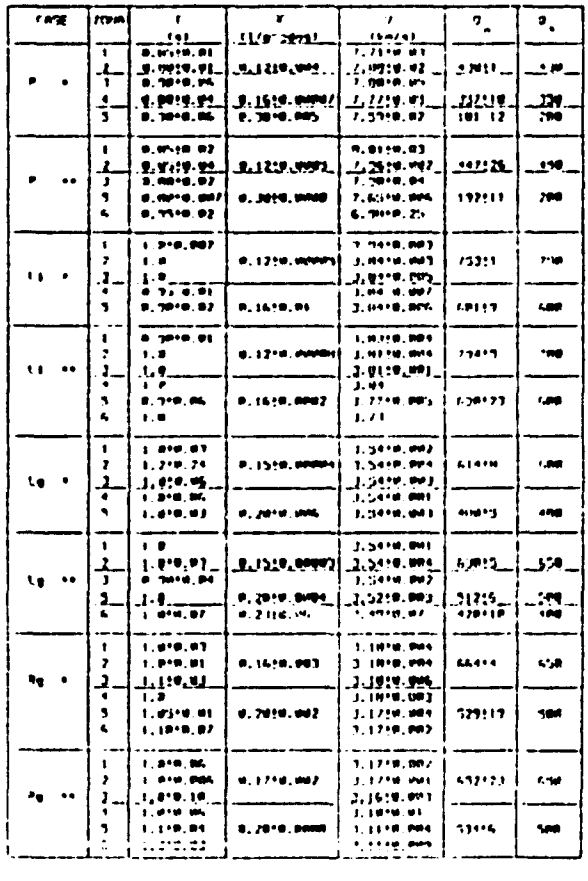

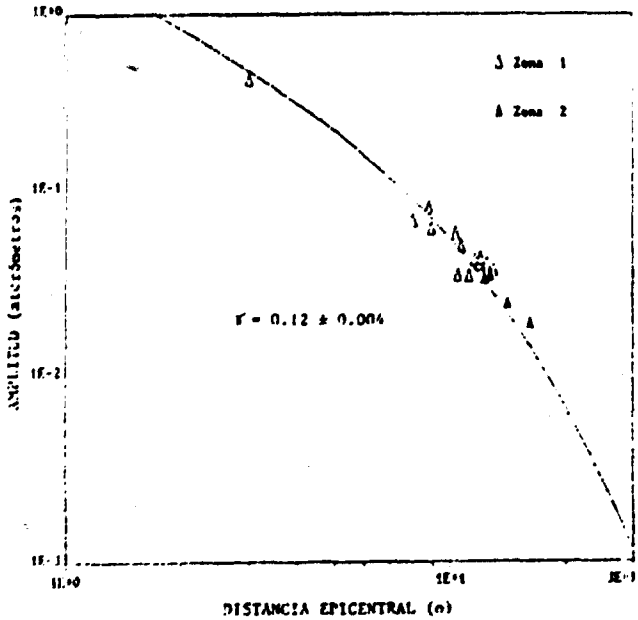

Fig. 12a. Valor de Y Fase P, sismos superficiales.

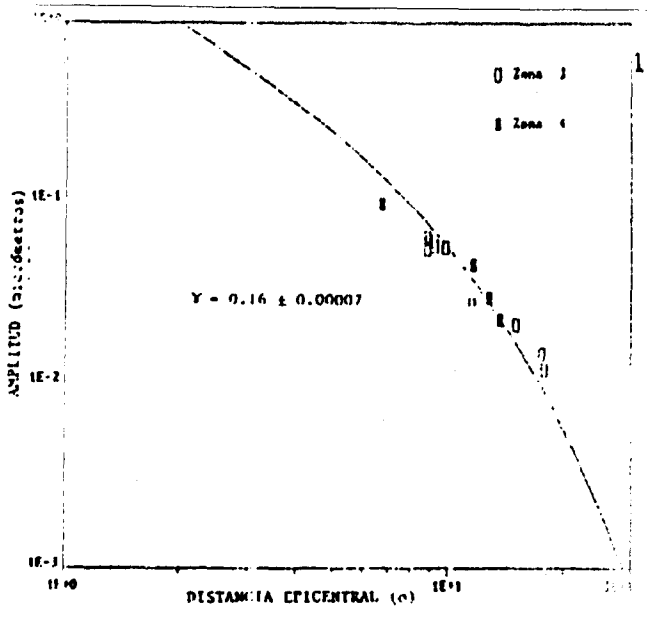

Fig. 12b. Valor de Y Fase P, sismos superficiales

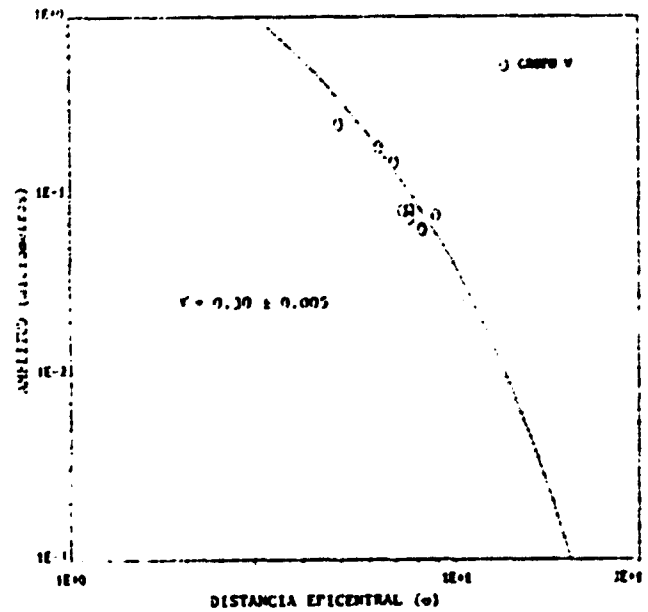

Fig. 12c. Valor de Y Fase P, sismos superficiales

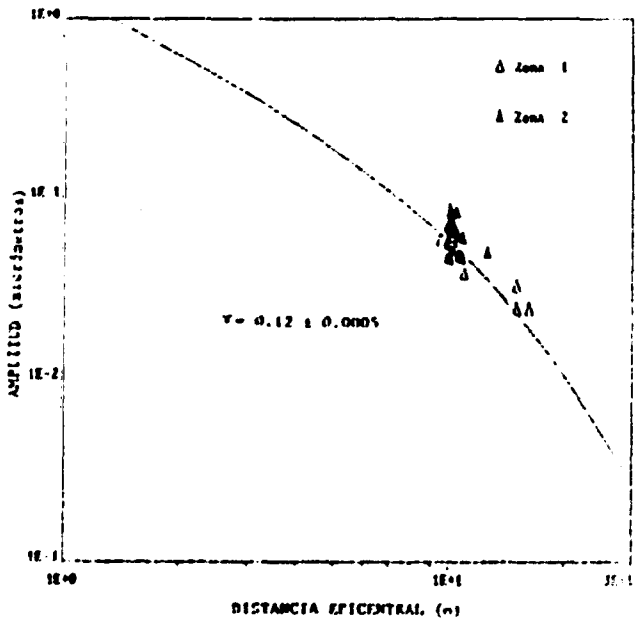

Fig. 13a. Valor de Y Fase P, sismos intermedios

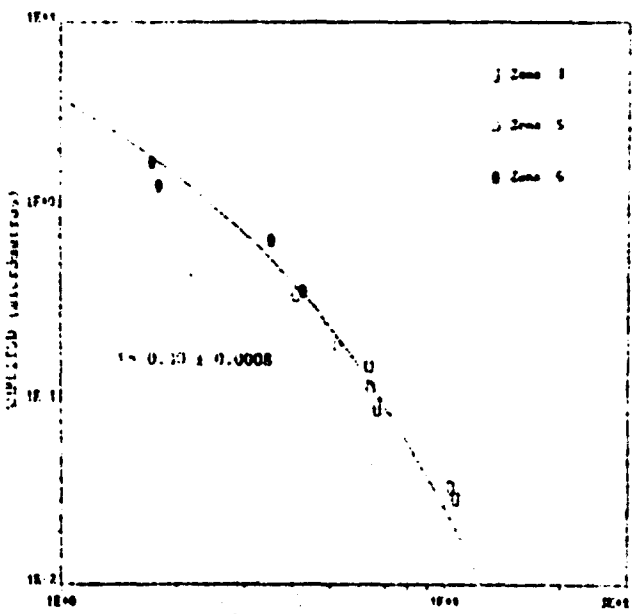

Fig. 13b. Valor de Y Fase P, sismos intermedios

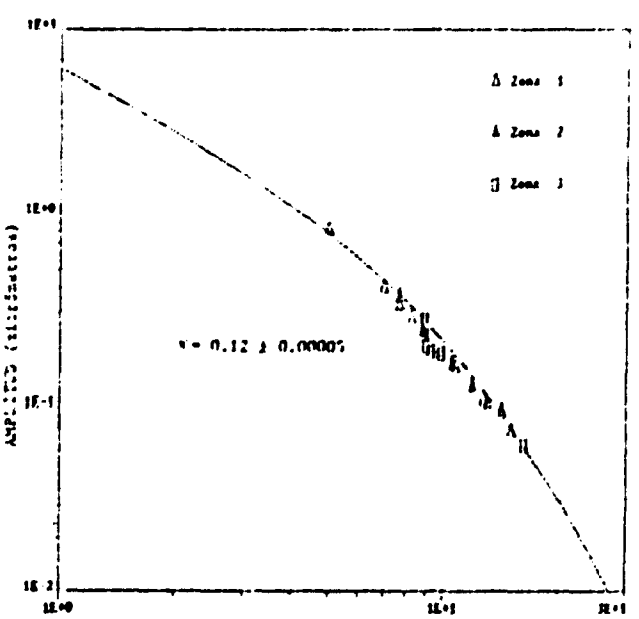

Fig. 14a. Valor de Y Fase LL, sismos superficiales

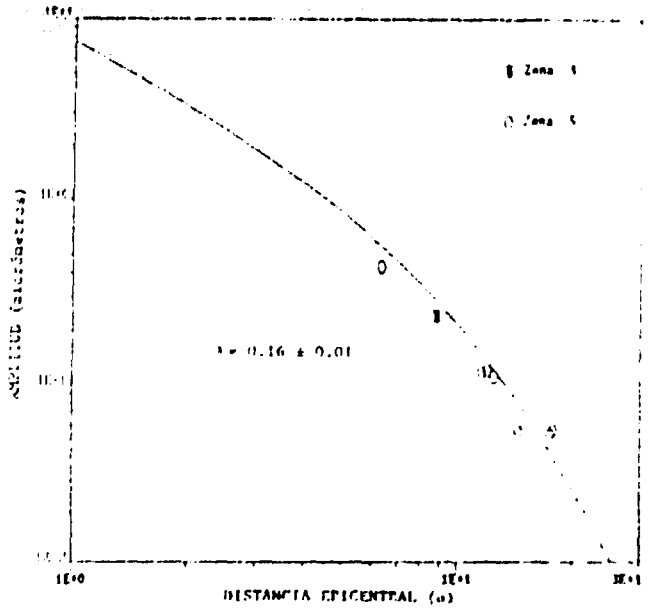

Fig. 14b. Valor de γ Fase Lg, sismos superficiales

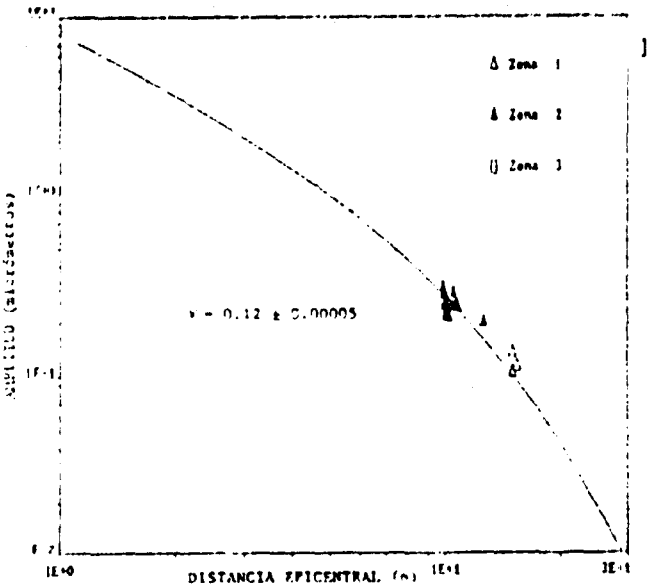

Fig. 15a. Valor de γ Fase Lg, sismos intermedios.

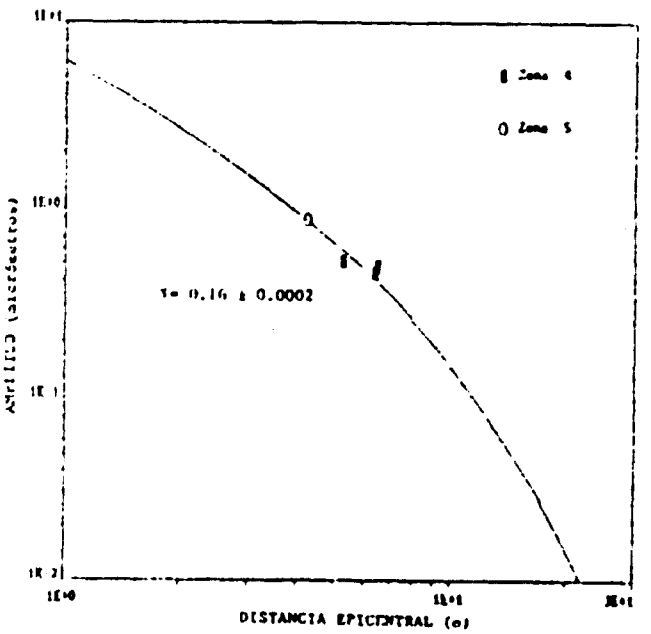

Fig. 15b. Valor de γ Fase Lg, sismos intermedios

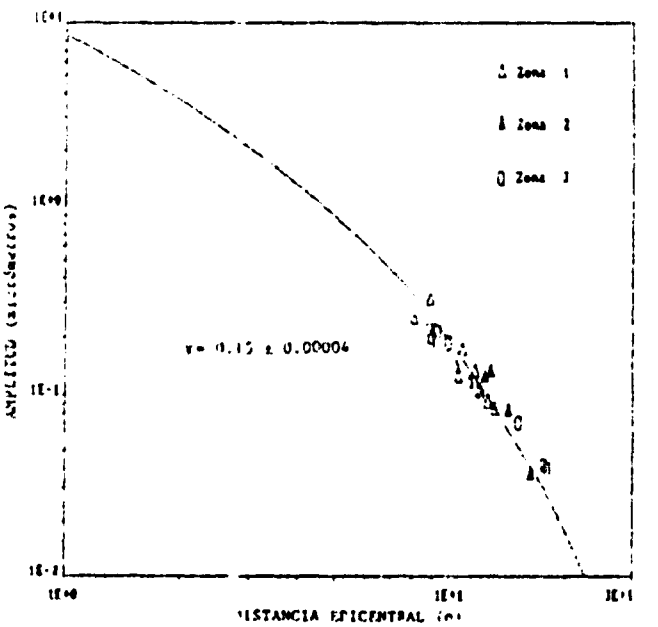

Fig. 16a. Valor de γ Fase Lg, sismos superficiales

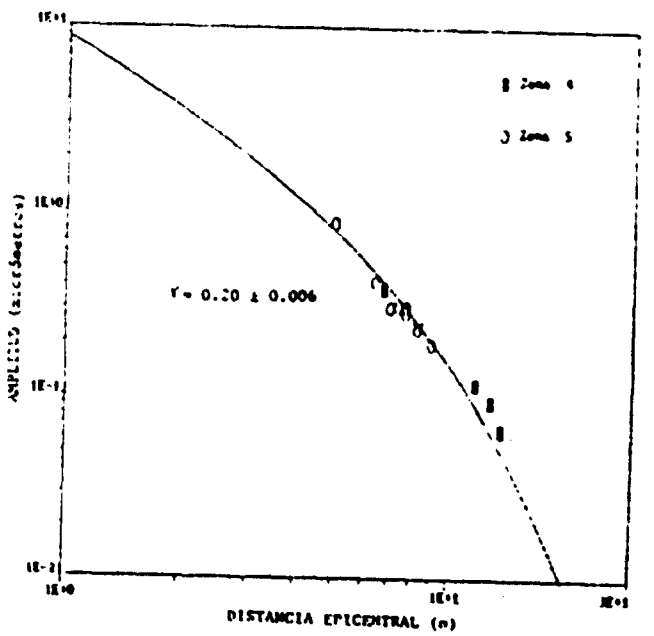

Fig. 16b. Valor de γ Fase Lg, sismos superficiales.

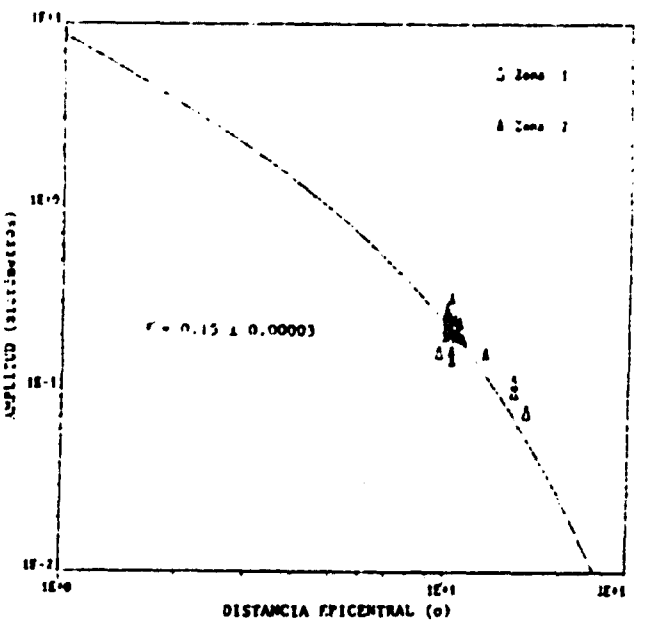

Fig. 17a. Valor de γ Fase Lg, sismos intermedios.

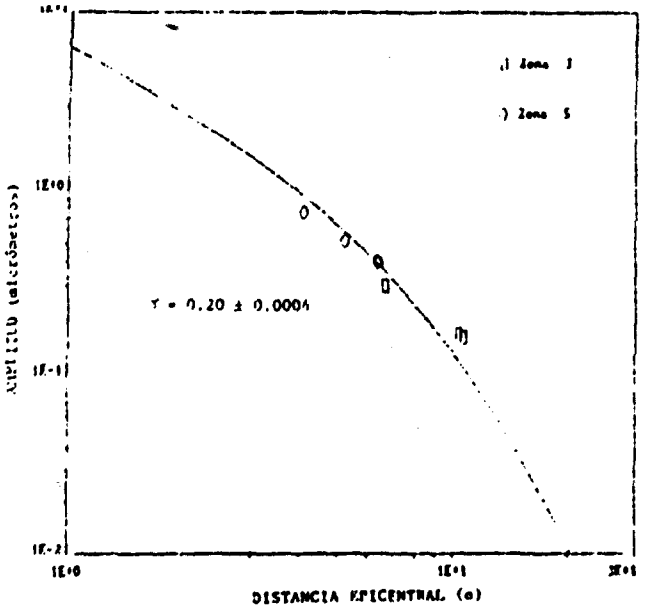

Fig. 17b. Valor de γ Fase Lg, sismos intermedios

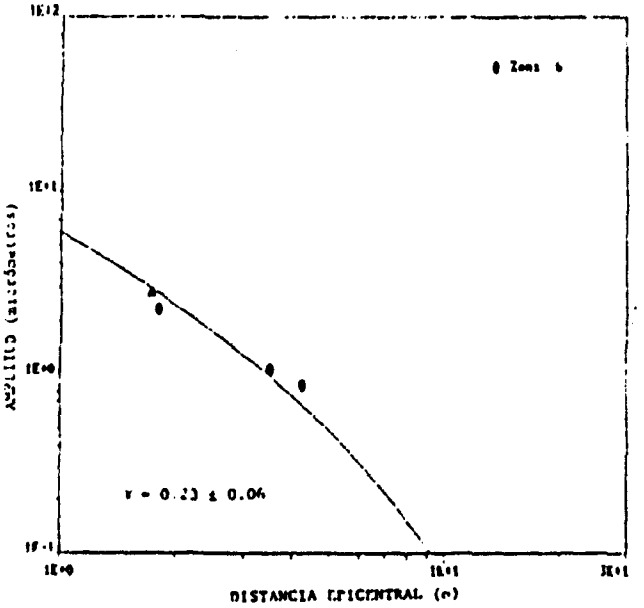

Fig. 17c. Valor de γ Fase Lg, sismos intermedios

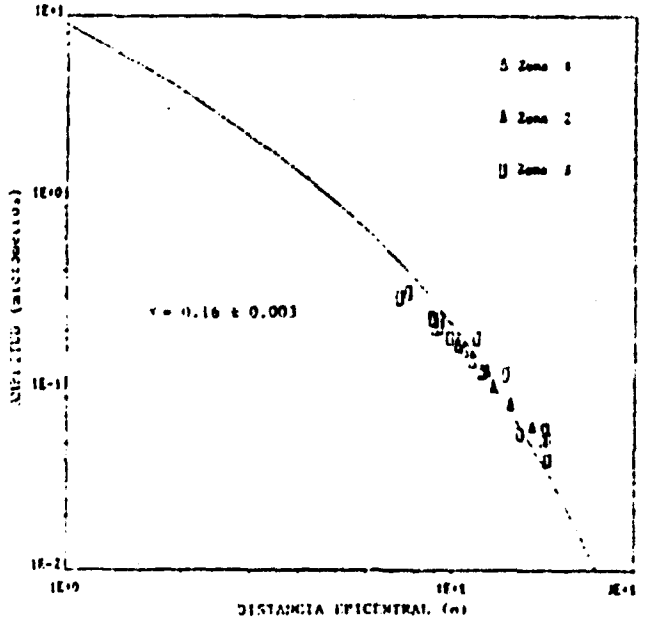

Fig. 18a. Valor de γ Fase Rg, sismos superficiales

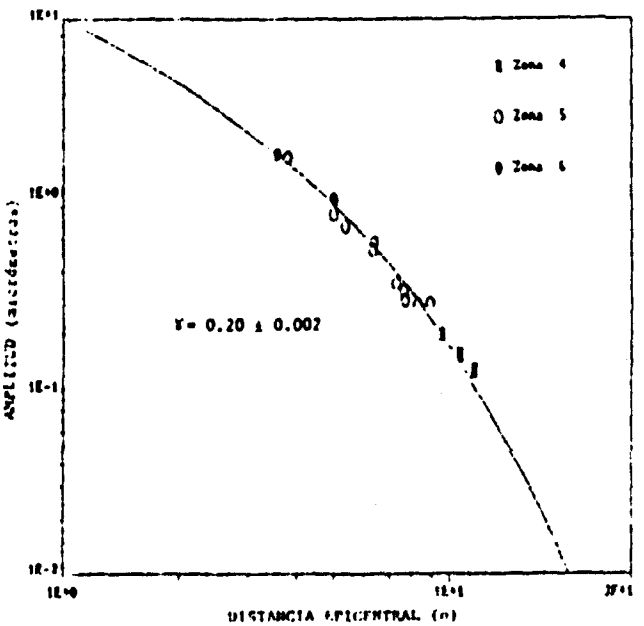

Fig. 18b. Valor de γ Fase Rg, sismos superficiales

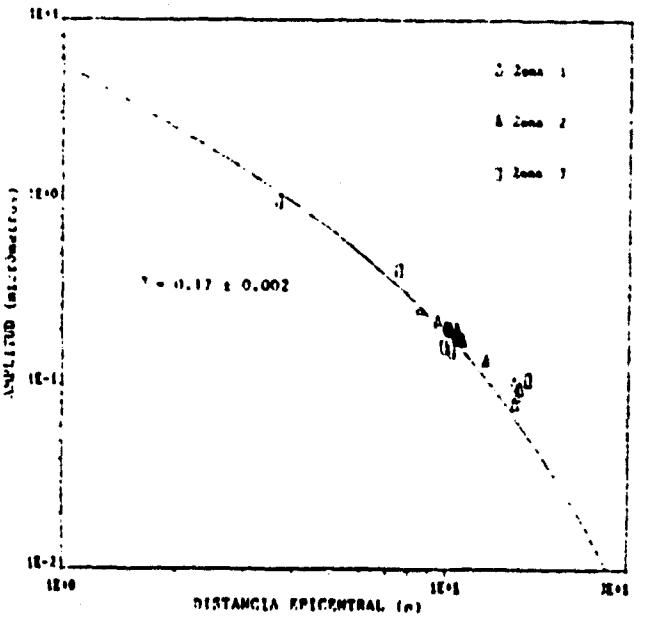

Fig. 19a. Valor de γ Fase Rg, sismos intermedios

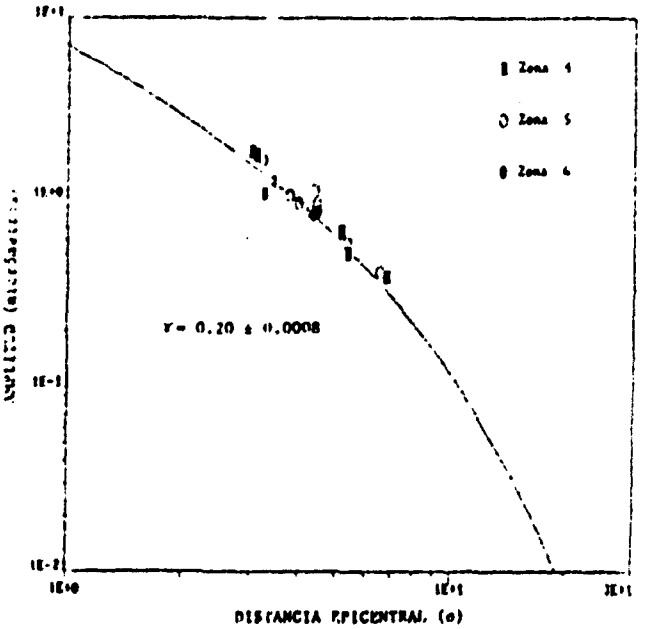

Fig. 19b. Valor de γ Fase Rg, sismos intermedios

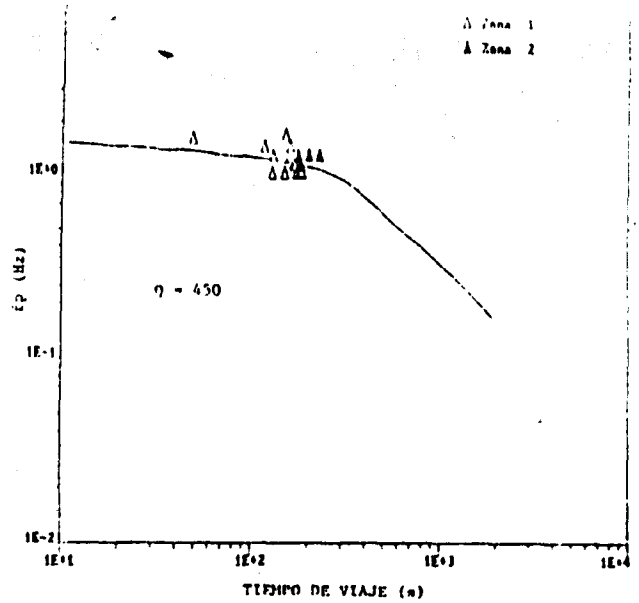

Fig. 20a. Valor de Q Fase P, sismos superficiales.

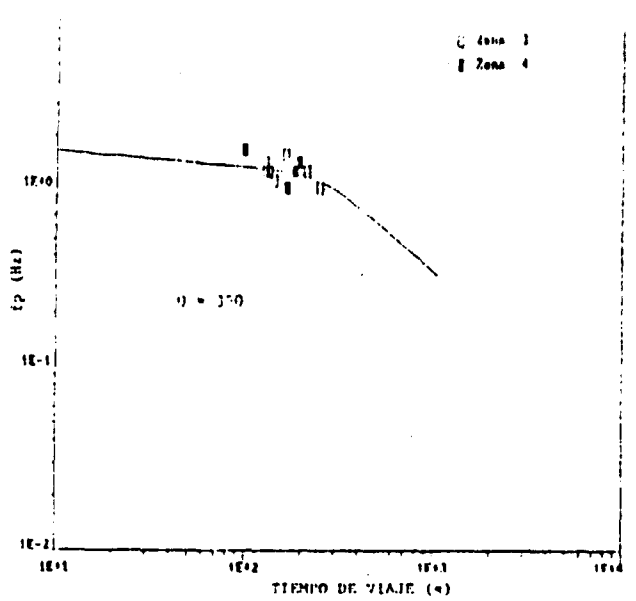

Fig. 20b. Valor de Q Fase P, sismos superficiales.

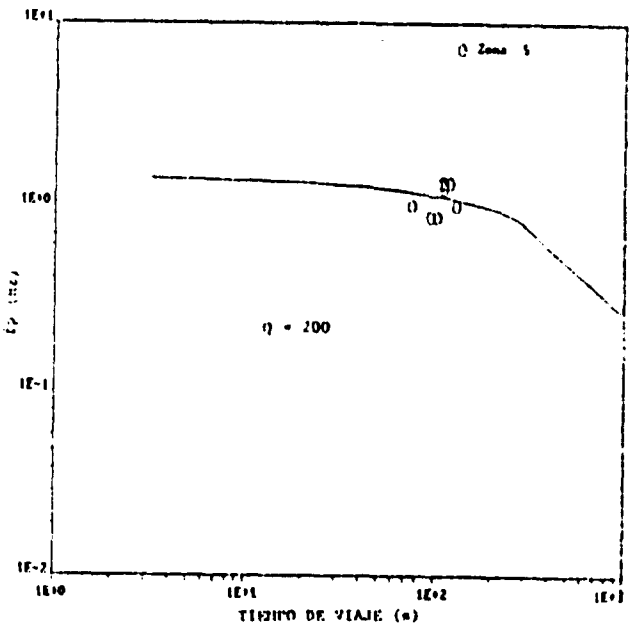

Fig. 20c. Valor de Q Fase P, sismos superficiales.

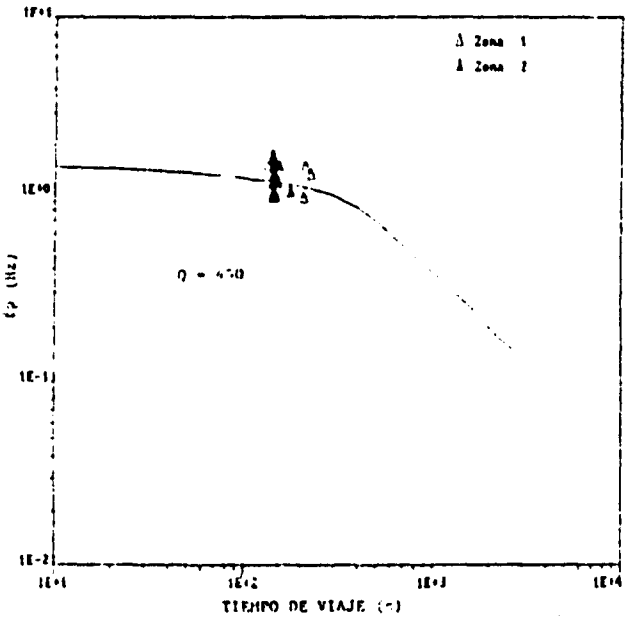

Fig. 21a. Valor de Q Fase P, sismos intermedios.

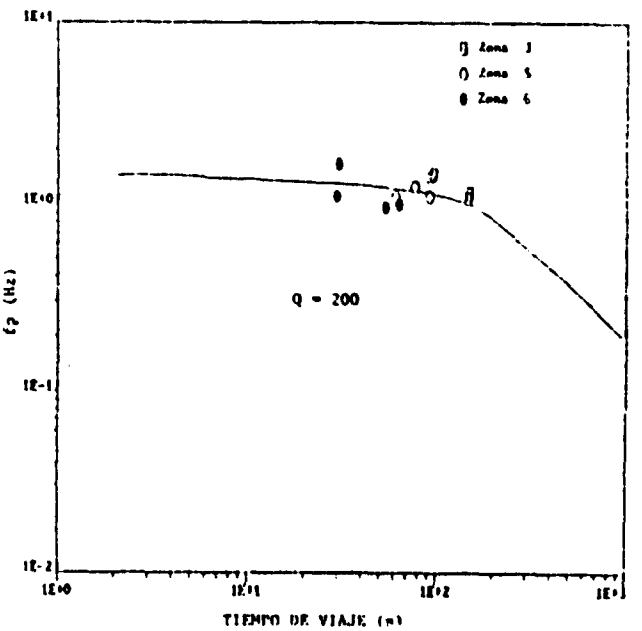

Fig. 21b. Valor de Q Fase P, sismos intermedios

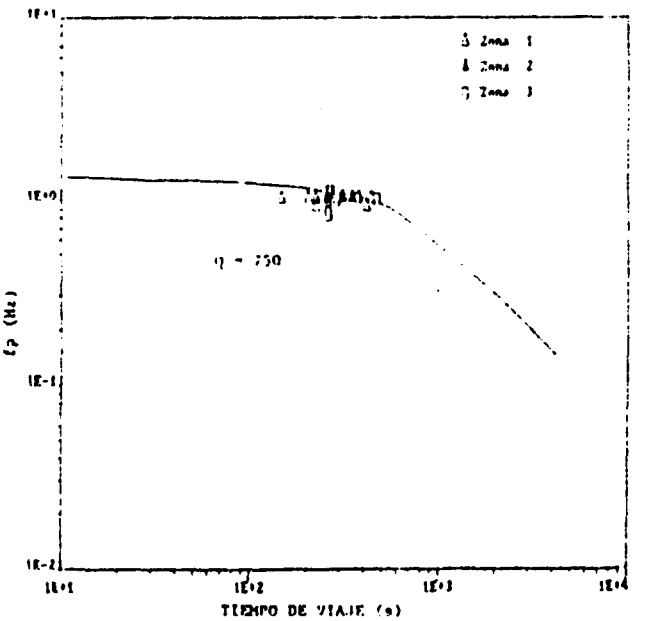

Fig. 22a. Valor de Q Fase Lg, sismos superficiales.

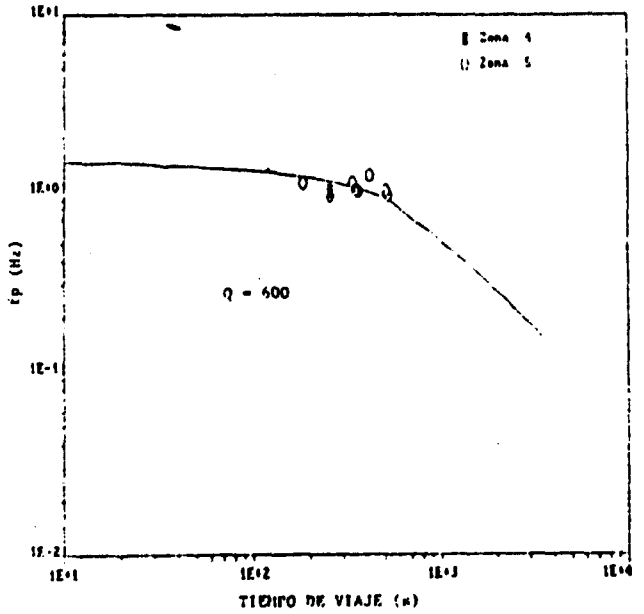

Fig. 22b. Valor de Q Fase Ll, sismos superficiales.

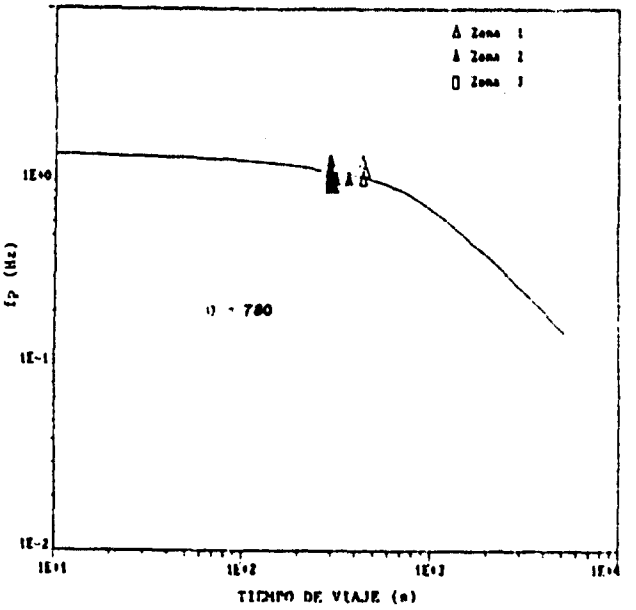

Fig. 23a. Valor de Q Fase Ll, sismos intermedios.

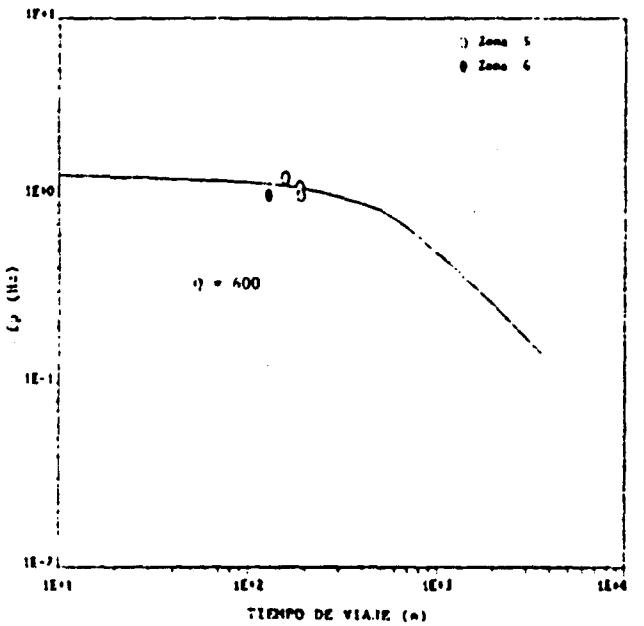

Fig. 23b. Valor de Q Fase Ll, sismos intermedios.

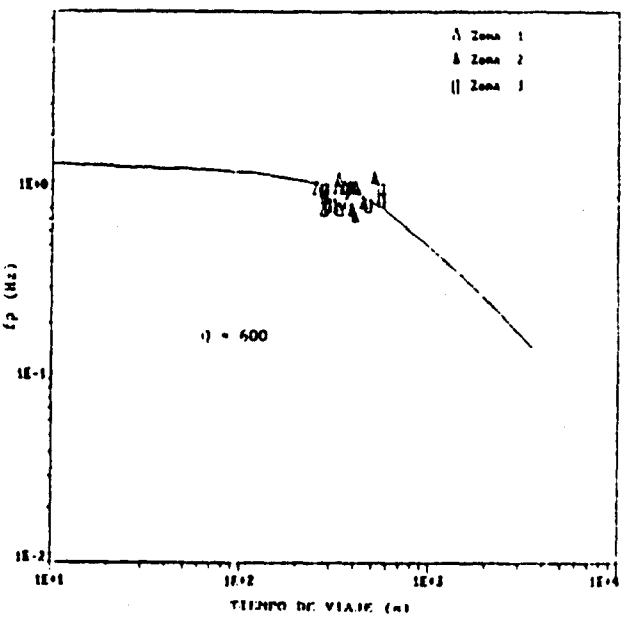

Fig. 24a. Valor de Q Fase Lg, sismos superficiales.

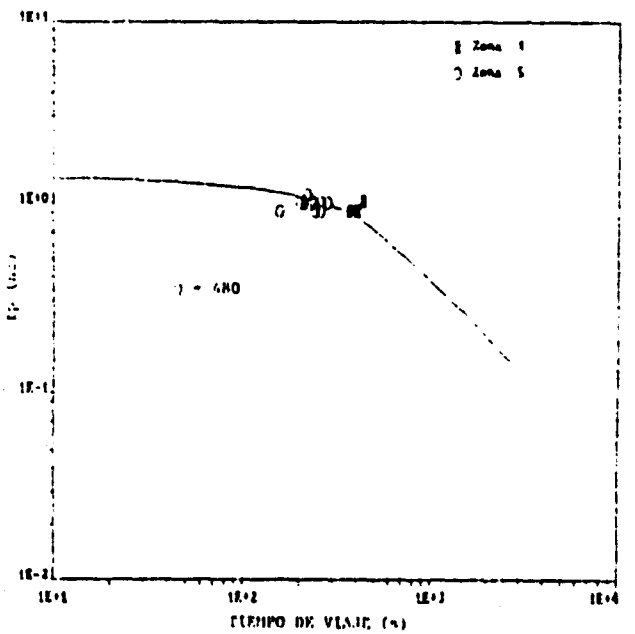

Fig. 24b. Valor de Q Fase Lg, sismos superficiales.

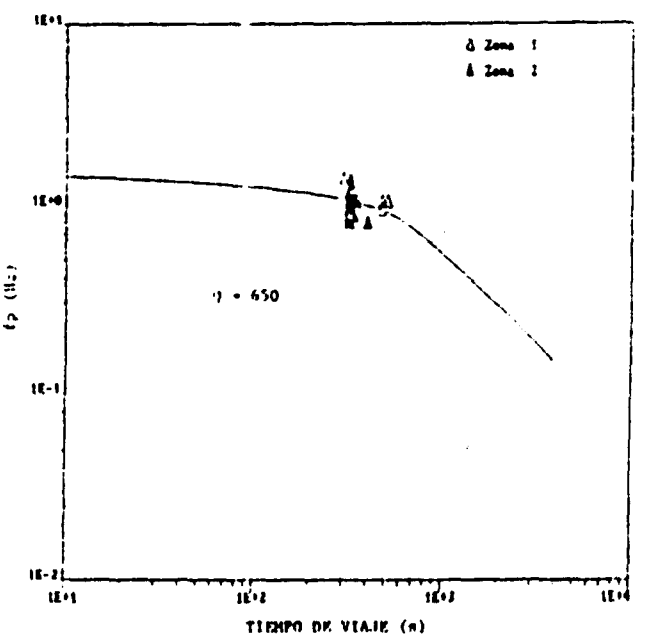

Fig. 25a. Valor de Q Fase Lg, sismos intermedios.

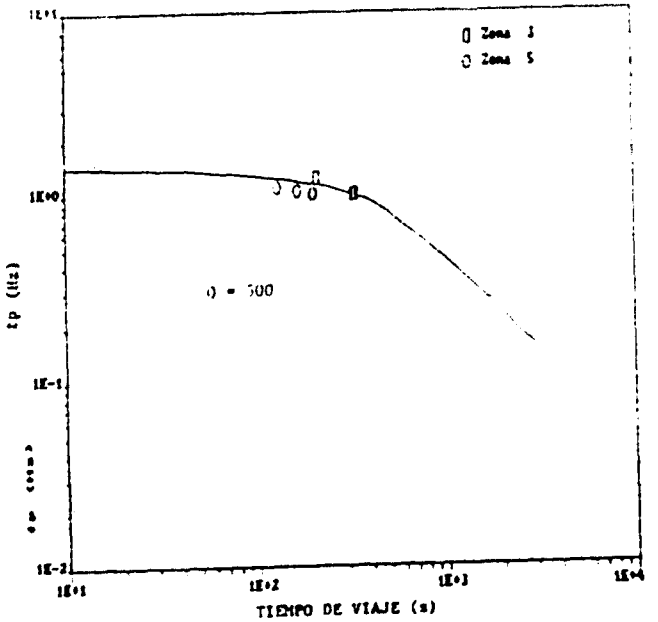

Fig. 25b. Valor de Q Fase Lg, sismos intermedios.

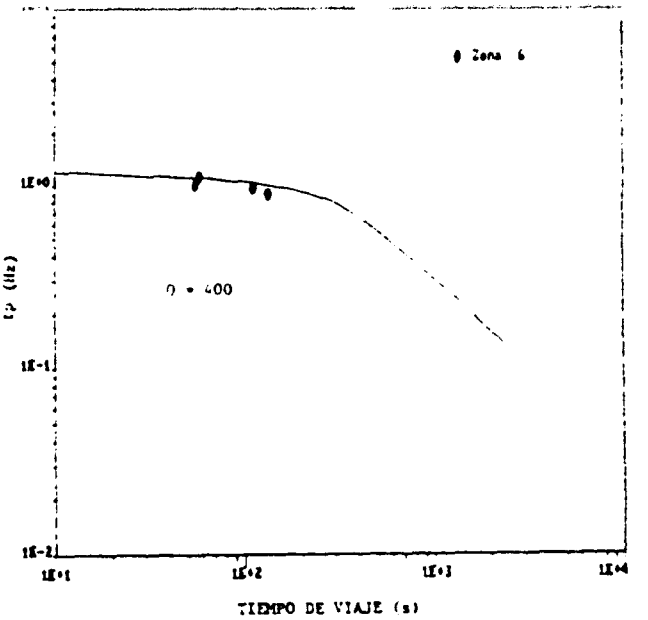

Fig. 25c. Valor de Q Fase Lg, sismos intermedios.

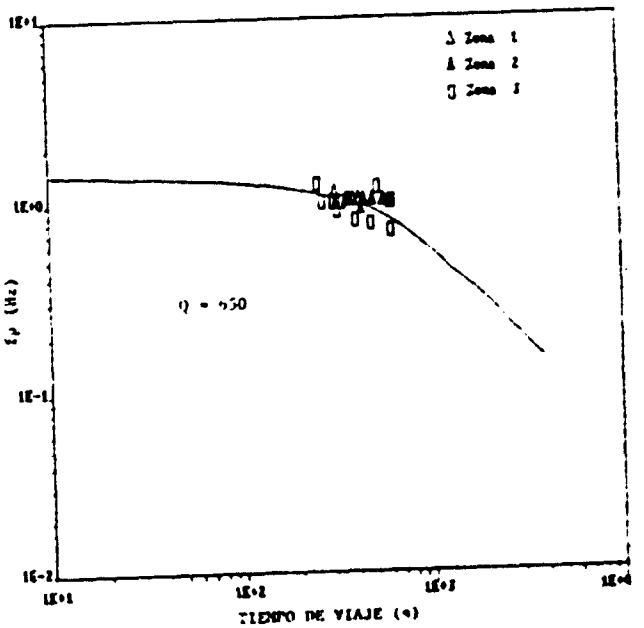

Fig. 26a. Valor de Q Fase Rg, sismos superficiales.

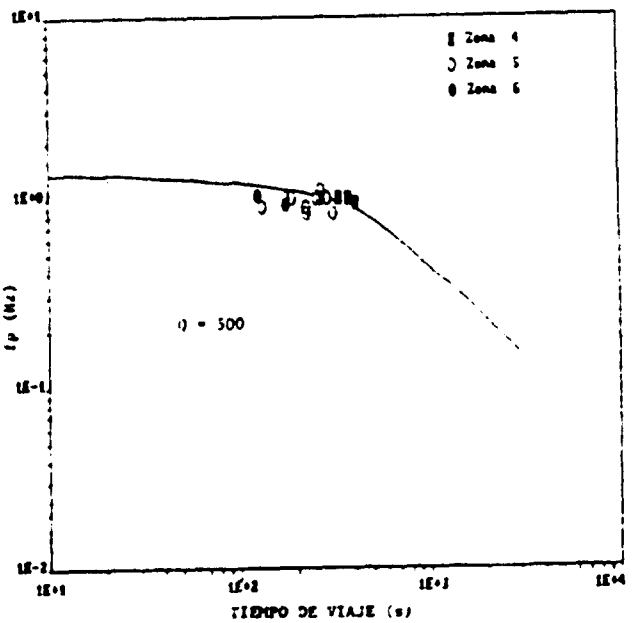

Fig. 26b. Valor de Q Fase Rg, sismos superficiales.

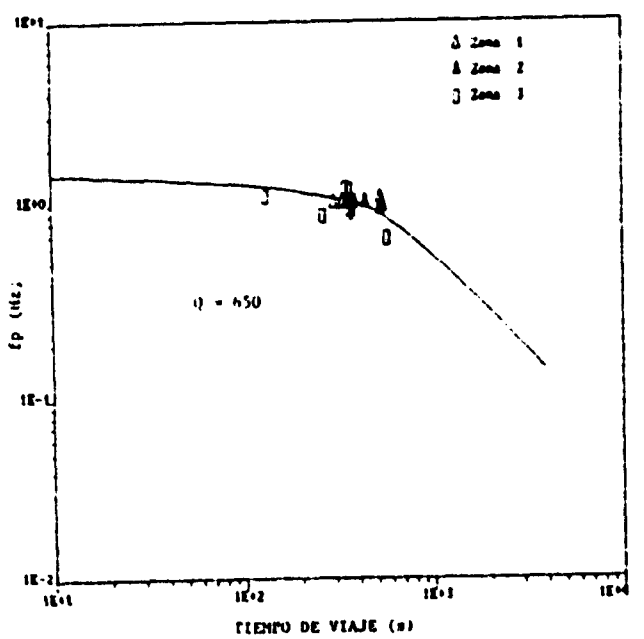

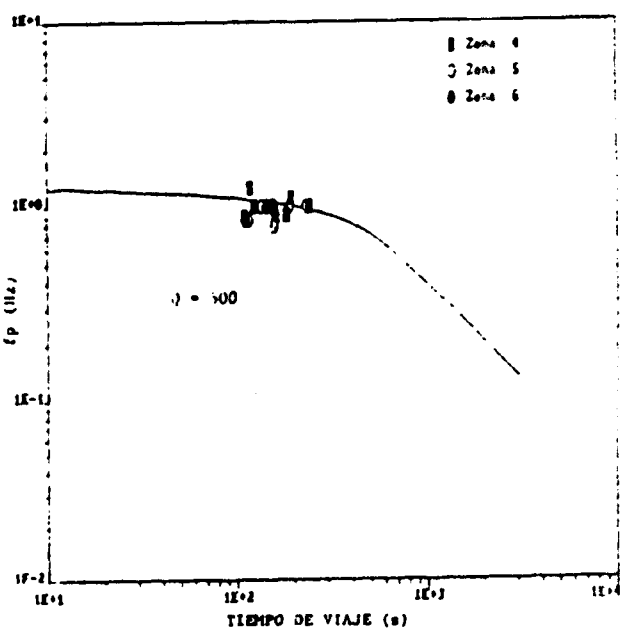

Fig. 27b. Valor de Q Fase Rg, sismos intermedios.

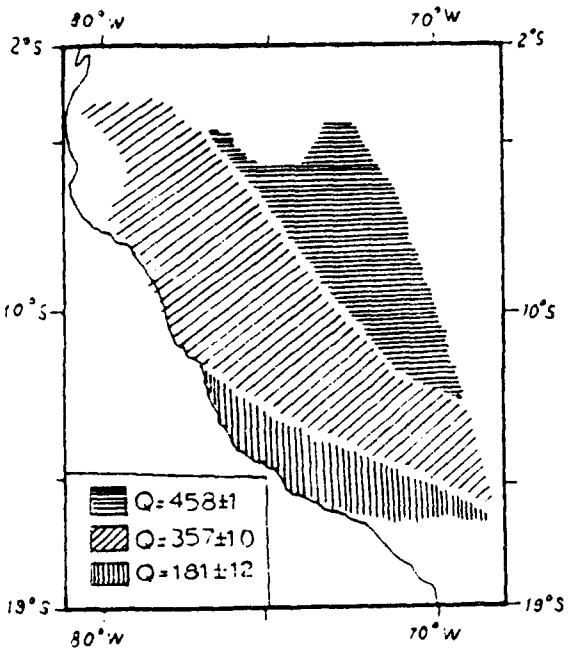

Fig. 28a. Regiones de Q Fase P, focos superficiales.

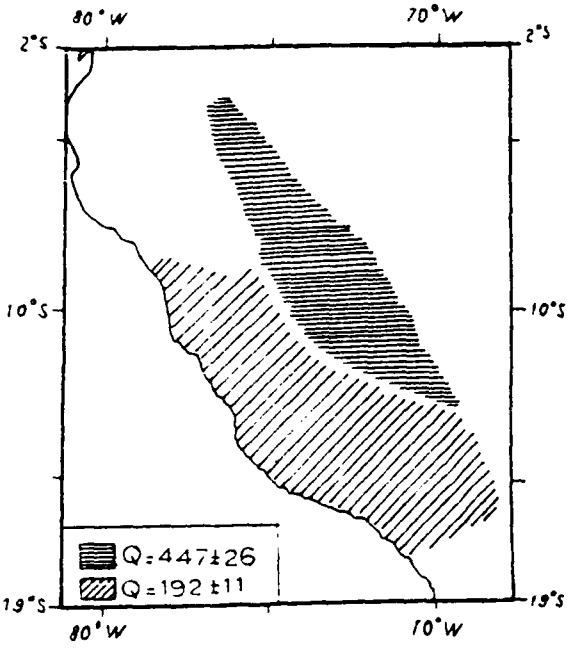

Fig. 28b. Regiones de Q Fase P, focos intermedios.

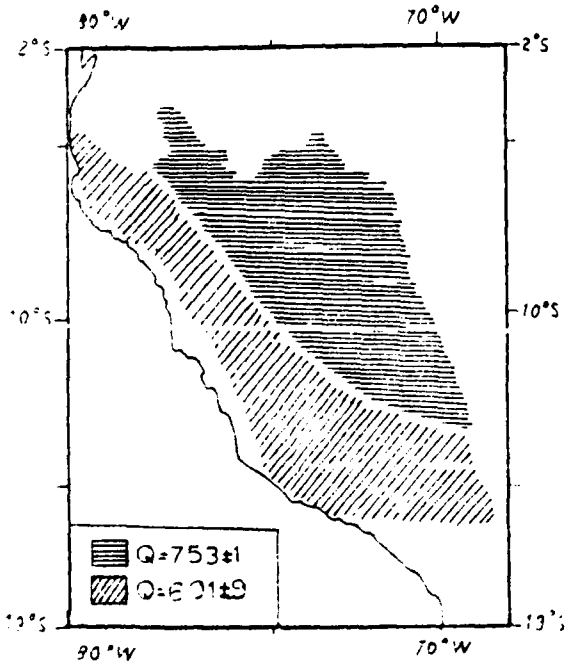

Fig. 29a. Regiones de Q Fase L1, focos superficiales.

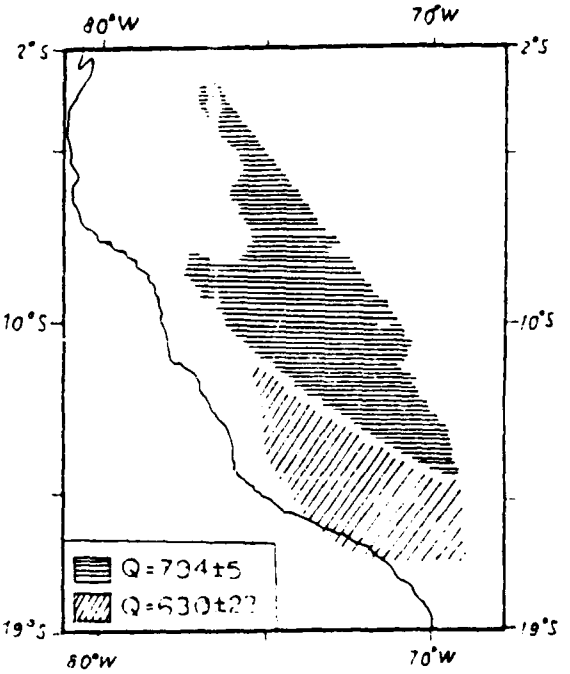

Fig. 29b. Regiones de Q Fase L1, focos intermedios.

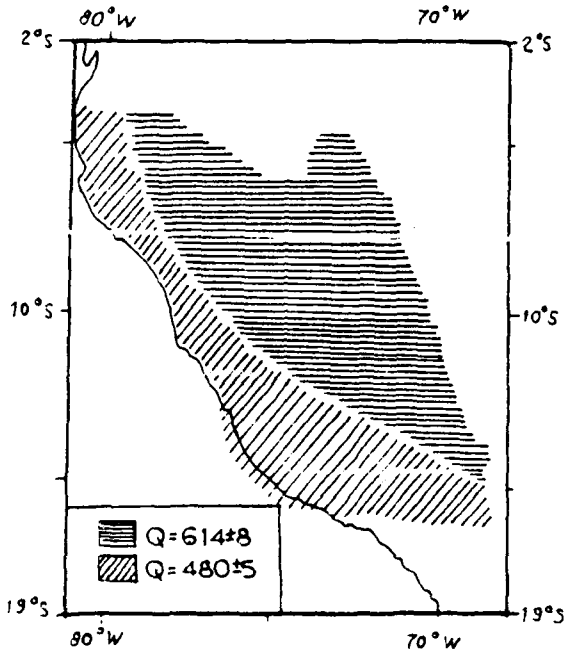

Fig. 30a. Regiones de Q Fase Ly, focos superficiales.

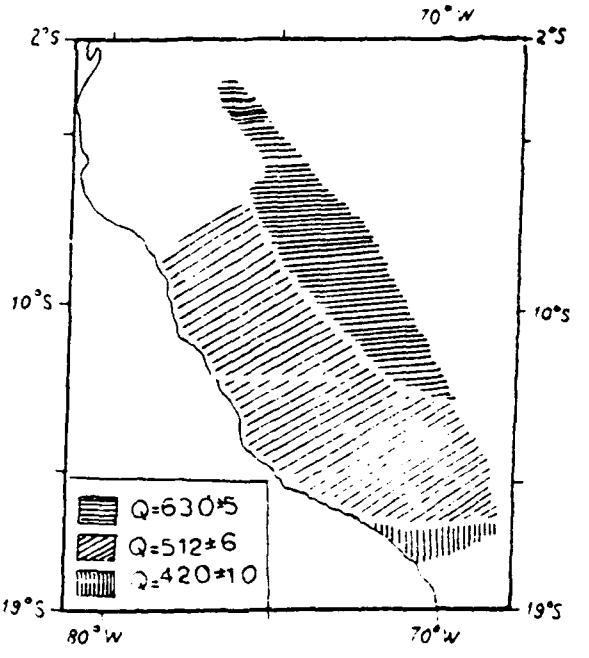

Fig. 30b. Regiones de Q Fase Ly, focos intermedios.

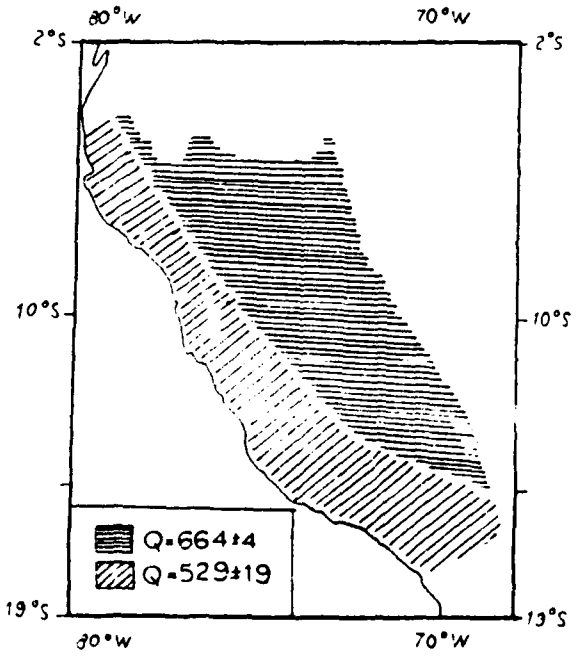

Fig. 31a. Regiones de Q Fase Ry, focos superficiales.

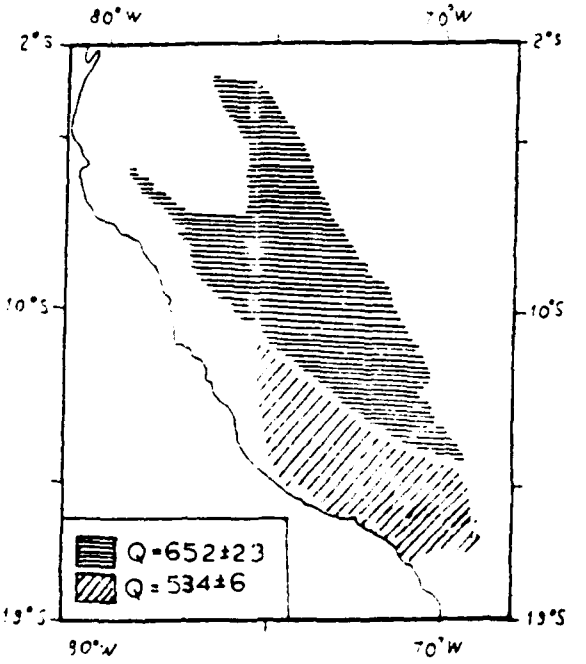

Fig. 31b. Regiones de Q Fase Ry, focos intermedios.

INTERPRETACION

Comparando la velocidad de grupo calculada para las ondas P con el modelo de velocidad (Fig. 32) para la región (Ayala, 1991), notamos que éstas se transmiten hasta el manto superior, incluyendo su capa de baja velocidad. Para focos superficiales se distinguen tres regiones en relación a Q, la primera con menor atenuación correspondiente al Escudo Brasileño y Subandino, con los valores más altos de Q; la segunda zona corresponde a la cordillera, con una mayor atenuación, debido sin duda a la complejidad en la estructura. y la tercera para el Altiplano y parte activa de la cordillera Occidental. Para focos intermedios, se presentan dos regiones con un aumento de la atenuación en dirección oeste; la primera para el Escudo Brasileño, Subandino y parte cordillera Oriental y la segunda para el Altiplano y cordillera Occidental.

Los valores calculados de Q de la Tabla 2 corresponden a un promedio de toda la trayectoria; analizándolos en función de la distancia epicentral, se presenta una tendencia a un ligero aumento de Q con la distancia, que se estudiará posteriormente. Para los eventos más distantes hay una mayor penetración de las ondas P y un consiguiente aumento en la densidad y homogeneidad del material del manto.

La Fig. 33 muestra la variación de la profundidad de la discontinuidad de Mohorovicic entre Perú y Bolivia (mod. de James, 1971), el espesor máximo de la corteza debajo de los Andes centrales es de 70 km (Fernández, 1968, James, 1971 y Molina, 1977), el cual disminuye en dirección este hasta 40 km, para mantenerse casi constante con un espesor de 39 km para la región del Escudo Brasileño (Oblitas, 1972); hacia el oeste el espesor de la corteza oceánica en la Placa de Nazca es de 5 kilómetros (Guzmán, 1972).

Para las ondas guiadas se tienen dos casos; para los focos superficiales se presentan dos regiones de valores de Q, con una menor atenuación en la región del escudo, la cual aumenta en dirección oeste en la cordillera.

Para los focos intermedios se tiene mejor resolución, posiblemente debido a que el efecto atenuador del paquete sedimentario de la corteza continental es menor; estudiando los valores del factor de calidad, notamos que se pueden discriminar dos regiones y sólo para las Lg tres; notando un mayor valor de Q (menor atenuación) para la región del Escudo Brasileño y también para el límite escudo-cordillera (Subandino); Q disminuye en la cordillera Oriental, mayor atenuación, y aún aumenta más álla en el Altiplano y en la cordillera Occidental; estas variaciones verticales y laterales en la estructura se manifiestan en la variación de Q, expresado en un modelo preliminar de Q para la corteza continental entre Perú y Bolivia (Fig. 34), que nos muestra la complejidad de la estructura debajo de los andes centrales.

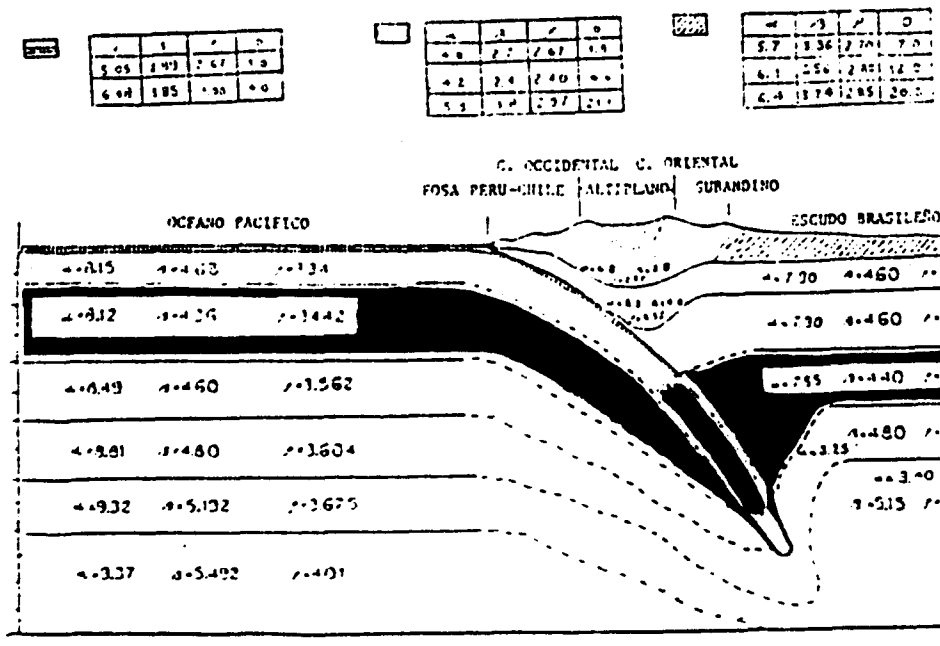

Fig. 32. Modelo generalizado de velocidad para la corteza y manto superior, entre Perú y Bolivia (Ayala, 1981).

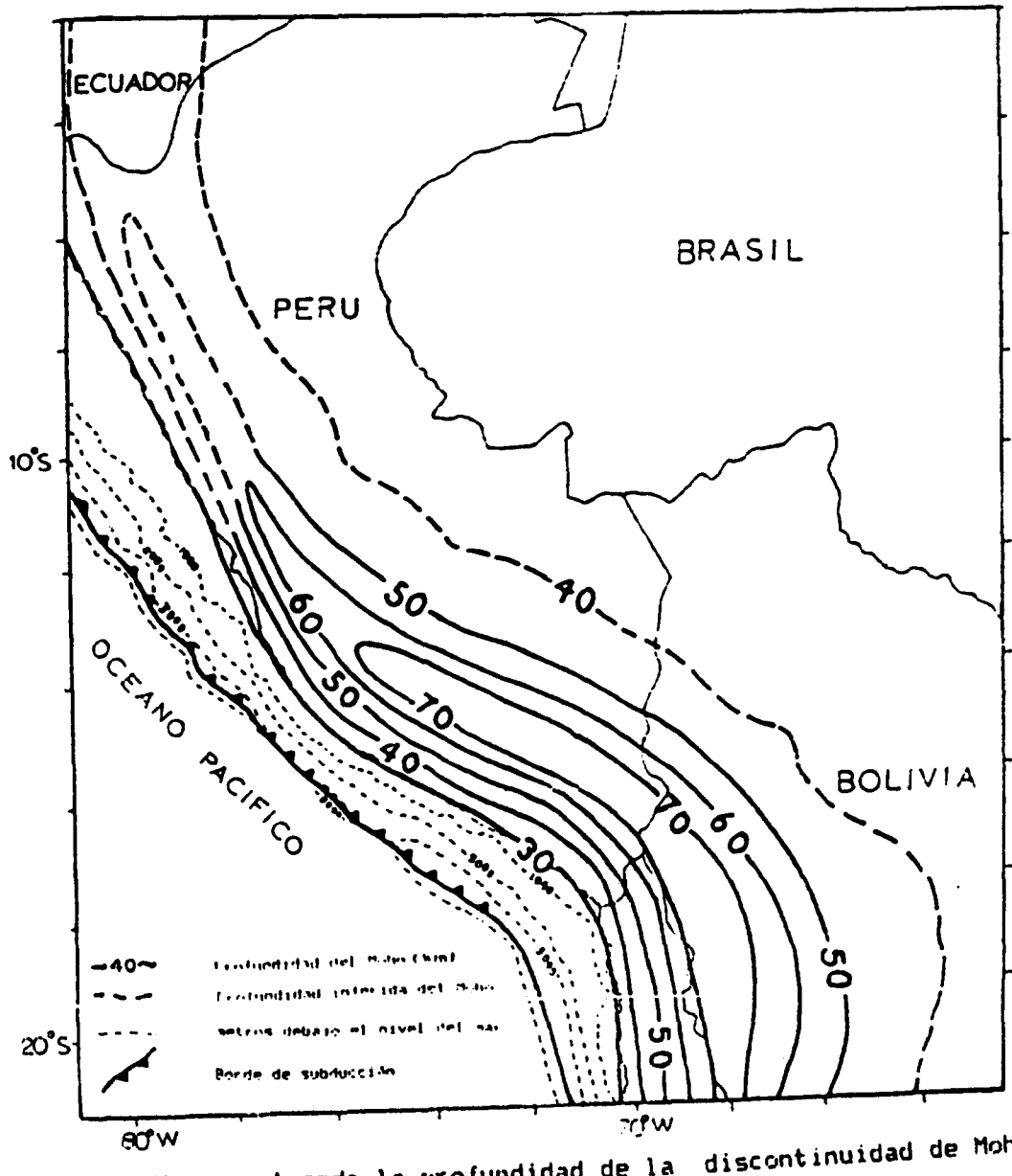

Fig. 33. Mapa mostrando la profundidad de la discontinuidad de Mohorovicic (mod. de James, 1971).

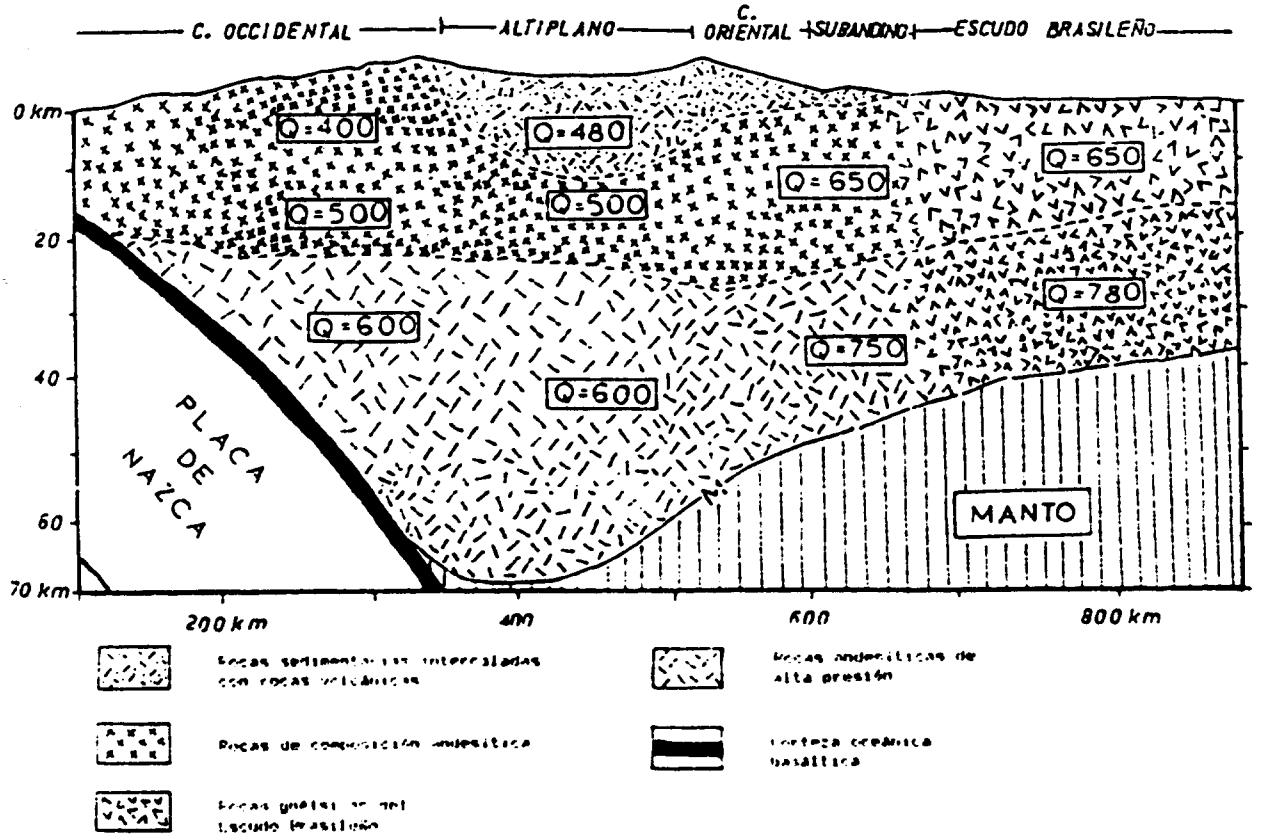

Fig. 34 . Modelo preliminar de Q para la corteza continental entre el Perú y Bolivia (en base a James, 1976).

Por todo lo anterior notamos que estudiando la atenuación de ondas guiadas de corto periodo y focos intermedios se puede discriminar mejor diferentes estructuras.

AGRADECIMIENTOS

Este estudio ha sido auspiciado por el Air Force Office of Scientific Research, Air Force Systems Command, USAF, bajo el Grant Número AFOSR-89-0532A.

BIBLIOGRAFIA

Ayala, R. (1991). Deriva continental y tectónica de placas con relación a la evolución de la placa de Nazca y los Andes Centrales (en prensa).

Bath, M.(1954). The Elastic waves Lg and Rg along Euroasiatic paths, Arkiv. Geofys. 2, 295-324.

Bath, M. (1956). A continental channel wave guided by the intermediate layer in the crust, Geofis. Pura Appl. 38, 19-31.

Bollinger, G. A. (1979). Attenuation of the Lg Phase and the determination of mb in the Southeastern United States, Bullletin Seismological Society of America, Vol. 69, No. 1, 45-63.

Cabré, R. S.J., E. Minaya, I. Alcócer and R. Ayala (1989). Propagation and attenuation of Lg waves in South America, Final Report, Geophysics Laboratory, Air Force Systems Command, United States Air Force, Hanscom Air Force Base, Massachusetts 01731-5000. GL-TR-89-0273, ADA218853

Cabré, R. S.J., E. Minaya, R. Ayala and C. Mora (1990). Lg and other regional phases in South America, Final Report, Geophysics Laboratory, Air Force Systems Command, United States Air Force, Hanscom Air Force Base, Massachusetts 01731-5000. GL-TR-90-0298, ADA232087

Centro Regional de Sismologia, CERESIS (1985). Mapa Neotectónico Preliminar de América del Sur, Proyecto SISRA, Instituto Geográfico Militar de Chile.

Fernández, L. and J. Careaga (1968). The Thickness of the crust in Central United States and La Paz, Bolivia, from the Spectrum of longitudinal Seismic Waves, Bulletin Seismological Society of America, Vol. 58, No. 2, 711-741.

Guzmán, R. J.(1972). Estructura de la Placa de Nazca a partir de la dispersión de ondas superficiales, Tesis de Grado, Universidad de Chile, Santiago, Chile.

Herrmann, R. B. (1980). Q estimates using the coda of local earthquakes, Bulletin Seismological Society of America, Vol. 70, No. 2, 447-468.

James, D. E. (1971). Andean Crustal and Upper Mantle Structure;J.Geophys. Res., Vol. 76, Number 14, 3246-3271.

James, D. E. (1976). Evolución de los Andes Centrales, Deriva Continental y Tectónica de Placas, Selecciones de Scientific American, H. Blume, Madrid, España.

Jeffreys, A., J. R. Aires (1988). Gravity anomalies and flexure of the Lithosphere at the Middle Amazon Basin, Brazil, J. Geophys. Res., Vol. 93, Number B-1, 415-428.

Molina, A. (1977). Estructura de los Andes Centrales a través de residuos y atenuación de ondas sismicas, Tesis de Grado, Universidad Mayor de San Andrés.

Minster, J. B. and T. H. Jordan (1978). Present day Plate Motion, J. Geophys. Res.,Vol. 76, Number B11, 5331-5354.

Morrison R., P. (1962). A Resume of the Geology of South America, Institute of Earth Sciences, University of Toronto.

Nuttli, O. W. (1973). Seismic wave attenuation and magnitude relations for Eastern North America, J. Geophys. Res., Vol. 78, Number 5, 876-885.

Nuttli, O. W. (1980). The Excitation and Attenuation of seismic crustal phases in Iran, Bulletin Seismological Society of America, Vol. 70, No. 2, 469-485.

Oblitas, L. (1972). Estructura del Escudo Brasileño a partir de la dispersión de las ondas superficiales, Tesis de Grado, Universidad de Chile, Santiago, Chile.

Press, F. and M. Ewing (1952). Two slow surface wave across North América, Bulletin Seismologycal Society of America, 42, 219-228.

Raoof, M. M. and nuttli, O. W. (1984). Attenuation of High Frecuency Earthquake Waves in South America, PAGEOPH., Vol. 22, 619-644.

Schlater, I., E., Nederlof (1966). Bosquejo de la Geologia y Paleografia de Bolivia, Bol. Geobol No. 8.